EVALUATION OF COMPUTER CODES FOR COMPLIANCE DETERMINATION PHASE II

Prepared for

Nuclear Regulatory Commission

Contract NRC-02-88-005

Prepared by

Center for Nuclear Waste Regulatory Analyses
San Antonio, Texas

January 1994

EVALUATION OF COMPUTER CODES FOR COMPLIANCE DETERMINATION PHASE II

Prepared for

**Nuclear Regulatory Commission
Contract NRC-02-88-005**

Prepared by

**Amitava Ghosh
Sui-Min Hsiung
Goodluck I. Ofoegbu
Asadul H. Chowdhury**

**Center for Nuclear Waste Regulatory Analyses
San Antonio, Texas**

January 1994

PREVIOUS REPORTS IN SERIES

Number	Name	Date Issued
CNWRA 93-005	Evaluation of Coupled Computer Codes for Compliance Determination	June 1993
NUREG/CR-6022	A Literature Review of Coupled Thermal-Hydrologic-Mechanical-Chemical Processes Pertinent to the Proposed High-Level Nuclear Waste Repository at Yucca Mountain	July 1993

ABSTRACT

The objective of this study was to select a computer code that can be used by the U.S. Nuclear Regulatory Commission (NRC) and the Center for Nuclear Waste Regulatory Analyses (CNWRA), with appropriate modifications, for determining U.S. Department of Energy (DOE) compliance with NRC regulations on thermal loads. A phased approach was adopted for this study. Phase II of the study is reported herein. In Phase I of the study, the finite-element code ABAQUS and the distinct-element code UDEC were selected for further evaluation. According to reported information, ABAQUS has several features that are useful in modeling various coupled phenomena associated with the proposed high-level waste (HLW) repository at Yucca Mountain (YM). For example, it has the capability for mechanical-effect-dependent coupled modeling of unsaturated fluid flow through porous media. Also, the properties of the medium, as modeled in ABAQUS, can be temperature- and degree-of-saturation-dependent. In Phase II of the study, four benchmark mechanical response problems that were previously analyzed by UDEC, as well as two problems with intersecting fractures, were analyzed using ABAQUS. Although the results from these analyses show that ABAQUS can model rough fractures as well as UDEC, it cannot model rock joint networks, especially when the expected shear displacements along different joints are large. On the other hand, although UDEC can model joint network effectively and has the capability for mechanical-effect-dependent saturated fracture flow modeling, it does not have the ability for matrix flow modeling. Neither of these two codes is found to be able to adequately model all of the important coupled thermal-mechanical-hydrological (TMH) processes of the near field of the proposed HLW repository at YM. It is neither practical nor cost effective to select and modify only one of these codes for near-field TMH coupled analysis. Instead, an alternative approach that takes advantage of the best features of each code for analyzing different areas of concerns may be necessary. UDEC is recommended for use in underground excavation stability problems where coupled thermal and mechanical effects, including earthquakes, are important. It is recognized that many problems relevant to a proposed HLW repository are truly three-dimensional (3D). Therefore, in addition to UDEC, the use of 3DEC code, which is in essence a 3D version of UDEC, appears to be necessary. Several modifications are necessary to the 3DEC/UDEC codes so that the problems associated with the effect of thermal-mechanical coupling can be adequately analyzed. The scope of the modification work is outlined in this report. ABAQUS may be used in problems where mechanical-effect-dependent unsaturated fluid flow, vaporization of water, recondensation of the vapor, and condensate dripping through the potential preferential pathways need to be modeled. The evaluation of ABAQUS conducted in this report is primarily based on the qualification study results on the mechanical process and some other reported information. Consequently, the options for the TMH analysis in the ABAQUS code have not been verified. It is recommended that these options be tested using relevant benchmark problems currently under development, laboratory coupled TMH tests to be conducted under the Seismic Rock Mechanics research project, and some benchmark problems and test cases from the DEvelopment of COupled models and their VALidation against EXperiments (DECOVALEX) program.

CONTENTS

CONTENTS (Cont'd)

FIGURES

TABLES

ACKNOWLEDGMENTS

EXECUTIVE SUMMARY

The design and performance assessment of the proposed high-level waste (HLW) repository at Yucca Mountain (YM), Nevada, likely will be based on simulations of several coupled processes. These simulations may consider thermal (T), mechanical (M), hydrological (H), and chemical (C) processes and their interactions (TMHC) over a variety of spatial and temporal scales (Tsang, 1991; Manteufel et al., 1993). The spatial scale of interest in the code selection study is the near field, which includes both emplacement drift and borehole. A recent U.S. Nuclear Regulatory Commission (NRC) staff technical position (Nataraja and Brandshaug, 1992) provided an acceptable methodology for systematically considering thermal loads and thermally induced mechanical, hydrological, and chemical processes for the design and performance assessment of a geologic repository for demonstration of compliance by the U.S. Department of Energy (DOE) with the NRC regulations on thermal loads (U.S. Nuclear Regulatory Commission, 1992). The objective of the code selection study was to select a computer code that can be used by the NRC and the Center for Nuclear Waste Regulatory Analyses (CNWRA), with required modifications, for determining DOE compliance with NRC regulations on thermal loads. Only the coupled interactions among the TMH processes that are relevant to HLW disposal at YM were considered in the study. The effect of chemical reactions on TMH processes and vice versa were not considered in the code selection study, primarily because no code is available that can deal with all four processes. If found to be appropriate, the effect of chemical reactions on TMH processes will be considered at a later date.

A phased approach was adopted for the study. The Phase II results of the study are reported herein. During Phase I of the study (Ghosh et al., 1993), 15 codes were evaluated based on reported information regarding their TMH capability to model the disturbed and fractured near field of the repository. The three-dimensional (3D) finite-element code ABAQUS (Hibbitt, Karlsson & Sorensen, Inc., 1992a,b,c) and the two-dimensional (2D) distinct-element code UDEC (ITASCA Consulting Group, Inc., 1992a,b) were selected for further evaluation in Phase II of the study.

In Phase II, a list was established of features that are considered necessary for compliance determination code(s) to effectively assess the potential effects of coupled TM and TMH processes relevant to YM. The development of this list was based primarily on a recent report by Manteufel et al. (1993) in which important coupled processes relevant to YM were identified, as well as on other newly acquired information (Makurat et al., 1990a,b; Tsang, 1990; Hofmann, 1993). An assessment of the UDEC and ABAQUS codes was made against this list using information from the qualification studies on these codes and other reported information.

ABAQUS was subjected to a qualification study similar to the study of UDEC (Brady et al., 1990). Four benchmark problems, originally modeled by UDEC, were analyzed by ABAQUS. These problems were to facilitate the evaluation of the mechanical aspect of the capabilities of the ABAQUS code. Results from the ABAQUS analysis show that its capabilities to model rough fractures and infinite medium under pseudostatic and dynamic loads are comparable to those of UDEC. Moreover, based on reported information (Hibbitt, Karlsson & Sorensen, Inc., 1992a,b,c), ABAQUS has several features that are useful in modeling various coupled phenomena associated with the proposed HLW repository at YM. For example, it has the capability for mechanical-effect-dependent unsaturated fluid flow through porous media and fractures. The properties of the medium, as modeled in ABAQUS, can be temperature- and degree-of-saturation-dependent. Two more problems were modeled in Phase II of the study using ABAQUS to determine its capability to model the rock joint network. Results of this analysis show that

the interface element, available in ABAQUS to model rough interfaces, is incapable of modeling the rock joint intersecting network, since the mechanism is not in place for a rock block at one quadrant of two intersecting joints to recognize the existence of the rock block at the opposite quadrant. As a result, one block can numerically penetrate another block without generating any stress. On the other hand, UDEC can model the joint network effectively and has the capability for mechanical-effect-dependent fracture flow modeling, but it does not have the option for matrix flow modeling. With the present state-of-the-art in finite-element method, it is neither practical nor cost effective to develop capabilities in ABAQUS to model the joint network. Alternatively, it is also not cost effective to incorporate unsaturated fluid flow through porous media capability in UDEC. It is also recognized that many problems relevant to a HLW repository are truly 3D and cannot be modeled with any 2D idealization of UDEC. Therefore, the use of 3DEC code (ITASCA Consulting Group, Inc. 1992c,d), which is in essence a 3D version of UDEC, in addition to UDEC appears to be necessary.

It is apparent that none of these three codes can adequately model all of the important coupled TMH processes of the near field of the proposed HLW repository at YM. It is neither practical nor cost effective to select and modify only one of these codes for near-field TMH coupled analysis. Toward this end, an alternative approach may be necessary for addressing different concerns that are relevant to the near field of the HLW repository by making use of the best features of each code. It was decided that both 3DEC and UDEC will be used in underground excavation stability problems where coupled thermal and mechanical effects, including earthquakes and nuclear explosions, are important. However, several aspects of these codes need modification. The rock joint constitutive models available in UDEC and 3DEC are inadequate for predicting the shear strength and dilation during cyclic pseudostatic and dynamic loads. A new rock joint model is being developed using the experimental results of the Seismic Rock Mechanics research project. Once developed, this rock joint model needs to be incorporated in these codes.

ABAQUS, on the other hand, may be used in problems where mechanical-effect-dependent unsaturated fluid flow, vaporization of water, recondensation of the vapor, and condensate dripping through the potential preferential pathways need to be modeled. It should be noted that the primary objective of the coupled TMH modeling is to provide estimates of the changes in permeability with time and space so that they can be taken into account in subsystem near-field performance assessment (PA) and total system PA calculations. ABAQUS will also be used to verify the various assumptions relevant to mechanical-effect-dependent fluid flow that the available hydrological codes will make in the near-field PA and total system PA calculations. However, the capabilities identified in the ABAQUS code that are suitable for the coupled TMH analysis relevant to the proposed HLW repository at YM are based on reported information. Further assessment of the ABAQUS code is recommended to confirm these capabilities before it can be recommended for modeling problems involving TMH phenomena. Development of relevant benchmark problems for this assessment is currently under way. Results from laboratory coupled TMH experiments, currently undertaken in the Seismic Rock Mechanics research project, will also be used in this evaluation process. To the extent practical, some benchmark problems and test cases from the DECOVALEX program will be used for the ABAQUS evaluation.

1 INTRODUCTION

## 1.1 BACKGROUND AND OBJECTIVES

Yucca Mountain (YM), located approximately 160 km northwest of Las Vegas, Nevada, has been designated by the United States Congress for characterization as a potential repository site for high-level nuclear waste (HLW) disposal. A general description of the YM site for the proposed repository has been given in the U.S. Department of Energy (DOE) Site Characterization Plan (SCP) (U.S. Department of Energy, 1988). The area is characterized by north to northwest trending mountain ranges composed of volcanic and volcanoclastic strata that dip eastward. The strata are broken into en-echelon fault blocks. The geomechanical conditions at the site are characterized by a highly fractured rock mass with prominent vertical and sub-vertical faults and joints. It should be noted that the terms fracture, crack, and joint are used interchangeably in this report. Arid climate prevails in the YM area, with less than 25 cm of rain per year, and no perennial streams exist in this region. The potential repository location is in the densely welded, devitrified part of the Topopah Spring (TSw2 unit) member of the Paintbrush tuff (Figure 1-1), which is about 350 m below the ground surface and 225 m above the water table (Klavetter and Peters, 1986). At YM, the zone above the water table contains capillary water held in pores and perched water zones (Figure 1-2). The emplacement of radioactive waste in this partially saturated geologic medium will cause major perturbations to the system involving coupled thermal, mechanical, hydrological, and chemical (TMHC) processes. Under the coupled conditions, the behavior of the repository and its surrounding rock mass cannot be predicted by considering each process independently.

The fractured rock mass will be perturbed in several ways. First, the construction of the repository changes the state of stress, which, in turn, causes mechanical deformation of the rock, including joint normal and shear deformations. Joint normal and shear deformations have implications regarding the stability of excavations. They also affect fluid flow and solute transport in the rock mass, which are particularly important to the performance of a geologic nuclear waste repository and its environment. Second, the nuclear waste provides a heat source that is active over an extended period of time. This thermal load induces rock expansion. The rock expansion may cause dilation, closure, and shear failure of fractures. The permeability of both matrix and fracture may change accordingly. The thermal load may also cause (i) degradation of the mechanical properties of rock, (ii) changes to the chemical sorption and retardation capabilities, and (iii) healing of rock fractures. Third, dynamic ground motions due to earthquakes, nearby underground weapons testing, etc., will take place in the environment of *in situ* stresses and thermally induced phenomena in the repository. The dynamic ground motions, including the cumulative effect of repetitive seismic motions, will cause further dilation, closure, and shear of fractures, which may change the fracture and matrix permeabilities.

There is a consensus in the literature concerning the importance of coupled processes at the proposed nuclear waste repository at YM (Tsang, 1991; Manteufel et al., 1993). A recent U.S. Nuclear Regulatory Commission (NRC) staff technical position provided an acceptable methodology for systematically considering thermal loads and thermally induced mechanical, hydrological, and chemical processes (Nataraja and Brandshaug, 1992). The primary purpose of the NRC technical position is to outline an acceptable method of comprehensively, systematically, and logically understanding and evaluating TMHC response for the design and performance assessment of a geologic repository and for demonstration of compliance by the DOE with NRC regulations on thermal loads (U.S. Nuclear Regulatory Commission, 1992).

m	DEPTH	ft	THERMAL/ MECHANICAL UNIT	LITHOLOGIC EQUIVALENT
			UO	ALLUVIUM
			TCw	WELDED, DEVITRIFIED TIVA CANYON
			PTn	VITRIC, NONWELDED TIVA CANYON, YUCCA MOUNTAIN, PAH CANYON, TOPOPAH SPRING
200	500		TSw1	LITHOPHYSAL TOPOPAH SPRING; ALTERNATING LAYERS OF LITHOPHYSAE-RICH AND LITHOPHYSAE-POOR WELDED, DEVITRIFIED TUFF
	1,000		TSw2	NONLITHOPHYSAL TOPOPAH SPRING POTENTIAL REPOSITORY HORIZON (CONTAINS SPARSE LITHOPHYSAE)
400			TSw3	VITROPHYRE, TOPOPAH SPRING
	1,500		CHn1	ASH FLOWS AND BEDDED UNITS, TUFFACEOUS BEDS OF CALICO HILLS; MAY BE VITRIC (v) OR ZEOLITIZED (z)
			CHn2	BASAL BEDDED UNIT OF CALICO HILLS
			CHn3	UPPER PROW PASS
600	2,000		PPw	WELDED, DEVITRIFIED PROW PASS
			CFUn	ZEOLITIZED LOWER PROW PASS AND UPPER BULLFROG
	2,500		BFw	WELDED, DEVITRIFIED BULLFROG
800			CFMn1	ZEOLITIZED LOWER BULLFROG
CFMn2			CFMn3	UPPER ZEOLITIZED TRAM / ZEOLITIZED BASAL BEDDED UNIT OF BULLFROG
	3,000		TRw	WELDED, DEVITRIFIED TRAM

Figure 1-1. Thermal/mechanical stratigraphy at Yucca Mountain (after U.S. Department of Energy, 1988)
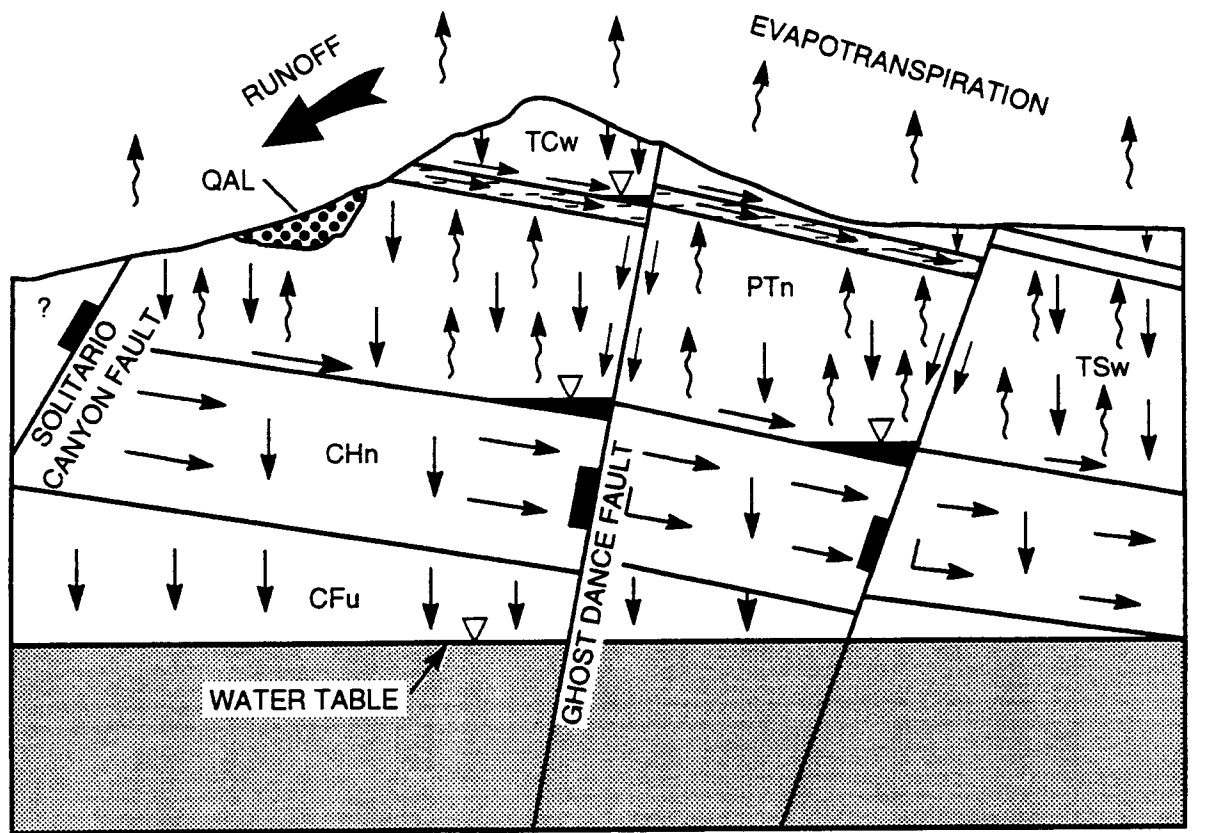
Figure 1-2. Generalized east-west section through Yucca Mountain showing conceptual moisture-flow system under natural conditions (after U.S. Department of Energy, 1988)

The spatial scale of interest in this code evaluation study is the near field that includes both emplacement boreholes and drifts. In general, there are two issues that involve mechanical effect in the near-field environment of the HLW repository: (i) stability of underground excavations, including emplacement boreholes and drifts for both opening design and providing input for design and performance assessment of waste packages, and (ii) mechanical-effect-dependent hydrological properties determination and fluid flow calculation resulting from vaporization of water, recondensation of the vapor, and condensate dripping through the potential preferential pathways, for providing input for both the waste package and the system performance assessment.

The stability of underground openings, including emplacement boreholes and drifts, will primarily depend on thermomechanical (TM) effects. The TM effects are those due to *in situ* stresses; excavation-induced stresses; dynamic motions, including the cumulative effect of repetitive seismic motions; and the thermally induced stresses and deformations. The movement along the joints of the disturbed jointed rock mass forms the primary mode of deformation of the near-field rock mass (Kana et al., 1991). Excessive slippage of a rock block along failed joints may affect the performance of the waste canisters inside emplacement boreholes and drifts. In addition to the TM effects, the behavior of the joints is also influenced by the presence of water in the joints (Jaeger and Cook, 1979; Hoek and Brown, 1980).

Buscheck and Nitao (1993) have shown, through numerical calculations, that matrix-dominated flow will not result in significant vertical transport of radionuclides and that fracture-dominated flow is the only credible mechanism capable of bringing water to the waste package and transporting radionuclides to the water table. During radioactive decay of the HLW, the resulting temperature field will generate thermal stresses which produce normal and shear displacements of the fractures. Additionally, the most likely serious effect of earthquakes on hydrology is to change the fracture permeability, for example, similar to what happened in California during the Loma Prieta earthquake[1] (Hofmann, 1993). In the case of the Loma Prieta earthquake in California, it has been inferred that the increased fracture permeability allowed the water table in the mountains to drop more than 30 m while greatly increasing the flow of springs and streams in the foothills. At YM, the change of fracture permeability may occur due to the ground motion from earthquakes and underground nuclear explosions at the Nevada Test Site. Recent observations (Hill et al., 1993) that a large earthquake can induce smaller earthquakes at great distances from its epicenter makes this issue much more significant than previously thought. Cumulative effects of repetitive seismic loads may form preferential pathways connecting the emplacement area with condensation zones above the emplacement area, perched water zones, or neighboring steep hydraulic gradient zone. Heating of the groundwater in the near field of the repository produces vaporization, vapor flow, condensation, and condensate flow. Hence, the coupled system becomes one involving thermal, mechanical, and hydrological interactions (TMH). Furthermore, the thermal load may also cause the healing of rock fractures (Lin and Daily, 1989) and, hence, a change of fracture permeability. However, the effect of chemical reactions on these TMH processes and vice versa were not considered in this code evaluation study, primarily because no code is available that can deal with all four processes. The effect of chemical reactions on TMH processes will be considered at a later date, if found to be appropriate.

---

[1]Personal communication with Prof. G.A. Thompson, Stanford University, Stanford, California, June 1993.

The objective of the code selection study was to select a computer code for NRC and Center for Nuclear Waste Regulatory Analyses (CNWRA) use, with appropriate modifications, in determining DOE compliance with NRC regulations on thermal loads. A phased approach was adopted for this purpose. During Phase I of the code selection study (Ghosh et al., 1993), 15 codes were evaluated based on reported information regarding their TMH capability to model the disturbed and fractured near field of the repository. The two-dimensional (2D) distinct-element code UDEC and the three-dimensional (3D) finite-element code ABAQUS were selected for further evaluation during Phase II of the code selection study.

The objectives of Phase II of the code selection study were to: (i) evaluate the ABAQUS and UDEC codes further for the coupled TMH analysis capabilities of the two codes based on a combination of qualification studies and reported information (Hibbitt, Karlsson & Sorensen, Inc., 1992a,b,c; ITASCA Consulting Group, Inc., 1992a,b); (ii) develop an approach for the use of one or both codes for further development as a compliance determination code(s) (CDCs); and (iii) recommend any alternative approach if any aspect of the TMH coupled phenomena could not be modeled. In this report, ABAQUS was subjected to a qualification study similar to that of UDEC (Brady et al., 1990) to evaluate its mechanical analysis capabilities. Four benchmark problems, originally analyzed by UDEC in the Seismic Rock Mechanics research project (Brady et al., 1990), were analyzed by ABAQUS. Of the four problems, two were pseudostatic and two were dynamic, each containing a single joint. In addition to these four benchmark problems, two pseudostatic problems with intersecting joint network were also analyzed using ABAQUS as part of the qualification study. Since the simulation of the mechanical response of jointed rock mass is the fundamental requirement for the CDCs, the purpose of this qualification study on ABAQUS was to determine if the code can reproduce the rock joint response of these benchmark problems under pseudostatic and dynamic loads. The UDEC qualification study includes qualification against: (i) four benchmark problems (Brady et al., 1990), (ii) laboratory results (Hsiung et al., 1993a), and (iii) DECOVALEX modeling results (Ahola et al., 1992, 1993). The CDCs, after appropriate modifications, should be able to model the important coupled phenomena among TMH processes expected in the near field at the proposed repository at YM.

The CDCs will provide input, as applicable, to the subsystem Performance Assessment (PA) code EBSPAC (Sridhar et al., 1993), Iterative Performance Assessment (IPA) codes SOTEC (Sagar et al., 1992) and SEISMO, and Total System Performance Assessment code TPA (Sagar and Janetzke, 1993). This code will receive input as needed from EBSPAC, SOTEC, and seismic hazard code SEISM1 (currently under revision at the CNWRA), and will interact with various PA auxiliary analysis codes. The DOE is anticipated to use a number of finite-element, finite difference, and distinct-element codes with various degrees of TMH coupling. The CDCs will provide the NRC and the CNWRA tools to independently verify the DOE calculations in areas involving key technical uncertainties (KTUs).

1.2 SCOPE

The scope of Phase II of the multiphase study computer codes selection includes:

- establishment of a set of necessary features for the CDCs

- evaluation of the capabilities and deficiencies of UDEC against the necessary features based on the qualification studies of UDEC against benchmark problems (Brady et al., 1990), qualification studies of UDEC against laboratory results (Hsiung et al., 1993b),

DECOVALEX analysis results of UDEC (Ahola et al., 1992, 1993), and personal communications with ITASCA Consulting Group, Inc. (owner of UDEC)

- qualification of ABAQUS through a study using the four benchmark problems that have been used for the qualification study of UDEC (Brady et al., 1990), as well as using two problems with a pair of intersecting joints

- evaluation of the capabilities and deficiencies of ABAQUS against the necessary features based on the qualification studies and personal communications with Hibbitt, Karlsson & Sorensen, Inc. (owner of ABAQUS)

- assessment of the nature and scope of modifications of each ABAQUS and UDEC that will be necessary if only one of these two codes is selected as a CDC

- selection of code(s) for further modifications and proposed scope of appropriate modifications of CDCs and/or recommendation of any alternative approach if any aspect of the TMH coupled phenomena cannot be modeled

2 NECESSARY FEATURES OF THE COMPLIANCE DETERMINATION CODE(S)

Thermally induced TMH effects at YM are anticipated to be quite complex. The importance of individual processes and their coupled effects will depend upon the thermal loading of the repository, the design of the engineered barriers, properties of the geologic medium, and the time and spatial scales at which these processes are of interest. The CDCs, after appropriate modifications, should be able to simulate the important near-field coupled phenomena in problems relevant to the proposed HLW repository at YM. Brief discussions on the important aspects of TM and TMH coupled phenomena expected in the near-field environment of the proposed repository are provided in Chapter 1. In this chapter, the features of CDCs necessary to adequately model the expected coupled phenomena are discussed. However, any discussion on engineered barrier design has been excluded from this chapter as it is beyond the scope of this study.

As discussed in Chapter 1, there are two main issues that involve the near-field environment of the proposed HLW repository:

(i)   Stability problem associated with underground excavations, including emplacement drifts and emplacement boreholes due to gravity, repetitive seismic, and thermal loads [Figures 2-1(a) and 2-1(b)].

This issue primarily deals with TM effects for designing the excavations and providing input to design and performance assessment of waste packages. The effect of water that may be present in the joints and may affect stability of underground openings should also be considered. The relevant Compliance Determination Methods (CDMs) include those on Shafts and Ramps Design, Underground Facility Design, Retrievability of Waste, Waste Package Design, and Performance of Waste Packages.

(ii) Mechanical-effect-dependent hydrological properties determination and fluid flow calculation in the near field of the proposed repository from vaporization of water, recondensation of vapor, and condensate dripping through the potential preferential pathways [Figure 2-1(c)].

This issue deals with TMH effects and provides input for both the waste package and the system performance assessment. It may be necessary to deal with multiphase flow and phase change of fluid in an approximate way. Also, depending on the extent of dry-out zone around the emplacement borehole/drift, the spatial scale of interest for this issue may be larger than that in the first issue. The CDMs on the Performance Assessment of Waste Packages and Total System are relevant to this issue.

Features of the CDCs that are necessary to analyze TM phenomena pertinent to the first issue (stability problems) are:

(i)   simulation of thermal and seismic loading time histories

(ii) simulation of heat conduction and thermal stress field
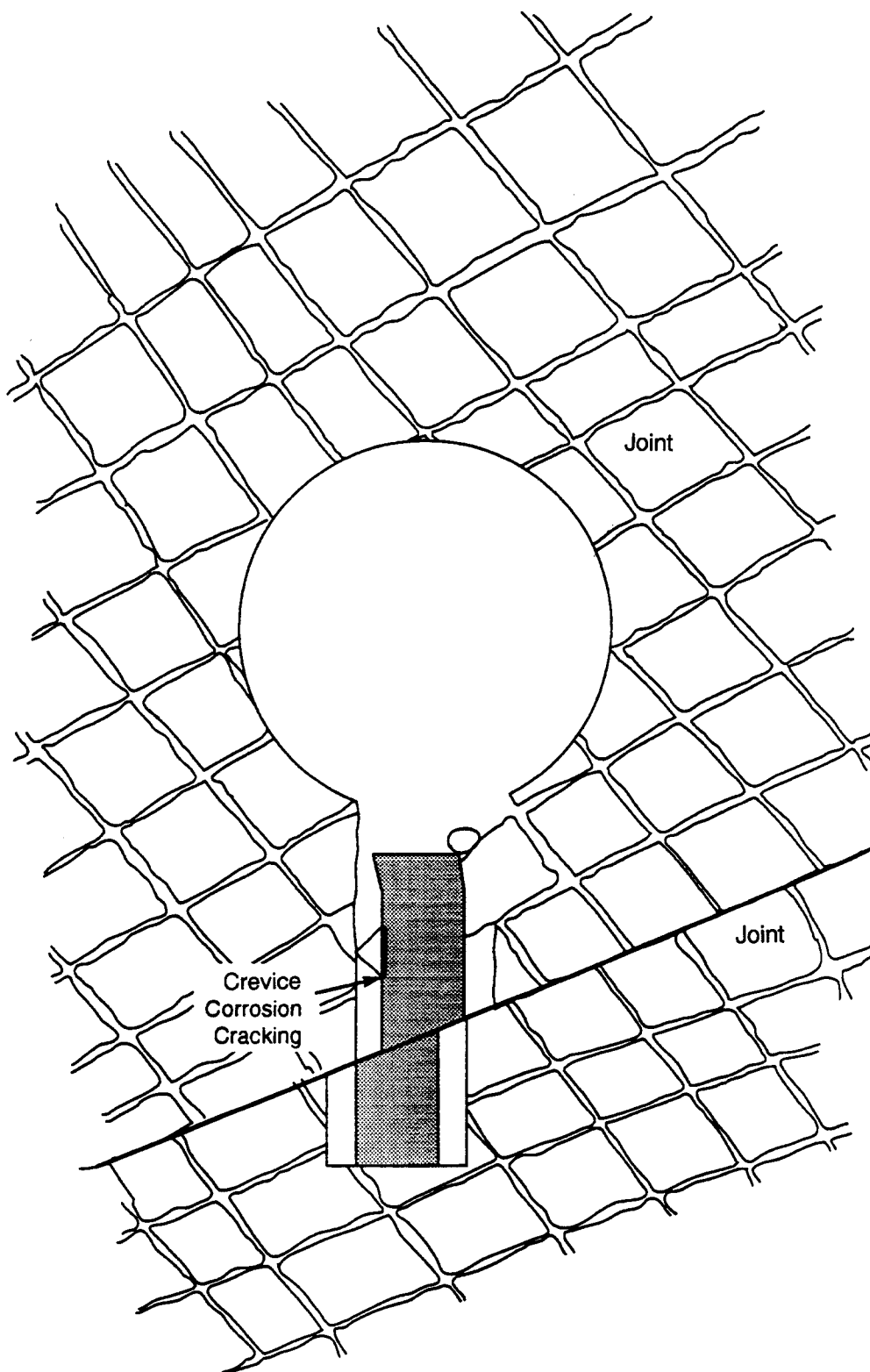
Figure 2-1(a). Schematic representation of near-field stability problems with coupled thermomechanical and seismic effects (vertical emplacement configuration)
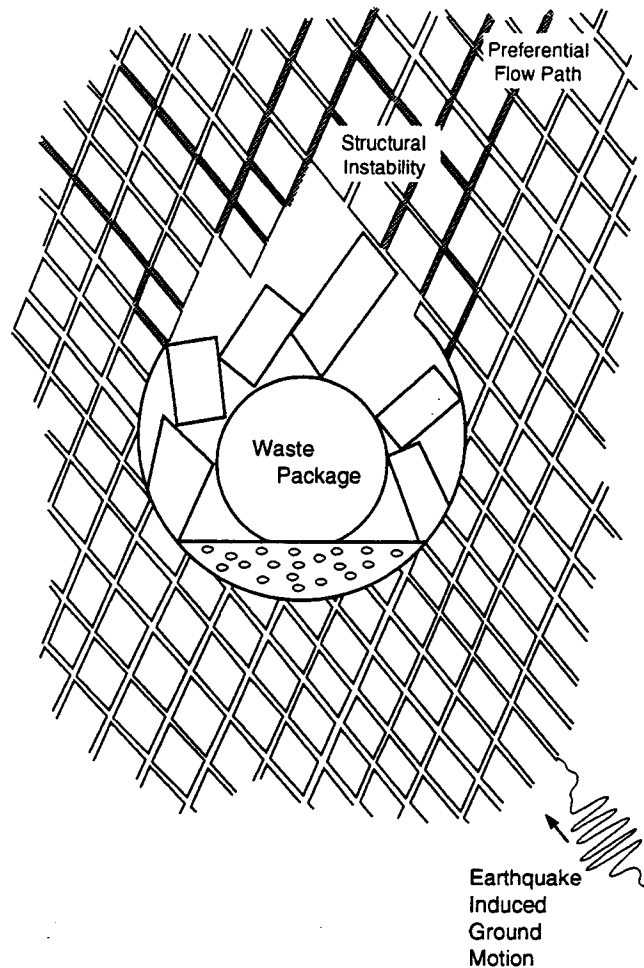
Figure 2-1(b). Schematic representation of near-field stability problems with coupled thermomechanical and seismic effects (horizontal emplacement configuration) before backfilling

(iii)   simulation of rock joints with appropriate constitutive law to model the normal and shear deformation under thermal and mechanical loads (including earthquakes and underground nuclear explosions)

(iv)   modeling of rock joint network

(v)   modeling of infinite region

(vi)   modeling of material constitutive laws

(vii)   simulation of *in situ* stress field

(viii)   modeling of excavation
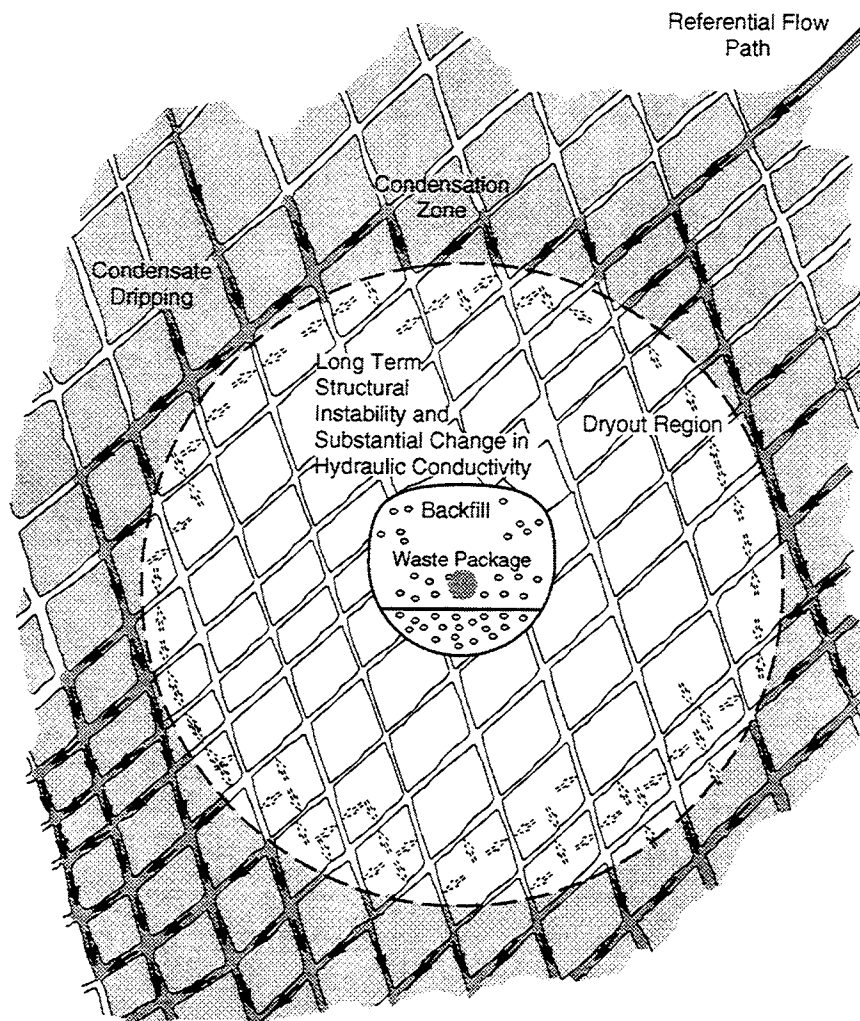
Figure 2-1(c). Schematic representation of problems with TMH effects

In addition to those noted above, features related to the second issue which are necessary to analyze the TMH phenomena in the near field of the proposed repository at YM are:

(i) modeling of poroelastic medium

(ii) modeling of mechanical-effect-dependent fluid flow through fracture

(iii) modeling of phase change of fluid

The features listed for the two concerns do not represent any particular order of importance or degree of difficulty of their implementation in a code and are discussed in more detail in following sections.

It is relatively simple and less time-consuming to model only a section through the rock mass (2D modeling) to get a good understanding of the problem. For many problems, it is sufficient to simulate the problem along one or more sections of the region to develop an understanding of the overall response of the system. However, there are some problems in connection with the proposed HLW repository at YM that are truly 3D; for example, modeling of an excavation in a fractured rock mass when strike of each joint set is not normal to the cross section of the excavation and are not amenable to 2D idealization. Flow of fluid through the fracture network makes it almost impossible to be analyzed acceptably by a 2D code. Any 2D modeling of 3D problems involves some assumptions about the TMH processes and their interactions. These assumptions may not be valid for certain problems pertinent to the proposed repository. In order to address these types of problems, a 3D code is necessary.

The abovementioned features were developed based primarily on the recent report on the coupled processes expected to be associated with the proposed nuclear waste repository at YM (Manteufel et al., 1993) and other newly acquired information (Tsang, 1990; Makurat et al., 1990a,b; Hofmann, 1993). If future research changes the basis for any possible scenario or adds new concerns, an update to the list of necessary features will be needed. Any feature newly added to the list will need to be incorporated in the CDCs if it produces a significant effect on performance.

2.1   SIMULATION OF THERMAL AND SEISMIC LOADING TIME HISTORIES

The thermal load at the proposed repository will be a result of heat generated due to the decay of nuclear waste stored inside canisters emplaced in boreholes or drifts. The magnitude of the thermal load depends on the age and form of the HLW and the number and configurations of spent fuel assemblies and vitrified waste containers for disposal. The magnitude of the thermal loading is expressed as Areal Power Density (APD) in units of W/m^2 or kW/acre. The APD may vary from location to location within the repository or a drift, and it decreases with time. Depending on the problems to be analyzed, these thermal loadings can be idealized as point, line, or volume loadings in the modeled space or expressed as thermal time histories. As a result, the codes should be able to model these various thermal loading conditions.

Natural geothermal gradient is another source of heat in the proposed repository. Data on temperature profile with depth show large variations in geothermal gradients near YM. Upper and lower bounds for the geothermal gradient are 37 and 20 °C/km, respectively (U.S. Department of Energy, 1988). *In situ* temperature at the repository horizon (about 300 m beneath the surface) is estimated to be about 22 to 30 °C. This temperature distribution is an initial temperature field, and the codes should have modeling features to simulate the effects from this geothermal temperature field.

The proposed repository is expected to be subjected to dynamic loads from earthquakes, nearby underground nuclear testing, etc., over its life span. The codes should be able to accept the time history of displacement, velocity, acceleration, stress, etc., applied on the model boundary as input.

2.2   MODELING OF HEAT CONDUCTION AND THERMAL STRESS FIELD

Heat generated by emplacement of HLW in underground excavations will, given time, spread throughout the surrounding rock mass and, consequently, cause the rock mass to expand. The codes should be able to calculate the distribution of temperature within the modeled region for a given thermal

loading either at the boundary or at any given point of the rock mass. Heat transfer may occur either by conduction, convection, or radiation. It is expected that heat transfer through a rock mass will be dominated by the conduction process (Manteufel et al., 1993). Restriction of the expansion by the surrounding rock will result in thermally induced mechanical stresses. This thermally induced stress field, in addition to the *in situ* stresses and the stresses induced by excavation, repeated seismic effects, and other loads, can induce normal and shear displacements of the rock joints. This increases the potential for rock mass failure resulting from excessive joint shear displacement and may cause change of fracture transmissivity. It may also induce microcracks in the rock which could reduce the stiffness of the rock and may lead to the formation or extension of a fracture network through coalescence and propagation of individual microcracks, thus creating the potential for preferential flow paths. The CDCs should be able to model thermally induced stresses from the calculated temperature field.

2.3 MODELING OF POROELASTIC MEDIUM

Rock at YM is a porous medium with extensive fractures. It is expected that the fluid will flow through both the rock matrix and the fracture network. The code should be able to simulate both of these flows. Fluid flow through fractures is discussed in Section 2.4.

When the medium is fully saturated, all the pores are completely filled with water. Air and/or water vapor exist at a point if the medium is partially saturated. The mechanical behavior of the porous medium is a combination of the responses of the water and solid materials to local pressure and of the overall response of the material to the effective stress. The effective stress principle [Biot's poroelastic medium formulation (Biot, 1955)] (a coupled MH process) should be used to characterize the response of the rock.

2.4 MODELING OF MECHANICAL-EFFECT-DEPENDENT FLUID FLOW THROUGH FRACTURE

Redistribution of mechanical stress acting on a rock joint can induce shear displacement along the joint. Excavation of the underground openings, ground motion from earthquakes and nearby underground nuclear testings, and imposed thermal load can cause this stress redistribution. Shear displacement along the joint causes dilation of the joint, which changes the joint aperture and transmissivity and, in turn, may change the preferential flow path. A similar effect will take place if the normal stress acting across the joint surfaces is reduced due to stress redistribution or the pressure of fluid flowing through the joint. As discussed in Section 1.1 of this report, the most likely serious effect of earthquakes on hydrology at YM is to change the fracture permeability, for example, similar to what happened in California during the Loma Prieta earthquake[2] (Hofmann, 1993). In the case of the Loma Prieta earthquake in California, it has been inferred that the increased permeability allowed the water table in the mountains to drop more than 30 m while greatly increasing the flow of springs and streams in the foothills. Raney (1988) has made similar inference about effects of 28 United States earthquakes in the Western North American Intermontane region on mine hydrology. Makurat (1985), Makurat et al. (1990a,b) and Tsang (1990) reported orders-of-magnitude increase of hydraulic conductivity of a joint under shear. This observation is based on laboratory experiments on natural joints in gneiss, granite,

---

[2]Personal communication with Prof. G.A. Thompson, Stanford University, Stanford, California, June 1993.

schist, syenite, and sandstone and numerical simulation using the Barton-Bandis rock joint model and the cubic law.

The CDCs should be able to model fluid flow through fractures present in the rock mass to provide estimates of the changes in permeability with time and space so that they can be taken into account in subsequent near-field PA and total system PA calculations.

2.5   MODELING OF PHASE CHANGE OF FLUID

The thermal load generated by the decaying of disposed HLW will raise the temperature of the surrounding rock mass. This increased temperature will, in turn, increase the vapor pressure of the groundwater. As a result, the water in the liquid phase will not be in equilibrium with the water in the gaseous phase. To restore thermodynamic equilibrium, part of the water in the liquid phase will vaporize. As the temperature reaches the nominal boiling point, boiling first starts along the fracture faces (perimeter of the rock blocks) and proceeds toward the interior of the blocks (Buscheck and Nitao, 1993; Buscheck et al., 1993). After reaching the fracture network, most of the vapor is calculated to be driven away from the emplacement region to areas with cooler temperatures, where it condenses along fracture surfaces. Most of the condensate (water) is calculated to drain down the fractures before being imbibed by the rock matrix. This phase change of water to vapor and vice versa will need to be considered in the TMH modeling.

2.6   SIMULATION OF ROCK JOINT

At the proposed HLW repository at YM, the rock mass deformation and the stability of the underground structures for all types of loadings, including thermal and repetitive seismic loadings, will be determined predominantly by both normal and shear responses of the discontinuities (Christianson, 1988; Kana et al., 1991), which include existing joints, faults, bedding planes (International Society for Rock Mechanics, 1978), and new fractures created during excavation. Furthermore, in the near field of the excavations, flow through fractures is considered to be the dominant mechanism in controlling the groundwater flow (Buscheck and Nitao, 1993).

Preliminary information from drill cores suggests two well-defined joint sets in the TSw2 unit of Topopah Spring tuff, the proposed emplacement horizon (U.S. Department of Energy, 1988). The fracture frequency is 2 to 17 fractures/m^3, with a fracture spacing of 0.06 to 0.47 m. As the rock matrix in the TSw2 unit is quite strong, it is expected that most of the rock mass deformation will take place along the joints, and the stability problems will mostly be structurally controlled. Stability problems of the excavation will be due to (i) gravity fall of blocks from the roof and sidewalls, and (ii) sliding of a rock block on one of the joint surfaces or one of the lines of intersection of joint surfaces (Hoek and Brown, 1980). Excavation-induced stress concentrations may either open or close the pre-existing discontinuities, depending on the fracture orientation with respect to the underground openings, and cause slippage if the shear stress developed exceeds the mobilized shear strength. Shear displacement along a joint surface will cause dilation of the joint. As the fluid flow is extremely sensitive to the joint aperture (proportional to almost the third power of the aperture), the characteristics of fluid flow in the rock mass surrounding the openings can change drastically (several orders of magnitude) with shear displacement along joint surfaces (Makurat, 1985; Tsang, 1990; Makurat et al., 1990b). Makurat et al. (1990a) reported increase of flow by a factor of 20,000 to 150,000 due to joint dilation. Old preferential paths for fluid flow may dry up, and new preferential paths may form with different flow rates.

Ground motion from earthquakes and underground nuclear explosions at the Nevada Test Site can affect the stability of the openings at the proposed repository. Recent observations (Hill et al., 1993) that a large earthquake can induce smaller earthquakes at great distances from the epicenter make this issue much more significant than previously thought. The excavations subjected to repetitive seismic loads ultimately fail by accumulation of shear displacements along the joints (Kana et al., 1991). These shear displacements can change the fluid flow characteristics in the rock mass (Raney, 1988) and may induce major roof fall.

Heat generated by the emplaced HLW in underground excavations will result in a thermally induced stress field. Depending on the magnitude of these stresses and the strength of the joints, excessive joint slippage may occur. Numerical simulations by Christianson and Brady (1989) showed that thermal load may increase the stability of a fractured rock mass when the joints are dipping in some directions. When the joints are dipping in unfavorable directions, thermal load can produce serious instability of the excavations. The failed joints will dilate, which may change the flow characteristics around the openings.

It is clear from the previous discussion that the pre-existing discontinuities and fractures created during the excavation process may have a significant effect on the TMH responses of the rock mass surrounding the excavation at the proposed repository. As a result, explicit modeling of rock joints is necessary to simulate these behaviors.

2.7   MODELING OF ROCK JOINT NETWORK

Since rock joints are expected to dominate the mechanical and hydrological behavior of the rock mass at YM, the CDCs should be able to simulate the fracture network realistically. There are two aspects in simulating the fracture network: (i) modeling intersecting discontinuities with proper transfer of stress and displacement from one fracture to another, and (ii) generating fractures in 3D.

It is realized that it is not practical to obtain accurate information on all existing fractures with their 3D locations in the rock mass. As a result, stochastic simulation of the fracture network is necessary by synthesizing the information available from the outcrop, borehole, drifts, etc. It may be cumbersome to have this capability included in the CDCs, as the computation involved will be quite different from the core computational scheme of the codes, that is, finite-element, finite difference, boundary-element, or discrete element. It may be simpler to have these capabilities in a preprocessor to these codes. The preprocessor could develop the joint geometry model and write the information in a format readable by the CDCs, as has been done for DECOVALEX Phase II modeling (Ahola et al., 1993).

2.8   MODELING OF EXCAVATION

Creation of a new excavation in the rock mass is a sequential process. Before the construction of the excavation, the rock mass was in equilibrium with the material that was in place of the excavation. As the excavation is constructed, the stress field is redistributed around the excavation. If the induced stress field is too high to be accommodated by the surrounding rock mass, failure occurs. Stress redistribution around an excavation will also change apertures of the joints in the region that, in turn, modify the hydrological properties of the rock mass. The CDCs should be able to simulate the excavation effects on the rock mass. For numerical simulation, the excavation process can be modeled by instantaneous excavation of several stages of excavation. In that case, the code should be able to simulate the effects on the rock mass at different stages of excavation.

2.9 SIMULATION OF *IN SITU* STRESS FIELD

The rock mass is always subjected to a nonzero stress field due to the weight of the overlying rock, confinement, and past stress history (Goodman, 1980). The vertical stress is generally taken as the weight of the overlying rock. The horizontal stress, however, may vary significantly from the value predicted due to the Poisson's effect (Hoek and Brown, 1980). The principal stress directions are primarily a function of surface topography. When the surface topography is nearly horizontal, the principal stress directions are vertical and horizontal. However, the presence of hilly terrain may change these stress directions significantly. Presence of this *in situ* stress field in the rock mass should be taken into account by the code as an initial stress field present in the modeled region when calculating the stress distribution around any excavation.

2.10 MODELING OF INFINITE REGION

Many problems in geomechanics involve infinite or unbounded regions. Alternatively, the region of interest can be small compared to the surrounding medium, such as the near field of the proposed repository which is small compared to the size of YM. In static analysis, the model may be extended far enough so that the effect of the model boundaries on the region of interest are negligible. However, this approach is done at the expense of extra computation, decreased computational speed, and additional time needed to develop the model. In the case of dynamic analysis, however, the approach with extended modeling region as adopted in the static analysis may not be practical especially with problems involving wave propagation in which proper modeling of infinite boundary is extremely important to minimize the reflection of dilational and shear waves back into the mesh of the modeled region. Therefore, an ability in the CDCs to properly simulate infinite boundary using techniques such as nonreflecting boundary or infinite elements is a must.

2.11 MODELING TWO- VERSUS THREE-DIMENSIONAL GEOMETRY

It is relatively simple and less time-consuming to model only a section through the rock mass (2D modeling) to get a good understanding of the problem. For many problems, it is sufficient to simulate the problem along one or more sections of the region to develop an overall response of the system. However, there are many problems that are not amenable to a 2D approximation. Presence of rock joint sets whose orientations are not normal to the plane of the model will make accurate analysis of the problem intractable in 2D. Modeling of fluid flow through the joints also makes the problem unsolvable using 2D analysis. Thus, the use of a combination of 2D and 3D codes will be most cost effective.

2.12 MODELING OF MATERIAL CONSTITUTIVE LAWS

The partially saturated rock mass around the excavations in the proposed HLW repository will be subjected to mechanical (*in situ* stress field, excavation-induced stress concentration, and ground motion) and thermal (heat due to decay of HLW and geothermal temperature distribution) loads. All of these processes can affect the response of the rock mass in two ways. First, the material properties may be directly dependent on the stress, temperature, or degree of saturation. Second, the imposed temperature distribution and the stress field can change the material properties.

The material constitutive laws available in the code should be able to adequately model the response of the fractured rock mass under any mechanical load. They should take into account the material degradation close to and beyond the yield point. The capability to simulate the time-dependent behavior of the rock mass should also be included. Application of stress on the rock mass produces microcracks. The number of microcracks and crack coalescence increases as the material goes toward failure (Kemeny and Cook, 1990; Ghosh, 1990). These microcracks not only reduce the stiffness of the rock matrix but also increase the bulk permeability. The material model available in the code should be able to account for this reduction of stiffness and the increase of permeability.

The mechanical properties of a rock mass are also affected by the temperature field. Young's modulus of a rock sample from the potential repository horizon decreased by about 16 percent as temperature was increased from 22 to 150 °C under both uniaxial and biaxial compression (5 MPa) (Price et al., 1987). It is well known that the brittle ductile-transition pressure decreases with increasing temperature (Jaeger and Cook, 1979). However, the temperature anticipated for HLW emplacement at YM (U.S. Department of Energy, 1988) is not high enough to cause a substantial decrease of the transition pressure.

The temperature field present in the rock mass also can affect the thermal properties of the material. There are evidences in the literature (Nimick and Connolly, 1991) that the thermal expansion coefficient and thermal conductivity of rock are dependent on temperature. Therefore, it is expected that the change in heat conduction due to change in temperature field will also change the thermal stress field.

Presence of pore fluid in the rock can change the mechanical and thermal properties. The coefficient of friction increases for some minerals and decreases for other minerals when water is present in the interfaces (Jaeger and Cook, 1979). Average strength of saturated specimens of Topopah Spring tuff is approximately 30 percent less than the average strength of dry samples. Samples from tuffaceous rock of Calico Hills showed a decrease in strength by 23 percent (U.S. Department of Energy, 1988). It was observed in laboratory investigations that the attenuation of a stress wave was directly related to both void ratio and degree of saturation (Crowley, 1973). Less porous and more saturated materials were found to produce larger stresses as the same seismic wave passes through.

Moisture content of a porous medium also can influence the thermal conductivity of rock. Rasmussen et al. (1990) reported that the thermal conductivity for Apache Leap tuff decreases 30 percent from a fully saturated to an oven-dried condition. The relation between the thermal conductivity and the degree of saturation is nonlinear. The decrease of thermal conductivity is more pronounced for drier samples.

Commonly available material models may not be able to acceptably simulate the response of partially saturated rock mass subjected to mechanical and thermal loads. Therefore, it may become necessary to develop or adopt from other researchers a material constitutive model specially designed for the rock in the proposed repository. A provision to include user-supplied material models with relative ease should be available in the code(s).

3 CODE COMPARISON AND PROPOSED UTILIZATION OF COMPLIANCE DETERMINATION CODE(S)

Depending on the purposes, areas of utilization, and solution schemes used, different computer codes may have distinctly different capabilities and limitations. In this section, the ABAQUS and UDEC computer codes are evaluated and compared based on the features necessary in the CDCs to assess the design and performance of a HLW repository at the proposed YM site. The features of CDCs that are considered necessary to model the coupled TM and TMH processes in the near field of a proposed repository are given in Chapter 2 and are used for this evaluation. This evaluation is based on a combination of a qualification study and reported information on these two codes.

3.1 COMPARISON OF ABAQUS AND UDEC CODES AGAINST NECESSARY FEATURES

3.1.1 Simulation of Thermal and Seismic Loading Time Histories

Both ABAQUS and UDEC are capable of accepting thermal and seismic loading histories. The time-varying perturbation can be read from a file. They can model the distribution of temperature within the modeled region for a thermal load given either at the boundary or at any given point in the rock mass.

3.1.2 Modeling of Heat Conduction and Thermal Stress Field

Both ABAQUS and UDEC can calculate the distribution of temperature within the modeled region for a thermal load either at the boundary or at any given point in the rock mass. Uncoupled heat-transfer analysis in ABAQUS can model heat conduction through the material with temperature-dependent conductivity. ABAQUS can also model convection and radiation boundary conditions and forced convection. UDEC also has the capability to model convection and radiation boundary conditions, but it lacks the capability of simulating forced convection. It is important to note that the heat transfer through a rock mass at YM is expected to be dominated by conduction process (Manteufel et al., 1993).

UDEC can simulate the conductive transient flow of heat (Fourier's law) in materials and the resulting stress field. Heat loadings in the material may be from either line or volume sources. Both implicit and explicit solution schemes are available. The solution scheme can be switched from one to another at any time during the analysis.

The usual procedure for solving coupled TM problems in UDEC is to decouple the processes. The problem is first cycled to equilibrate mechanically. Any desired alterations to the model, such as an excavation, can be carried out, followed by cycling to equilibrate mechanically again. The heat sources can be turned on at this point. The thermal timesteps will be taken until the desired time is reached or the thermally induced out-of-balance forces in the blocks are large. The model needs to be cycled again to bring it into mechanical equilibrium. This process of thermal timesteps followed by mechanical timesteps needs to be repeated until sufficient time has been simulated. If the thermally-induced stresses and displacements are considered too large, the step may have to be repeated with smaller allowed temperature change.

Three types of thermal stress analyses may be performed with ABAQUS: (i) temperature does not depend on mechanical solution, (ii) coupled analysis in which mechanical and thermal solutions affect each other strongly, and (iii) adiabatic.

If the stress solution is not dependent on the temperature solution, temperature is calculated in a heat transfer analysis and is used as a predefined field. Temperature can vary with location and is also time-dependent. Coupled temperature-displacement analysis is required when the stress analysis is dependent on the temperature distribution and the temperature solution is dependent on the stress solution. Adiabatic analysis may be carried out in cases where the heat is generated so rapidly that it does not get time to be dissipated. This analysis scheme may not be necessary in the context of the proposed repository.

3.1.3 Modeling of Poroelastic Medium

UDEC cannot model matrix flow. ABAQUS models the porous medium as a multiphase material and uses the effective stress principle to characterize its response (Hibbitt, Karlsson & Sorensen, Inc., 1992a). Two fluids are present in the medium. One is the wetting fluid, which is assumed to be relatively incompressible. Generally, the other fluid is gas, which is compressible. When the medium is fully saturated, all of the voids are completely filled with the liquid. Both fluids exist at a point if the medium is partially saturated. ABAQUS can also take into account any wetting fluid trapped in the particles of the medium in the formulation. Nonlinear equilibrium equations are solved by Newton's method in the implicit time integration scheme.

The mechanical behavior of the porous medium is a combination of the responses of the fluid and solid materials to local pressure and of the overall response of the material to the effective stress. Density of the wetting liquid can change with temperature. Solid material is assumed to have the local mechanical response, which is dependent on the degree of saturation with the wetting fluid.

A porous medium is modeled by attaching the finite-element mesh to the solid phase. Fluid flows through the porous medium. Darcy's law describes the flow of liquid. The continuity equation is satisfied approximately by defining the excess wetting-liquid pressure as a nodal variable interpolated over the element. Backward Euler approximation is used to integrate the equation in time. The total derivative of this integrated continuity equation with respect to nodal variables is required for Newton iterations for solving the nonlinear, coupled equilibrium, and continuity equations. ABAQUS directly solves these equations for rapid convergence, even if the equations are highly nonlinear. The equations are also nonsymmetric due to change in geometry, dependence of permeability on void ratio, change in saturation, and inclusion of fluid gravity load in total pore pressure analysis.

3.1.4 Modeling of Mechanical-Effect-Dependent Fluid Flow Through Fracture

UDEC has the capability to model the liquid flow through saturated fractures on a system of impermeable blocks. A coupled mechanical and hydraulic analysis is performed in which the conductivity of the fracture is dependent on the mechanical deformation, and, conversely, the pressure of fluid in the fracture affects the mechanical stress distribution. For a closely packed system, a network of domains exists. Each domain is filled completely with fluid at uniform pressure and communicates with other neighboring domains through the contact points. The degree of refinement of the numerical representation of the flow through the fracture network is directly linked with the mechanical discretization and can be

specified by the user. Flow is determined from the difference in pressure between adjacent domains. The hydraulic aperture is calculated from the joint aperture at zero-normal stress and the joint normal displacement. A minimum aperture is assumed below which the mechanical closure does not affect the hydraulic conductivity. A maximum value is assumed, which can be changed by the user. A more elaborate empirical relation between joint mechanical and hydraulic apertures, given by Barton et al. (1985), can also be used in the analysis. The flow rate through the fracture is calculated using the hydraulic aperture, and the new domain pressure is then calculated taking into account the net flow into the domain and changes in the domain volume due to incremental motion of surrounding blocks. The forces exerted by the fluid on the surrounding blocks are calculated from the new domain pressure. These forces are then added to the forces at the grid points in mechanical calculation. This procedure produces effective normal stresses for the mechanical contacts and total stresses for the impermeable blocks. For numerical stability of the explicit fluid flow, the algorithm requires a stable timestep that is inversely proportional to fracture conductivity. UDEC can also model the flow of Bingham fluids, such as cement grout, through the fractures. Bingham fluids have visco-plastic properties and require a yield stress to initiate flow.

ABAQUS has interface elements that are coupled with either temperature or pore pressure. These are the same contact elements used in mechanical analysis, with either temperature or pore pressure as additional nodal degrees of freedom. The pore fluid can flow across and tangential to the interface. In other words, fluid inside the fracture can flow to the matrix, and fluid in the matrix can flow into the fracture network.

3.1.5 Modeling of Phase Change of Fluid

Neither ABAQUS nor UDEC at present can model any phase change of the fluid in the modeled region due to the imposed temperature distribution. The effect of temperature on vaporization of the groundwater and condensation of the vapor and subsequent flow through fractures cannot be modeled at present. It is recognized that these equations will be highly nonlinear, and the equation solvers currently used in ABAQUS may be inadequate to handle such severe nonlinearity. A new equation solver that can handle these nonlinear equations may be necessary. This could create a substantial amount of work.

3.1.6 Simulation of Rock Joint

The joint element in the CDCs should be able to model the normal and the shear deformations of the joints in the rock mass. To account properly for the deformations, a joint element should have two features: (i) the ability to incorporate the normal and shear stiffnesses of the joint; and (ii) constitutive laws describing the relations among the shear stress, dilation, normal stress, and shear displacement, taking into account the roughness of the joint.

The rock joint models in the UDEC code (Version 1.83) take both normal and shear stiffnesses directly into formulation. It should be noted that the rock joint model mentioned here describes the behavior of a single joint. Three constitutive laws for rock joint model simulation have been included in the code: Mohr-Coulomb, Continuously-Yielding, and Barton-Bandis.

In ABAQUS Version 5.2, rock joint behavior is simulated by Amonton's law (Jaeger and Cook, 1979). The shear stiffness required for rock joint simulation in the code is determined indirectly using a user-specified maximum elastic displacement and the limiting shear stress. Although there is no

provision for directly incorporating the normal stiffness, an indirect method is available. A fictitious spring element can be added in the normal direction, which always moves with the crack surfaces and remains normal to the surface to which it is attached. A contact stiffness can be prescribed to this spring. There are two types of joint elements currently available in the ABAQUS code: interface and slideline. Both interface and slideline elements can handle shear displacement. No fracture flow capability is available in the current slideline element formulation. Substantial effort is going to be required to add this option. The interface element, on the other hand, is coupled with fluid flow through the fracture in the ABAQUS formulation and, therefore, is more desirable than the slideline element. Consequently, the assessment of the capability of rock joint simulation in ABAQUS in the rest of this report is primarily based on the interface element.

It has been observed in the Seismic Rock Mechanics research project (Hsiung et al., 1993b) that the conceptual rock joint models included in both the UDEC and ABAQUS codes are inadequate in predicting the shear strength and dilation during shear reversal. Therefore, it is necessary to develop a new constitutive model for rock joint and incorporate this model into both UDEC and ABAQUS to replace the current rock joint models of these two codes.

3.1.7 Modeling of Rock Joint Network

The capability for explicitly simulating rock joint networks (rock mass response with intersecting joints) is a must for the CDCs to be selected to assess short- and long-term excavation stability and to estimate the potential for creating preferential pathways and near-field hydraulic properties, since the proposed repository is located in a jointed rock mass. Due to its unique formulation, the UDEC code can model a network with a large number of joints. The code, in its present form, limits joint input to ten different material property sets. However, only minor modifications to the code are needed in order for it to accept more than ten joint property sets.

The interface element in the ABAQUS code is judged to be incapable of handling joint networks, since a mechanism is not in place for a rock block at one quadrant of two intersecting joints to recognize the existence of the rock block at the opposite quadrant. As a result, the former block can penetrate the latter block with no stress building up in either block. Appendix A is a detailed discussion on the analysis of ABAQUS joint network modeling capability. This deficiency readily disqualifies the ABAQUS code for modeling the short- and long-term stability problems related to excavations (including emplacement drifts and emplacement boreholes) where pattern of the rock joint network has great impact.

3.1.8 Modeling of Excavation

Both ABAQUS and UDEC can simulate the excavation process in rock engineering problems. In UDEC, the null material model needs to be used to model the excavation sequence. ABAQUS uses element birth and death options.

3.1.9 Simulation of *In Situ* Stress Field

Both ABAQUS and UDEC have capabilities to simulate *in situ* stress fields. The ABAQUS code uses the GEOSTRESS command to incorporate this stress field as an initial condition into the model and the UDEC code uses the *IN SITU* command.

3.1.10 Modeling of Infinite Region

ABAQUS provides infinite elements to model the absorbing boundary. These elements are used in conjunction with the regular finite elements that model the region of interest with the infinite elements modeling the far-field region. Infinite elements (both 2D and 3D) are available for static uncoupled stress analysis and coupled stress-pore fluid pressure analysis. In dynamic analysis, the infinite elements have additional normal and shear tractions on the finite-element boundary that are proportional to normal and shear components of the plane wave velocity at the boundary. Boundary damping constants are selected automatically to minimize the reflection of dilation (P) and shear (S) wave energies back into the modeled region. The infinite elements transmit all the normally impinging plane body wave energy, provided the material behaves elastically at the boundary. These elements also work quite well in cases involving nonplanar body waves, Rayleigh surface waves, and Love waves, provided that they are arranged so that the dominant propagation direction is orthogonal to the surface. The infinite elements should be placed at some reasonable distance from the region of interest to avoid distortion of stress and displacement field within the area of interest by the infinite stiffness of infinite elements.

In UDEC, the nonreflecting or viscous boundaries are part of the boundary conditions to be applied. These boundaries provide viscous normal and shear tractions to the boundaries proportional to the P and S wave velocities, respectively. These tractions are calculated and applied to grid points at every timestep in the same way as the boundary loads. Since viscous forces are calculated from velocities lagging by half a timestep, there is a remote potential for numerical instability.

3.1.11 Two- Versus Three-Dimensional Modeling

For many problems in rock engineering, it may be sufficient to model along one or more sections of the region to develop an overall understanding of the response of the system, assuming plane strain or plane stress conditions. As a result, 2D modeling of the problem is acceptable. On the other hand, there are many problems that are not amenable to 2D idealization. Presence of rock joints with flow of fluid through them makes some problems truly 3D. ABAQUS has both 2D and 3D analysis capabilities, whereas UDEC can analyze only 2D problems. The companion code 3DEC can address 3D problems.

3.1.12 Modeling of Material Constitutive Laws

Both ABAQUS and UDEC have several material constitutive models to describe the material response under applied load. For example, UDEC has null, isotropic elastic, Drucker-Prager plasticity, ubiquitous joint, double-yield, and strain hardening/softening models. An excavated region can be modeled by changing the material constitutive law to a null model. Backfilling can be modeled by changing the material from null to an appropriate one. At present, all the material models are independent of temperature.

Both mechanical and thermal properties used in UDEC are invariant of temperature. The temperature-dependent material properties option could be incorporated into UDEC with a small amount of effort.

ABAQUS has a large library of material models for different material behaviors:

- purely elastic response

- viscoelastic response due to some energy dissipation during rapid loading

- yielding with considerable ductility beyond the yield point

- particle flow with some dominant frictional mechanism

- brittle materials (rocks, concrete, ceramics)

An equivalent continuum material model containing a high density of parallel joints in different orientations (JOINTC) is also available. The model provides for opening of the joints and frictional sliding in each of these systems. Under compressive stress, the joints can slide following the Coulomb criterion. Bulk failure of the medium is based on the Drucker-Prager failure criterion. ABAQUS has a user subroutine, UMAT, to incorporate any user-defined material model.

The material property definition in ABAQUS can be dependent on any state variable, such as temperature and degree of saturation. Young's modulus, Poisson's ratio, shear modulus, material stiffnesses, thermal conductivity, coefficient of thermal expansion, etc., can be described as a function of temperature and degrees of saturation. This information can be provided in a tabular form with data at several discrete points. Linear interpolation is carried out for material properties between two given data points. Alternatively, this information may be supplied with the user-defined material property subroutine UMAT.

3.2 COMPARISON OF ABAQUS AND UDEC CODES

Preliminary comparison between the ABAQUS and UDEC codes for their capabilities to model different coupled interactions among TMH processes was carried out in Phase I of this study (Ghosh et al., 1993). That comparison was based on the published information given in different users' manuals and is reproduced in Appendix B.

A further comparison of the ABAQUS and UDEC codes on their capabilities for assessing the design and performance of a HLW repository at the proposed YM site is provided in Table 3-1. Table 3-1 clearly indicates the differences between the ABAQUS and UDEC codes. The ABAQUS code appears to have more capabilities than the UDEC code in dealing with coupled TMH effects, especially in the area of modeling unsaturated conditions. ABAQUS has several features that are useful in modeling various coupled phenomena associated with the proposed HLW repository at YM. For example, ABAQUS can model the porous rock as a multiphase material and can model the unsaturated flow of fluid through it. The wetting fluid is assumed to be relatively incompressible. Generally the other fluid is gas/vapor that is compressible. The mechanical behavior of the porous medium as calculated in ABAQUS is the combined response of the liquid and solid materials to local pressure and of the overall response of the material to the effective stress.

Furthermore, ABAQUS has the interface element that can model the behavior of an interface between two blocks quite well. The fluid flow capability is coupled with the mechanical analysis. Fluid flow into the fracture from the rock matrix and from the fracture into the rock matrix can be modeled by ABAQUS.

Table 3-1. Capability comparison of ABAQUS and UDEC

Evaluation Criteria	UDEC (Version 1.83)	ABAQUS (Version 5.2)
Simulation of Thermal and Seismic Loading Time Histories	✓	✓
Modeling of Heat Conduction and Thermal Stress Field	✓	✓
Modeling of Poroelastic Medium*	X	✓
Modeling of Mechanical Effect Dependent Fluid Flow Through Fracture	✓	✓
Modeling of Phase Change of Fluid	X	X
Simulation of Rock Joint	✓	✓
Modeling of Rock Joint Network	✓	X
Modeling of Infinite Region	✓	✓
Modeling of Material Constitutive Models	✓†	✓
Simulation of *In Situ* Stress Field	✓	✓
Modeling 2D versus 3D Geometry	2D‡	2D and 3D
Modeling of Excavation	✓	✓
✓ Denotes that the code has the capability		
X Denotes that the code does not have the capability		
2D, 3D Two-dimensional and three-dimensional		
* Does not include change of permeability due to progressive damage of rock		
† UDEC (Version 1.83) cannot simulate thermal and saturation dependent material properties of the medium		
‡ Companion code 3DEC provides 3D capability		

However, ABAQUS has a serious shortcoming. The interface element in the ABAQUS code is judged to be incapable of handling rock joint networks, since one interface element does not recognize the existence of other nearby interface elements. As a result, a rock block at one quadrant of two intersecting joints can penetrate the rock block at the opposite quadrant without developing any stress in either block. This shortcoming readily disqualifies ABAQUS for modeling the short- and long-term stability problems related to excavations (including emplacement drifts and boreholes) where substantial shear displacement along some joints is possible. Furthermore, ABAQUS has been subjected to only a very limited amount of qualification study only on mechanical responses. All of its other capabilities are

based on reported information and are in need of qualification study before ABAQUS can be considered for selection to be modified for use as a CDC.

On the other hand, UDEC has capabilities of effectively modeling the joint network. The code can model relatively large shear displacements along the block interfaces with proper redistribution of resulting stresses. Therefore, this code is most suited for analyzing problems in the near field of the waste emplacement where large shear displacements of joints are likely and the pattern of joint network has great impact on the response of excavations, including stability. However, UDEC treats the medium as impermeable and can only model the flow of fluid through the joints or interfaces.

It is clear that neither of the two codes can acceptably model all the coupled TMH processes expected in the proposed HLW repository at YM. It will be impractical and not cost-effective to develop UDEC to a state so that it can handle unsaturated fluid flow like ABAQUS does. On the other hand, with the present state-of-the-art in finite-element technology[3], it is not possible to incorporate the joint network modeling capabilities in ABAQUS, although it has a very powerful capability of modeling unsaturated flow through a porous medium, which is an essential element in assessing the performance of a repository.

As discussed in Chapter 2, two main issues that involve mechanical effect are recognized to be associated with the near-field environment of the HLW repository. Recognizing the difficulties of upgrading either code and that each code has its distinct capabilities, an alternative approach that takes advantage of the strong features of each code is considered herein.

The UDEC code is proposed to be used to analyze static and dynamic problems where stability of the underground excavations (emplacement boreholes and drifts) is of main concern. As discussed in Chapter 2, some problems in connection with the HLW repository at YM are truly 3D and are not amenable to 2D idealization. To address these types of problems, adoption of the 3DEC code (ITASCA Consulting Group, Inc., 1992c,d) in addition to UDEC is suggested. The 3DEC code is essentially a 3D version of the UDEC code. The capabilities of these two codes are similar in the context of TM analysis. Furthermore, 3DEC has undergone a qualification study similar to that of UDEC in the Seismic Rock Mechanics research project, and it has been used for the pretest modeling of the dynamic direct shear test of a single jointed Apache Leap tuff specimen (Hsiung and Chowdhury, 1991, 1993). In solving the stability problems associated with underground excavations, the coupled TM effects (including earthquakes) will be considered, with an approximate consideration for the effect of presence of water in the joints on the stability of underground openings.

For the problems associated with the second issue, that is, unsaturated coupled TMH analysis, it is neither practical nor cost-effective to modify only UDEC/3DEC or ABAQUS for use as CDCs. Instead, a practical approach is to evaluate the unsaturated coupled TMH analysis capabilities of ABAQUS and the possibility of its utilization to provide estimates of the changes in permeability with time and space so that they can be taken into account in subsequent near-field PA and total system PA calculations. ABAQUS will also be used to verify the various assumptions relevant to mechanical-effect-dependent fluid flow that the available hydrological codes will make in the near-field PA and total system PA calculations. ABAQUS cannot model the phase change of fluid. The issue of phase change of water to vapor and vice versa in TMH coupling will be considered during evaluation of ABAQUS.

---

[3]Personal communication with Hibbitt, Karlsson & Sorensen, Inc., Pawtucket, Rhode Island, 1993.

4 PROPOSED SCOPE OF MODIFICATIONS OF THE SELECTED CODES

As discussed in Chapter 3, two codes, UDEC and its 3D version, 3DEC, have been selected to analyze stability problems of underground excavations, including emplacement drifts and boreholes of the proposed HLW repository at YM. UDEC and 3DEC have undergone qualification studies at the CNWRA to verify their capabilities to model stability problems of the excavations. The scope of modification work that will be necessary so that these codes can be used for TM coupled analysis associated with excavation stability problems is discussed in Section 4.1. Evaluations of both ABAQUS and UDEC show that neither of these codes is capable of simulating all of the important phenomena associated with TMH coupling in the near field of YM, although ABAQUS has several features that are better suited for analyzing TMH problems. Only the mechanical capabilities of ABAQUS have been verified herein (Appendix A). The reported capabilities of ABAQUS to model several aspects of TMH coupled phenomena need to be verified by analyzing several benchmark problems involving TM, MH, TH, and TMH processes. The scope of verification work that will be necessary so that ABAQUS could be used for TMH coupled analysis is described in Section 4.2. The scope of work described herein is considered to be adequate with the present state of knowledge about these codes. If future work with these codes identifies other deficiencies, this scope will need to be updated.

4.1 MODIFICATIONS FOR UDEC/3DEC

4.1.1 Rock Joint Constitutive Model

As discussed in Chapter 3, the rock joint constitutive models available in 3DEC and UDEC do not accurately predict shear strength and dilation during cyclic pseudostatic and dynamic loads that were reported by Hsiung et al. (1993a), Wibowo et al. (1992), Huang et al. (1993), and Jing et al. (1992). These rock joint models were developed based on data taken under unidirectional pseudostatic loading conditions. The results of the direct shear tests on the Apache Leap tuff joints have indicated that under cyclic pseudostatic and dynamic loadings, the shear resistance upon reverse shearing is smaller than that of forward shearing, and the joint dilation resulting from forward shearing recovers during reverse shearing. Reverse shearing can result from earthquake, thermal loading, or both. Failure to consider this aspect of joint behavior in an underground structural design and performance analysis could result in (i) an overestimation of the stability of emplacement drifts and emplacement boreholes and (ii) prediction of an incorrect pattern of near-field flow (including preferential pathways for water and gas). It is therefore necessary to develop a new rock joint constitutive model. The development of this model is already in progress using the experimental results of the Seismic Rock Mechanics research project. This rock joint model will be incorporated in the selected codes.

4.1.2 Other Modifications

The other modifications of CDCs include the incorporation of temperature and saturation-dependent material properties in UDEC and 3DEC. If the future work with these codes identifies the need for other options, the options will need to be incorporated as applicable.

4.2 EVALUATION OF ABAQUS FOR THERMAL MECHANICAL HYDROLOGICAL MODELING CAPABILITIES

The primary objective of the coupled TMH code is to provide a definition of the changes in the permeability field resulting from TM processes. This input will be provided for use in near-field flow codes utilized for subsystem PA. In addition, the TMH processes will be abstracted for use in the total-system PA code. The TMH code will also be used to verify the various assumptions relevant to mechanical-effect-dependent fluid flow that the available hydrological codes will make in the near-field PA and total system PA calculations. It should be noted that the capabilities identified in the ABAQUS code for modeling the TMH phenomena associated with the near field of the proposed HLW repository are based on reported information. Consequently, their validity has not been tested. Therefore, further evaluation of these capabilities is proposed. This evaluation is to confirm that ABAQUS can reproduce the response of benchmark and test case problems of the performance of a jointed rock mass under coupled TM, MH, TH, and TMH conditions. One or two benchmark/test case problems for each coupled condition mentioned above will be analyzed using ABAQUS. Two test case problems have been selected and the development of other benchmark/test case problems are in progress at the CNWRA. The selected test case problems are: (i) coupled MH experiment of single rock joint specimen under unsaturated condition being conducted at the CNWRA, and (ii) coupled TMH experiment of the Power Reactor and Nuclear Fuel Development Corporation (PNC) of Japan.

The MH experiment being conducted at the CNWRA under the Seismic Rock Mechanics research project is designed to study the mechanical effect on the unsaturated fracture flow through a single-joint rock specimen. The natural joint welded tuff specimens have been collected from Apache Leap, Arizona. Detailed specifications of this problem are given by Hsiung et al. (1993c). The TMH experiment, called BIG-BEN, simulated one disposal pit. It was composed of an electric heater, a carbon steel overpack, buffer material, and cylindrical reinforced concrete block with a hole at the center. The concrete block had an outside diameter of 6 m and was 5 m in height. The hole was approximately 1.7 m in diameter and 4.5 m in depth. An electric heater with three cartridge heaters was set in the overpack, which was about 1 m in diameter and about 2 m in height. Sensors to monitor temperature, heat flux, water content, displacement of overpack, swelling pressure, and stress were installed in the buffer material and the concrete block. Detailed specifications of the BIG-BEN experiment are given in DECOVALEX (1993).

The modeling results from ABAQUS for the various coupled conditions will be compared, whenever possible, to either the modeling results of other computer codes with similar capabilities or the corresponding experimental results. After the confirmation of the reported capabilities of the ABAQUS code is completed, a sensitivity analysis on the various coupled processes will be performed to the extent that the associated models in the ABAQUS code permit.

5 SUMMARY AND CONCLUSIONS

The objective of the code selection study was to select a computer code that can be used by the NRC and the CNWRA, with appropriate modifications, for determining DOE compliance with NRC regulations on thermal loads. In Phase I, the 3D finite-element code ABAQUS and the 2D distinct-element code UDEC were selected for further evaluation. In Phase II, two issues associated with the near field of the proposed HLW repository at YM were identified: (i) stability problems of underground excavations (coupled TM processes), and (ii) mechanical-effect-dependent hydrological properties determination and fluid flow calculation resulting from vaporization of water, recondensation of vapor, and condensate dripping through the potential preferential pathways (coupled TMH processes). A list of features that were considered necessary for a code to adequately model different coupled phenomena associated with both issues was developed.

ABAQUS and UDEC were evaluated against this list of features based on the information reported in respective user's manuals (Hibbitt, Karlsson & Sorensen, Inc., 1992a,b,c; ITASCA Consulting Group, Inc., 1992a,b) and the experience gained in modeling several benchmark problems. Results from this analysis show that ABAQUS can model rough fractures as well as UDEC does, but it cannot model rock joint networks, especially when the expected shear displacements along different joints are large. As large shear displacements are expected along different joints, especially under thermal and seismic loads, ABAQUS is not suitable for near-field stability analysis. On the other hand, UDEC can model joint network effectively and has the capability to model mechanical-effect-dependent fracture flow. Therefore, UDEC is suitable for problems associated with stability of the excavations. It is recognized that many problems relevant to the HLW repository are truly 3D. Therefore, the use of 3DEC code, which is essentially a 3D version of UDEC, in addition to UDEC appears to be necessary.

Neither ABAQUS nor UDEC/3DEC can adequately model all the important coupled TMH processes at the near field of the proposed repository. It is not practical with the present state-of-the-art in finite-element method to modify ABAQUS to incorporate joint network modeling capabilities. Similarly, it is not practical to incorporate unsaturated matrix flow in UDEC and 3DEC. As a result, an alternative approach that takes advantage of the best features of each code for analyzing the concerns mentioned earlier may be necessary. It was decided that both 3DEC and UDEC will be used in underground excavation stability problems where coupled TM effects, including earthquakes and nearby nuclear explosions, are important. However, several aspects of these codes need to be modified before they can analyze the problems adequately. The rock joint constitutive models available in UDEC and 3DEC are inadequate in predicting the shear strength and dilation during cyclic pseudostatic and dynamic loads. A new model is under development at the CNWRA using the results from the Seismic Rock Mechanics research project. This new model will be incorporated into these codes. ABAQUS, on the other hand, may be used in problems where mechanical-effect-dependent unsaturated fluid flow, vaporization of water, recondensation of the vapor, and condensate dripping through the potential preferential pathways need to be modeled. It should be noted that the primary objective of the coupled TMH modeling is to provide estimates of the changes in permeability with time and space so that they can be taken into account in subsystem near-field PA and total system PA calculations. ABAQUS will also be used to verify the various assumptions relevant to mechanical-effect-dependent fluid flow that the available hydrological codes will make in the near-field PA and total system PA calculations. However, it should be noted that the capabilities identified in the ABAQUS code, that are suitable for the coupled TMH analysis relevant to the proposed HLW repository at YM, are based on reported information. Further assessment of the ABAQUS code is recommended to confirm these capabilities before it can be recommended for modeling

the problems involving TMH phenomena. Development of relevant benchmark problems is currently under way at the CNWRA. Results from laboratory coupled TMH experiments, currently undertaken in the Seismic Rock Mechanics research project, will be used for this verification process. To the extent practical, some benchmark problems and test cases from the DECOVALEX program will be used for the ABAQUS evaluation.

6 REFERENCES

Ahola, M.P., S.M. Hsiung, L.J. Lorig, and A.H. Chowdhury. 1992. *Thermo-Hydro-Mechanical Coupled Modeling: Multiple Fracture Model, BMT2; Coupled Stress-Flow Model, TC1. DECOVALEX — Phase I.* CNWRA 92-005. San Antonio, TX: Center for Nuclear Waste Regulatory Analyses.

Ahola, M.P., L.J. Lorig, A.H. Chowdhury, and S.M. Hsiung. 1993. *Thermo-Hydro-Mechanical Coupled Modeling: Near-Field Repository Model, BMT3. DECOVALEX — Phase II.* CNWRA 93-002. San Antonio, TX: Center for Nuclear Waste Regulatory Analyses.

Barton, N.R, S. Bandis, and K. Bakhtar. 1985. Strength, deformation and conductivity coupling of rock joints. *International Journal of Rock Mechanics and Mining Sciences & Geomechanics Abstracts* 22(3): 121-140.

Biot, M.A. 1955. Theory of elasticity and consolidation for a porous anisotropic solid. *Journal of Applied Physics* 26(2): 182-185.

Brady, B.H.G., S.M. Hsiung, and A.H. Chowdhury. 1990. *Qualification Studies on the Distinct Element Code UDEC Against Some Benchmark Analytical Problems.* CNWRA 90-004. San Antonio, TX: Center for Nuclear Waste Regulatory Analyses.

Buscheck, T.A., and J.J. Nitao. 1993. The analysis of repository-heat-driven hydrothermal flow at Yucca Mountain. *Proceedings of the 4th High-Level Radioactive Waste Management Conference.* New York, NY: American Society of Civil Engineers.

Buscheck, T.A., D.G. Wilder, and J.J. Nitao. 1993. Large-scale *in situ* heater tests for hydrothermal characterization at Yucca Mountain. *Proceedings of the 4th High-Level Radioactive Waste Management Conference.* New York, NY: American Society of Civil Engineers.

Christianson, M.C. 1988. *Sensitivity of the Stability of a Waste Emplacement Drift to Variation in Assumed Rock Joint Parameters in Welded Tuff.* NUREG/CR-5336. Washington, DC: U.S. Nuclear Regulatory Commission.

Christianson, M.C., and B.H.G. Brady. 1989. *Analysis of Alternative Waste Isolation Concepts.* NUREG/CR-5389. Washington, DC: U.S. Nuclear Regulatory Commission.

Crowley, B.K. 1973. Effects of porosity and saturation on shock-wave response in tuffs. *International Journal of Rock Mechanics and Mining Sciences & Geomechanics Abstracts* 10: 437-464.

DECOVALEX. 1993. *Phase 3, Test Case 3, BIG BEN.* DECOVALEX Doc 93-124. DECOVALEX Secretariat. Stockholm, Sweden: Royal Institute of Technology.

Ghosh, A. 1990. *Fractal and Numerical Models of Explosive Rock Fragmentation.* Ph.D. Dissertation. Tucson, AZ: University of Arizona.

Ghosh, A., S.M. Hsiung, M.P. Ahola, and A.H. Chowdhury. 1993. *Evaluation of Coupled Computer Codes for Compliance Determination.* CNWRA 93-005. San Antonio, TX: Center for Nuclear Waste Regulatory Analyses.

Goodman, R.E. 1980. *Introduction to Rock Mechanics.* New York, NY: John Wiley & Sons.

Hibbitt, Karlsson & Sorensen, Inc. 1992a. *ABAQUS Theory Manual Version 5.2.* Pawtucket, RI: Hibbitt, Karlsson & Sorensen, Inc.

Hibbitt, Karlsson & Sorensen, Inc. 1992b. *ABAQUS/Standard User's I Manual Version 5.2.* Pawtucket, RI: Hibbitt, Karlsson & Sorensen, Inc.

Hibbitt, Karlsson & Sorensen, Inc. 1992c. *ABAQUS/Standard User's II Manual Version 5.2.* Pawtucket, RI: Hibbitt, Karlsson & Sorensen, Inc.

Hill, D.P., et al. 1993. Seismicity remotely triggered by the magnitude 7.3 Landers, California, earthquake. *Science* 260: 1617-1623.

Hoek, E., and E.T. Brown. 1980. *Underground Excavations in Rock.* London, UK: The Institution of Mining and Metallurgy.

Hofmann, R.B. 1993. *Summary of the May 17-18, 1993, CNWRA Advisors Meeting and Reports on Fault Displacement and Seismic Hazard Analysis.* CNWRA Report to the Nuclear Regulatory Commission. San Antonio, TX: Center for Nuclear Waste Regulatory Analyses.

Hsiung, S.M., and A.H. Chowdhury. 1991. *Seismic Rock Mechanics. Report on Research Activities for Calendar Year 1990.* W.C. Patrick, ed. NUREG/CR-5718. Washington, DC: U.S. Nuclear Regulatory Commission.

Hsiung, S.M., and A.H. Chowdhury. 1993. *Seismic Rock Mechanics. NRC High-Level Radioactive Waste Research at CNWRA Calendar Year 1991.* W.C. Patrick, ed. NUREG/CR-5817. Washington, DC: U.S. Nuclear Regulatory Commission.

Hsiung, S.M., D.D. Kana, M.P. Ahola, A.H. Chowdhury, and A. Ghosh. 1993a. *Laboratory Characterization of Rock Joints.* CNWRA 93-013. San Antonio, TX: Center for Nuclear Waste Regulatory Analyses.

Hsiung, S.M., A. Ghosh, A.H. Chowdhury, and M.P. Ahola. 1993b. *Evaluation of Rock Joint Models and Computer Code UDEC Against Experimental Results.* CNWRA 93-024. San Antonio, TX: Center for Nuclear Waste Regulatory Analyses.

Hsiung, S.M., A.H. Chowdhury, M.P. Ahola, and S. Mohanty. 1993c. *Project Plan for Seismic Rock Mechanics Project.* Revision 4, Change 1. San Antonio, TX: Center for Nuclear Waste Regulatory Analyses.

Huang, X., B.C. Haimson, M.E. Plesha, and X. Qiu. 1993. An investigation of the mechanics of rock joints—Part I. laboratory investigation. *International Journal of Rock Mechanics and Mining Sciences & Geomechanics Abstracts* 30(3): 257-269.

International Society for Rock Mechanics. 1978. Suggested methods for the qualitative description of discontinuities in rock masses. Commission on standardization of laboratory and field tests. *International Journal of Rock Mechanics and Mining Sciences & Geomechanics Abstracts* 15: 319-368.

ITASCA Consulting Group, Inc. 1992a. *UDEC Universal Distinct Element Code Version 1.8 Volume I: User's Manual*. Minneapolis, MN: ITASCA Consulting Group, Inc.

ITASCA Consulting Group, Inc. 1992b. *UDEC Universal Distinct Element Code Version 1.8 Volume II: Verification and Example Problems Manual*. Minneapolis, MN: ITASCA Consulting Group, Inc.

ITASCA Consulting Group, Inc. 1992c. *3DEC Three Dimensional Distinct Element Code Version 1.2 Volume I: User's Manual*. Minneapolis, MN: ITASCA Consulting Group, Inc.

ITASCA Consulting Group, Inc. 1992d. *3DEC Three Dimensional Distinct Element Code Version 1.2 Volume II: Verification and Example Problem Manual*. Minneapolis, MN: ITASCA Consulting Group, Inc.

Jaeger, J.C., and N.G.W. Cook. 1979. *Fundamentals of Rock Mechanics*. 3rd Edition. London, UK: Chapman and Hall, Ltd.

Jing, L., E. Nordlund, and O. Stephansson. 1992. An experimental study on the anisotropy and stress-dependency of the strength and deformability of rock joints. *International Journal of Rock Mechanics and Mining Sciences & Geomechanics Abstracts* 29(6): 535-542.

Kana, D.D., B.H.G. Brady, B.W. Vanzant, and P.K. Nair. 1991. *Critical Assessment of Seismic and Geomechanics Literature Related to a High-Level Nuclear Waste Underground Repository*. NUREG/CR-5440. Washington, DC: U.S. Nuclear Regulatory Commission.

Kemeny, J.M., and N.G.W. Cook. 1990. *Rock Mechanics and Crusted Stresses. Demonstration of a Risk-Based Approach to High-Level Waste Repository Evaluation*. EPRI-NP-7507. Palo Alto, CA: Electric Power Research Institute.

Klavetter, E.A., and R.R. Peters. 1986. *Estimation of Hydrologic Properties of an Unsaturated Fracture Rock Mass*. SAND84-2642. Albuquerque, NM: Sandia National Laboratories.

Lin, W., and W.D. Daily. 1989. Laboratory study of fracture healing in Topopah Spring tuff — implications for near field hydrology. *Nuclear Waste Isolation in Unsaturated Zone Focus '89 Proceedings*. La Grange Park, IL: American Nuclear Society: 443-449.

Makurat, A. 1985. *The Effect of Shear Displacement of the Permeability of Natural Rough Joints*. Memoirs of International Association of Hydrogeologist, XVII(1): 99-106.

Makurat, A., N. Barton, G. Vik, P. Chryssanthakis, and K. Monsen. 1990a. Jointed rock mass modeling. *Proceedings of the International Conference on Rock Joints*. N. Barton and O. Stephansson, eds. Leon, Norway: 647-656.

Makurat, A., N. Barton, and N.S. Rad. 1990b. Joint conductivity variation due to normal and shear deformation. *Proceedings of the International Conference on Rock Joints*. N. Barton and O. Stephansson, eds. Loen, Norway: 535-540.

Manteufel, R.D., M.P. Ahola, D.R. Turner, and A.H. Chowdhury. 1993. *A Literature Review of Coupled Thermal-Hydrologic-Mechanical-Chemical Processes Pertinent to the Proposed High-Level Nuclear Waste Repository at Yucca Mountain*. NUREG/CR-6021. Washington, DC: U.S. Nuclear Regulatory Commission.

Nataraja, M.S., and T. Brandshaug. 1992. *Staff Technical Position on Geologic Repository Operations Area Underground Facility Design — Thermal Loads*. NUREG-1466. Washington, DC: U.S. Nuclear Regulatory Commission.

Nimick, F.B., and J.R. Connolly. 1991. *Calculation of Heat Capacities for Tuffaceous Units from the Unsaturated Zone at Yucca Mountain, Nevada*. SAND 88-3050. Albuquerque, NM: Sandia National Laboratories.

Price, J.G., S.T. Conlon, and C.D. Henry. 1987. Tectonic controls on orientation and size of epithermal veins. *North American Conference on Tectonic Control of Ore Deposits*. Rolla, MO: University of Missouri: 36-46.

Raney, R.G. 1988. *Reported Effects of Selected Earthquakes in the Western North American Intermontane Region 1852-1983, on Underground Workings and Local and Regional Hydrology: A Summary*. Spokane, WA: U.S. Bureau of Mines Report.

Rasmussen, T.C., D.D. Evans, P.J. Sheets, and J.H. Blanford. 1990. *Unsaturated Fractured Rock Characterization Methods and Data Sets at the Apache Leap Tuff Site*. NUREG/CR-5996. Washington, DC: U.S. Nuclear Regulatory Commission.

Sagar B., and R. Janetzke. 1993. *Total System Performance Assessment Computer Code: Description of Executive Module (Version 2.0)*. CNWRA 91-009. San Antonio, TX: Center for Nuclear Waste Regulatory Analyses.

Sagar B., R.B. Codell, J. Walton, and R. Janetzke. 1992. *SOTEC: A Source Team Code for High-Level Geologic Repositories — User's Manual (Version 1.0)*. CNWRA 92-009. San Antonio, TX: Center for Nuclear Waste Regulatory Analyses.

Sridhar, N., J.C. Walton, G.A. Cragnolino, and P.K. Nair. 1993. *Engineered Barrier System Performance Assessment Codes (EBSPAC) Progress Report — October 1, 1992 through September 25, 1993*. CNWRA 93-021. San Antonio, TX: Center for Nuclear Waste Regulatory Analyses.

Tsang, C.F. 1990. Coupled behavior of rock joints. *Proceedings of the International Conference on Rock Joints*. N. Barton and O. Stephansson, eds. Loen, Norway: 505-518.

Tsang, C.F. 1991. Coupled hydromechanical - thermochemical process in rock fractures. *Reviews of Geophysics* 29(4): 537-551.

U.S. Department of Energy. 1988. *Site Characterization Plan: Yucca Mountain Site, Nevada Research and Development Area*. DOE/RW-0199. Washington, DC: U.S. Department of Energy.

U.S. Nuclear Regulatory Commission. 1992. *Disposal of High-Level Radioactive Wastes in Geologic Repositories*. Title 10, Energy, Part 60 (10 CFR Part 60). Washington, DC: Office of Federal Register.

Wibowo, J.T., B. Amadei, S. Sture, and A.B. Robertson. 1992. Shear response of a rock joint under different boundary conditions: An experimental study. *Conference on Fractured and Jointed Rock Masses*. Preprint. June 3-5, 1992. Lake Tahoe, CA.

APPENDIX A

EVALUATION OF ABAQUS AND UDEC COMPUTER CODES

A. EVALUATION OF ABAQUS AND UDEC COMPUTER CODES

Both ABAQUS and UDEC were used to analyze exactly the same benchmark problems in the mechanics of discontinuous rock. UDEC had been subjected to this qualification study before (Brady et al., 1990), and most of the problems from that qualification study were used in this study to analyze the capabilities of ABAQUS. It should be recognized that ABAQUS is a finite-element program and UDEC is a discrete-element program. Available features of ABAQUS were used to simulate each problem as close to the UDEC formulation as possible, except the solution scheme. ABAQUS analyses used an implicit solution scheme whereas UDEC analyses used an explicit solution scheme. In this appendix, the results from both ABAQUS and UDEC are compared for each problem.

A.1 PROBLEM 1: CYCLIC LOADING OF A SPECIMEN WITH AN EMBEDDED SLIPPING CRACK

A rectangular elastic rock block is embedded with a closed crack inclined at an angle to the direction of loading (Figure A-1). The bottom of the block is fixed. A constant uniaxial compressive stress is applied at the top of the block, causing inelastic slip of the crack surfaces. At some point, the applied stress is gradually released until the original configuration is re-established.

The rock is assumed to be linearly elastic, homogeneous, and isotropic. The conceptual model for this problem is illustrated in Figure A-2. The elasticity of the intact rock specimen is represented in terms of the spring with stiffness, k. Intact rock at the ends of the crack resists displacement parallel to the plane of the crack. This has been represented by two similar springs with stiffness, K_s, oriented parallel to the plane of the crack. The stress-displacement relation for the specimen, shown in Figure A-3, is composed of three distinct components (Brady et al., 1985; Olsson, 1982):

- a loading segment, OA, which involves elastic deformation of the intact rock and inelastic slip along the crack

- an initial unloading segment, AB, where the crack does not slip and the measured deformation is truly elastic deformation of the rock

- a final unloading segment, BO, which represents elastic deformation of the rock block and inelastic slip of the joint

When a compressive load is applied at the top of the specimen, the slip along the crack is resisted by the frictional force developed and the tensile force developed at the transgressive springs. The slip will occur if and only if $\tan (90° - \alpha) \leq 1/\tan \phi$ (Olsson, 1982). Total axial compression of the specimen is due to the compression of the equivalent spring (representing deformation of the intact rock) and vertical component of the displacement along the plane of the crack. Therefore, the stiffness of the specimen, represented by the slope of line, OA, in Figure A-3, is less than that from a comparable intact rock specimen.

When an increment of axial load is removed from the specimen, an incremental displacement up the plane of the crack will take place. Frictional force between the crack surfaces again resists the springs to cause slip. The crack will not slip as long as the normal stress across the crack develops sufficient frictional
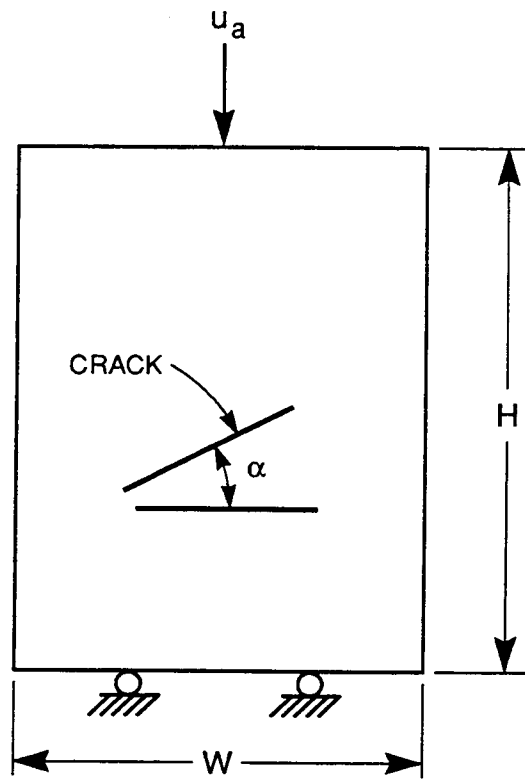
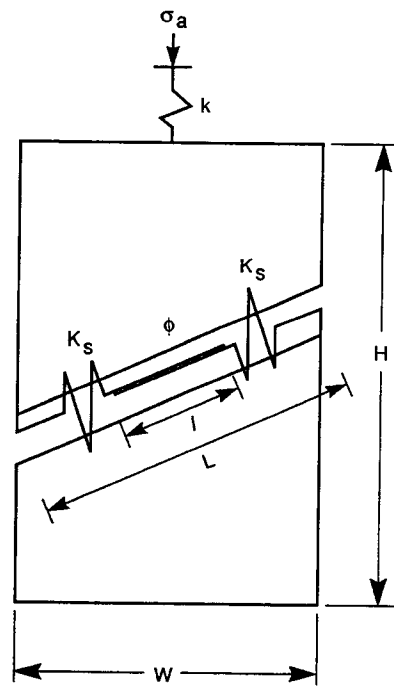**Figure A-1. Rock specimen with an embedded crack**

Figure A-2. Conceptual model of an elastic specimen with an embedded crack (after Brady et al., 1985)
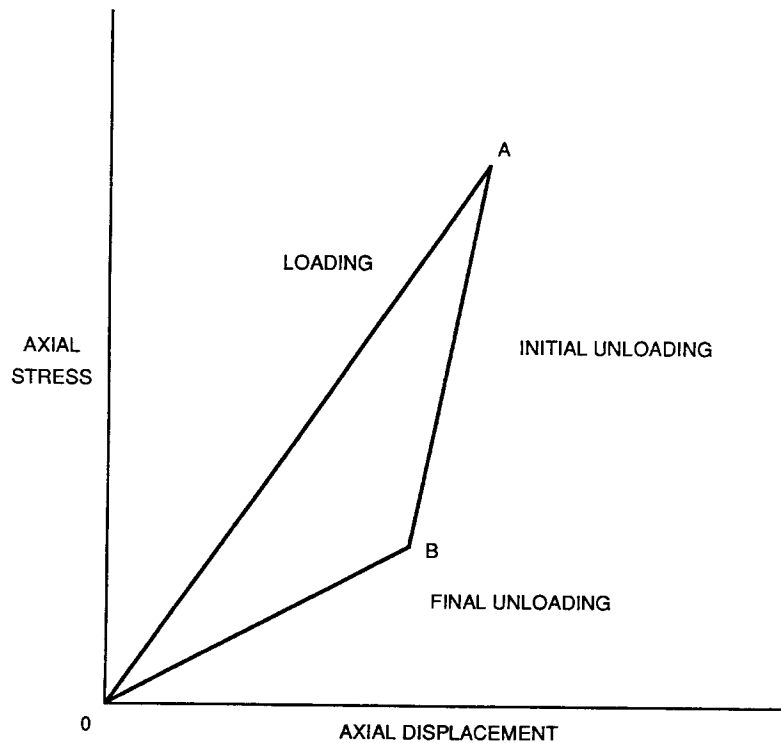
A-2

Figure A-3. Stress-displacement relationship of an elastic specimen with an embedded crack subjected to a uniaxial load cycle (after Olsson, 1982)

force. Thus, initially unloading the specimen will merely produce decompression of the equivalent spring. As a result, the slope of curve, AB, in Figure A-3 gives the true elastic stiffness of the intact rock (Brady et al., 1985).

As the axial load continues to decrease, the component of the force normal to the plane of the crack decreases which, in turn reduces the frictional force. After the critical value of load is reached, the crack surface will slip again. Figure A-3 shows that the load cycle is accompanied by hysteresis.

In the conceptual model, k is the equivalent axial elastic stiffness of the specimen, including the embedded discontinuity. The equivalent elastic stiffness of the specimen, assuming unit thickness and plane stress condition (Brady et al., 1990), is

$$\frac{1}{k} = \frac{H}{WE} + \frac{\cos^2\alpha}{K_n L} + \frac{\sin^2\alpha}{K_s L} \qquad \text{(A-1)}$$

where

$L = W/\cos\alpha$
α = inclination of the crack from horizontal

A-3

In Eq. (A-1), WE/H is the uniaxial elastic stiffness of the intact rock specimen. The second and third terms are the vertical component of the contributions from normal and shear stiffnesses of the crack, respectively. The stiffness of a specimen is represented by the slope of the applied stress versus the deformation curve. Stiffnesses of the specimen in three regions of the loading and unloading cycles are

$$\text{slope OA} = \frac{k}{1 + \dfrac{k \sin \alpha \sin (\alpha - \phi)}{K_s (L - l) \cos \phi}} \qquad \text{(A-2)}$$

$$\text{slope AB} = k \qquad \text{(A-3)}$$

$$\text{slope BO} = \frac{k}{1 + \dfrac{k \sin \alpha \sin (\alpha + \phi)}{K_s (L - l) \cos \phi}} \qquad \text{(A-4)}$$

The mechanical properties of the rock and the embedded crack are given below:

Young's modulus, E = 88.9 GPa
Poisson's ratio, v = 0.26
Joint normal stiffness, K_n = 220 GPa/m
Joint shear stiffness, K_s = 220 GPa/m
Joint friction angle, ϕ = 16°

The geometry of the problem is:

Height, H = 2 m
Width, W = 1 m
Joint inclination, α = 45°
Length of crack, l = 0.54 m

A.1.1 Analytical Solution

The equivalent elastic stiffness, k, of the specimen is k=38.89 GPa/m

Stiffness for the three regions are:

slope OA = 36.28 GPa/m
slope AB = 38.89 GPa/m
slope BO = 34.42 GPa/m

A.1.2 UDEC Solution

In UDEC, a crack must intersect the boundaries of the modeled region. Therefore, a through-going crack has been modeled. The part of the crack that is fictitious is given a high frictional resistance to prevent any slipping (friction angle = 89.4°).

The slipping portion of the crack is given the properties specified in the problem statement. UDEC solves a problem assuming plane stress condition. As a result, equivalent plane strain values of Young's modulus and Poisson's ratio were used in UDEC analysis. The equivalent material properties are

$$E_{UDEC} = E\frac{1 + 2v}{(1 + v)^2} = 88.1 \text{ GPa} \tag{A-5}$$

$$v_{UDEC} = \frac{v}{(1 + v)} = 0.206 \tag{A-6}$$

The specimen is discretized into several constant strain finite difference triangular elements to model the block as deformable. The mesh is shown in Figure A-4. A uniformly distributed axial load is applied at the top of the block. The axial load is increased in each loading step by a constant magnitude. Global stiffnesses were calculated directly from UDEC results using average vertical stress and maximum vertical displacement for each loading or unloading step. In this analysis, compression is taken as positive.

A.1.3 ABAQUS Solution

In ABAQUS, the problem is discretized using 8-noded, plane stress, quadrilateral elements. The mesh is shown in Figure A-5. This problem was analyzed using Version 5.2 of ABAQUS code. The fracture is modeled with interface elements. These elements can incorporate only the shear stiffness but not the normal stiffness. So the simulated fracture has only shear stiffness and no normal stiffness. A uniformly distributed axial load is applied at the top of the block. Maximum vertical displacement at each loading step is noted. The axial load is increased in each loading step by a constant magnitude. Global stiffnesses were calculated from the vertical-stress-versus-maximum-displacement curves. In this analysis, compression is taken as positive.

A.1.4 Comparison of Results

The results from ABAQUS and UDEC models are shown in Figure A-6. The results from the analytical solution are also shown in the figure. The stiffnesses at loading and unloading stages were calculated from the numerical results obtained in the ABAQUS and UDEC analyses (Table A-1). Stiffnesses calculated using the analytical solution are also given in Table A-1.

A.1.5 Discussion

There is no simple and completely rigorous analytical solution to the problem of an elastic body with an internal slipping crack. Results illustrated in Figure A-6 and given in Table A-1 show that both ABAQUS and UDEC can model the hysteresis observed in cyclic loading of a slipping crack in a specimen, although the hysteresis shown by ABAQUS is less than that in the analytical solution. The results agree
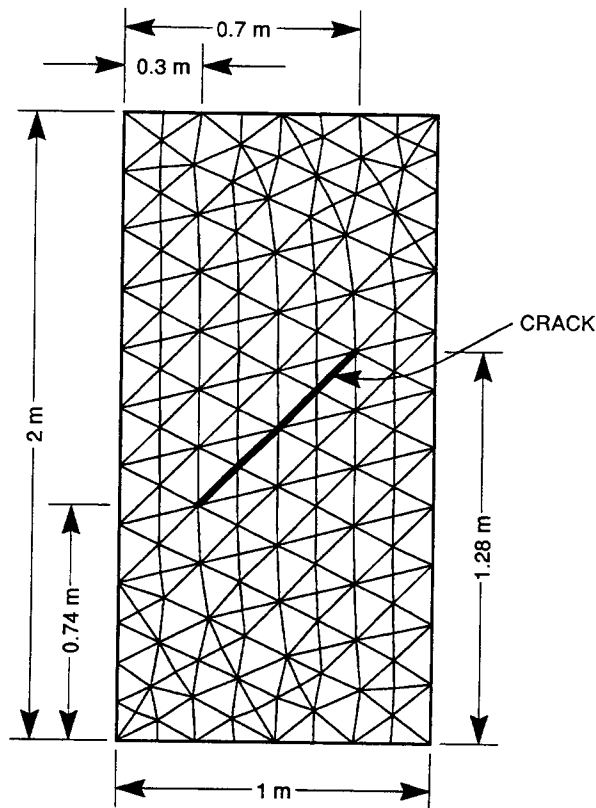
Figure A-4. Discretization of elastic medium into constant strain finite difference triangles in UDEC analysis

well with the conceptual model; however, the results will agree less closely as the length of the slipping crack increases with respect to the width of the specimen. This observation is expected because the conceptual model assumes uniform distribution of normal stress on the crack, and the elastic bridges and stress concentrations become more significant as the length of the elastic bridge between the crack and the specimen boundary decreases.

ABAQUS is somewhat stiffer, whereas UDEC is slightly softer than the analytical solution. This probably is due to the fundamental difference in the solution process. ABAQUS is a displacement-based finite element code. As the displacement is interpolated from element to element, it is expected that the model will be somewhat stiffer than the actual structure. Use of triangular elements to model the fracture might also have contributed in deviating from the analytical solution. Conversely, UDEC is energy or force based. Consequently, it produces a somewhat softer model of the structure.

A.2   PROBLEM 2: HORIZONTAL JOINT AT THE CROWN OF A CIRCULAR EXCAVATION IN AN INFINITE ELASTIC MEDIUM

A circular opening of radius 5 m is excavated in an elastic, homogeneous, isotropic, and infinite medium, as shown in Figure A-7. A horizontal weakness plane (joint) of infinite extent transects the excavation
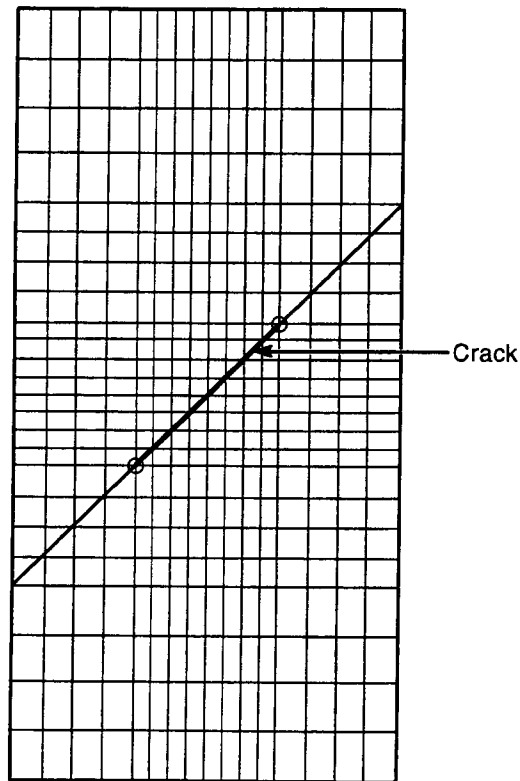
Figure A-5. Finite element mesh used in ABAQUS analysis

at $y=4.33$ m. The point of excavation between the excavation and the weakness plane is $60°$ measured counterclockwise from the x-axis. The *in situ* stress field is hydrostatic and equal to 24 MPa.

Properties of the rock medium are:

mass density, ρ = 10 kg/m³   0·62 w p·s

shear modulus, G = 35 GPa

bulk modulus, K = 60 GPa

Properties of the joint are:

normal stiffness, K_n = 200 GPa/m

shear stiffness, K_s = 200 GPa/m

cohesion, C = 0 MPa

friction angle, ϕ = 16.3°

tensile strength, T = 0 MPa

A.2.1 Analytical Solution

The state of stress around a circular excavation in a hydrostatic stress field, P, is (Brady and Brown, 1985)

A-7
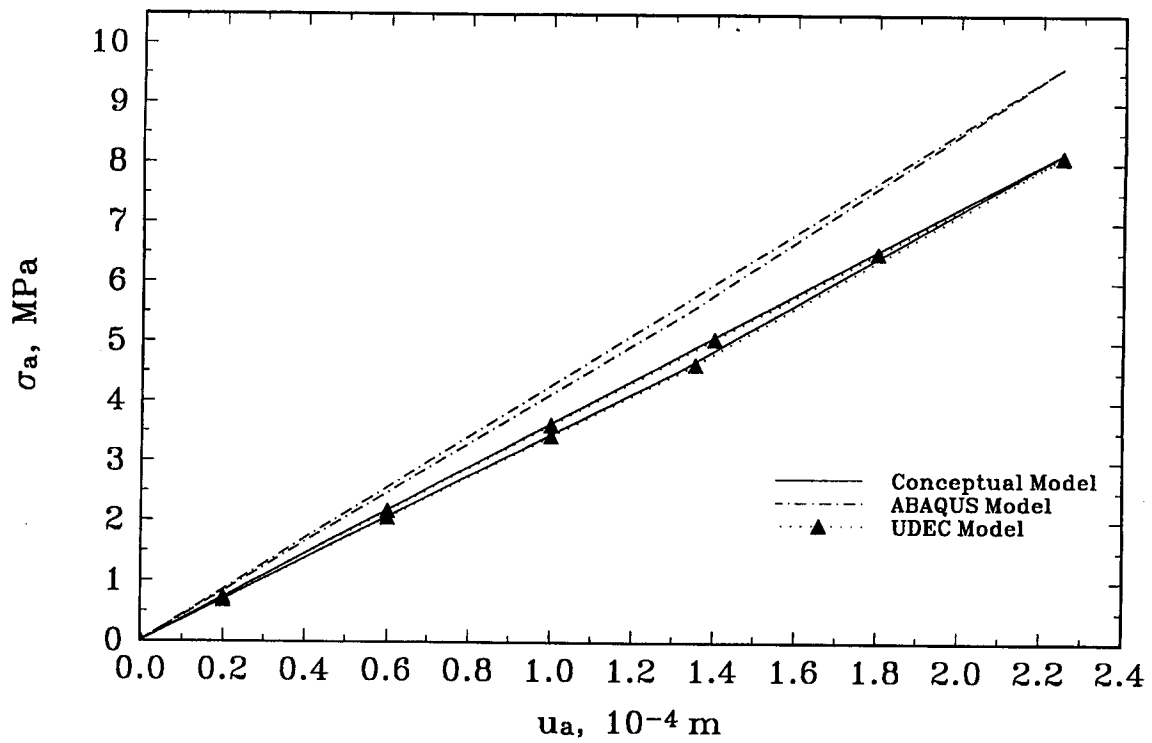
Figure A-6. Comparison of ABAQUS and UDEC results with the analytical solution
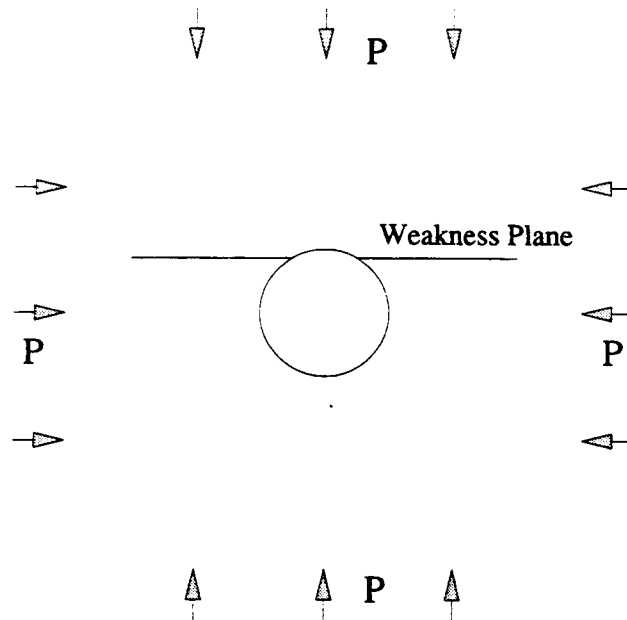
Figure A-7. Horizontal weakness plane near the crown of a circular excavation subjected to a hydrostatic stress field

A-8

Table A-1. Comparison of ABAQUS and UDEC results with conceptual model solution

Segment	Conceptual Model Stiffness (GPa/m)	ABAQUS Model Stiffness (GPa/m)	Error (percent)	UDEC Model Stiffness (GPa/m)	Error (percent)
Load OA	36.28	42.69	−17.7	36.04	+0.66
Unload AB	38.89	44.84	−15.3	38.91	−0.05
Unload BO	34.42	41.18	−19.6	34.14	+0.81

$$\sigma_{rr} = P\left[1 - \frac{a^2}{r^2}\right] = \sigma_1$$

$$\sigma_{r\theta} = 0$$

$$\sigma_{\theta\theta} = P\left[1 + \frac{a^2}{r^2}\right] = \sigma_3 \qquad \text{(A-7)}$$

where

a = radius of the circular excavation

r = radial distance from the center of the excavation to any point $(x,y) = \sqrt{x^2 + y^2}$

σ_1 = major principal stress

σ_3 = minor principal stress

The state of stress at any point along the weakness plane (Figure A-7) can be calculated using the stress transformation equations

$$\sigma_n = \frac{1}{2}[\sigma_1 + \sigma_3] + \frac{1}{2}[\sigma_1 - \sigma_3]\cos 2\beta$$

$$\sigma_s = \frac{1}{2}\left[\sigma_1 - \sigma_3\right]\sin 2\beta \qquad \text{(A-8)}$$

where

β = angle measured counterclockwise from σ_1 to σ_n

σ_n = normal stress acting on the weakness plane

σ_s = shear stress along the weakness plane

A-9

In this problem, $\beta = -\theta$ where θ is the angle measured counterclockwise from the x-axis to the point on the weakness plane. Therefore, the state of stress is

$$\sigma_n = P + P \frac{a^2}{r^2} \cos 2\theta \qquad \text{(A-9)}$$

$$\sigma_s = P \frac{a^2}{r^2} \sin 2\theta \qquad \text{(A-10)}$$

The strength mobilized by the weakness plane is

$$\tau = \sigma_n \tan \phi \qquad \text{(A-11)}$$

where ϕ is the friction angle. Equation (A-11) assumes that the weakness plane has zero cohesion and tensile strength and is nondilatant in shear. Slip of the weakness plane will take place if

$$|\sigma_s| \geq \tau$$

or

$$\frac{a^2}{r^2} \sin 2\theta \geq (1 + \frac{a^2}{r^2} \cos 2\theta) \tan\phi \qquad \text{(A-12)}$$

Equation (A-12) has been used to determine the extent of the joint failure. For a given friction angle of 16°, the joint fails up to 4.46 m from the excavation wall. It should be mentioned here that the approach suggested by Brady and Brown (1985) ignores the stress redistribution when a part of the joint fails. Therefore, the result from this approach should be taken as the lower bound solution. The actual failed region will be larger than 4.46 m.

At the boundary of the excavation, the normal and shear stress components on the plane of weakness are (Brady and Brown, 1985)

$$\sigma_{rr} = \sigma_{r\theta} = 0$$

$$\sigma_{\theta\theta} = 2 P \qquad \text{(A-13)}$$

$$\sigma_n = \sigma_{\theta\theta} \cos^2\theta \qquad \text{(A-14)}$$

$$\tau = \sigma_{\theta\theta} \sin \theta \cos \theta \qquad \text{(A-15)}$$

Therefore, the limiting condition for slip at the intersection of the excavation and the weakness plane under this state of stress is (Brady and Brown, 1985)

A-10

$$\sigma_{\theta\theta} \sin \theta \cos \theta = \sigma_{\theta\theta} \cos^2\theta \tan \phi \qquad \text{(A-16)}$$

or,

$$\tan \theta = \tan \phi \qquad \text{(A-17)}$$

The plane of weakness will slip if $\theta \geq \phi$. The sense of slip, given by the sense of the shear stress, shows outward displacement of the upper surface of the weakness plane relative to the lower surface. This implies boundary stresses lower than the elastic solution (Kirsch solution), determined without considering the plane of weakness at the crown of the opening. There is a possibility of tensile fracture formation in the crown.

The equilibrium state of stress at the intersection of the plane of weakness with the boundary can be established from Eq. (A-10). Rewriting Eq. (A-10), we get

$$\sigma_{\theta\theta} \frac{\sin (\theta - \phi)}{\cos \phi} = 0 \qquad \text{(A-18)}$$

For $\theta > \phi$, this condition can be satisfied only if $\sigma_{\theta\theta}=0$. Therefore, the regions near the intersection of the opening and the plane of weakness are either at destressed or having a low confining stress.

A.2.2 UDEC Solution

Due to symmetry along the vertical plane passing through the center of the opening, only the right side of the problem was modeled. The vertical principal *in situ* stress of 24 MPa was applied on the horizontal model boundaries located at 30 m above and below the center of the excavation. Horizonal principal *in situ* stress of 24 MPa was applied at the vertical model boundary placed 30 m from the center of excavation.

A.2.3 ABAQUS Solution

ABAQUS model, shown in Figure A-8(a) and (b), also exploited the symmetry of the problem using plane strain assumption. No displacement condition was imposed along the boundaries. The rock mass was modeled using 4-noded quadrilateral elements. The discontinuity was modeled using 4-noded interface elements. A slip tolerance of 1.0×10^{-4} m was assigned to the discontinuity to simulate the elastic shear stiffness. A vertical stress of 24 MPa was applied on the horizontal model boundaries located at 30 m above and below the center of the excavation. Horizontal stress of 24 MPa was applied at the vertical model boundary at 30 m from the center of excavation.

A.2.4 Comparison of Results and Discussion

Kirch solution and the frictional properties of the weakness plane indicate that the failure of the rock joint will take place up to 0.9 times the excavation radius into the rock from the excavation boundary. Results from both ABAQUS and UDEC are plotted in Figure A-9. The stresses are normalized by the vertical stress applied at the model boundaries. These results indicate joint slip up to about 1.6 times the excavation radius into the rock. The difference between the results obtained from ABAQUS and UDEC
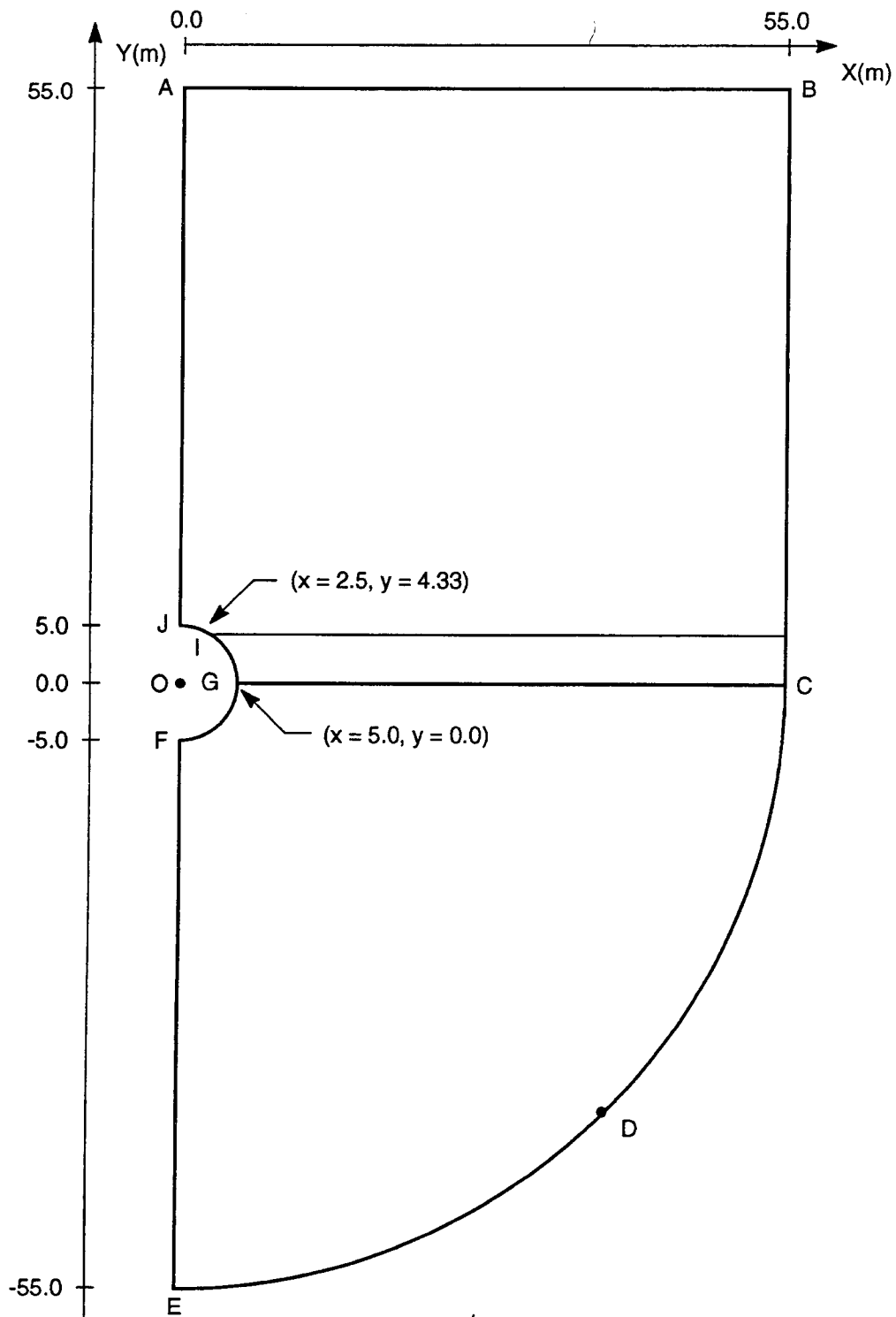
Figure A-8(a). Finite element model of the problem of a horizontal weakness plane near the crown of a circular excavation
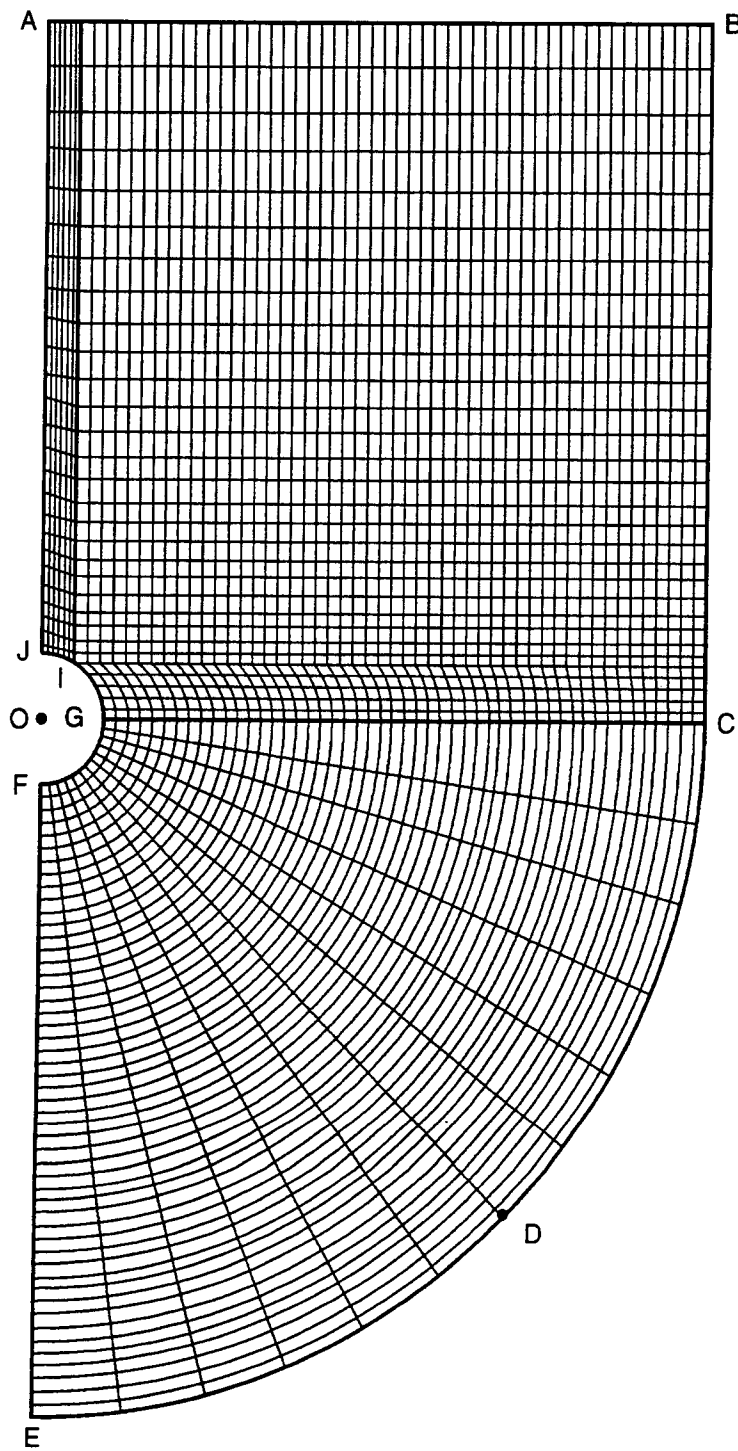
Figure A-8(b). Finite element mesh of the problem of a horizontal weakness plane near the crown of a circular excavation
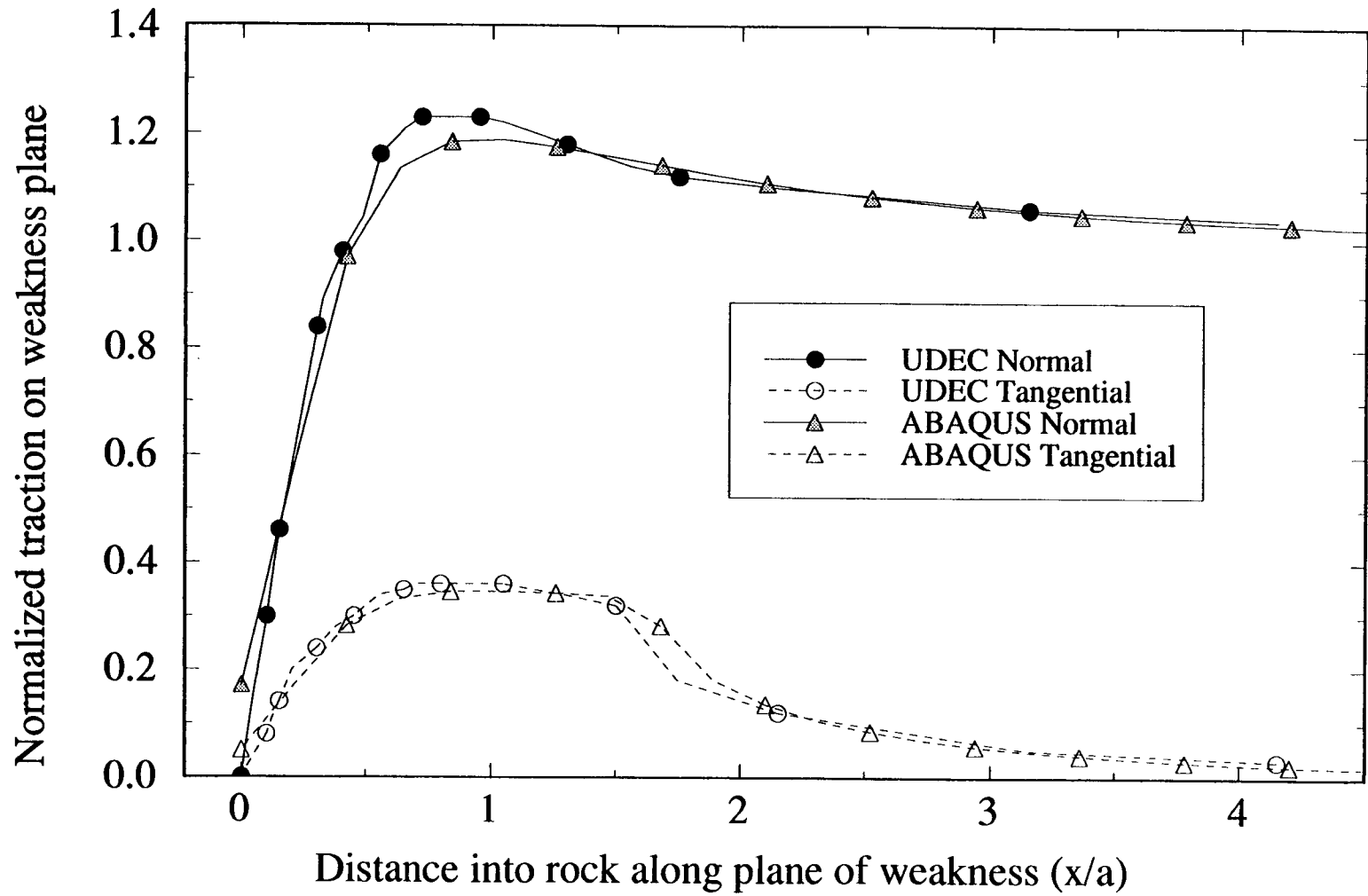
Figure A-9. Comparison of ABAQUS and UDEC results

is negligible. Failed region is larger in the ABAQUS and UDEC analyses as they also model the stress redistribution due to joint slip. The analytical approach using Kirch solution neglects this stress redistribution when a part of the joint fails.

A.3 PROBLEM 3: SLIP IN A JOINTED BODY INDUCED BY A HARMONIC SHEAR WAVE

This problem deals with the dynamic response of a planar discontinuity subjected to a normally incident plane harmonic shear wave. The geometry of the problem is illustrated in Figure A-10. A discontinuity of infinite extent is embedded in an infinite, homogeneous, and isotropic elastic medium. The shear strength is cohesive. As the friction angle is equal to zero, the shear strength is constant and independent of normal stress. The discontinuity will slip if the transient shear stress induced by the shear wave equals or exceeds the shear strength, τ_s. If slip occurs, the energy contained in the incident wave is partitioned between reflected and transmitted waves and absorption at the interface. This problem was previously analyzed using UDEC (Brady et al., 1990). It was analyzed again using ABAQUS in order to evaluate its capability to (i) model an interface under dynamic load and (ii) simulate nonreflecting boundary conditions.

A.3.1 Analytical Solution

Miller (1978) solved the problem considering two dissimilar media, 1 and 2, on opposite sides of the discontinuity. The incident wave at position, x, and at time, t, is expressed as

$$U_i = U \sin \left(\frac{wx}{ci} - wt \right)$$ (A-19)

where

$$C_i = \left[\frac{G_i}{P_i} \right]^{\frac{1}{2}} (i = 1,2) \text{ represents the shear wave velocity in medium } i$$

U = amplitude
w = angular frequency

The shear displacement at the interface between two dissimilar surfaces may be described as

$$d(t) = D \cos (wt - \phi)$$ (A-20)

where
D = amplitude of joint shear
ϕ = phase shift occurring at the boundary

The solution for D is

$$C^2 (D) + [\omega_1 \gamma_1 \gamma_2 D/(\gamma_1 + \gamma_2) - S(D)]^2 = [2\omega U \gamma_1 \gamma_2/(\gamma_1 + \gamma_2)^2]$$ (A-21)
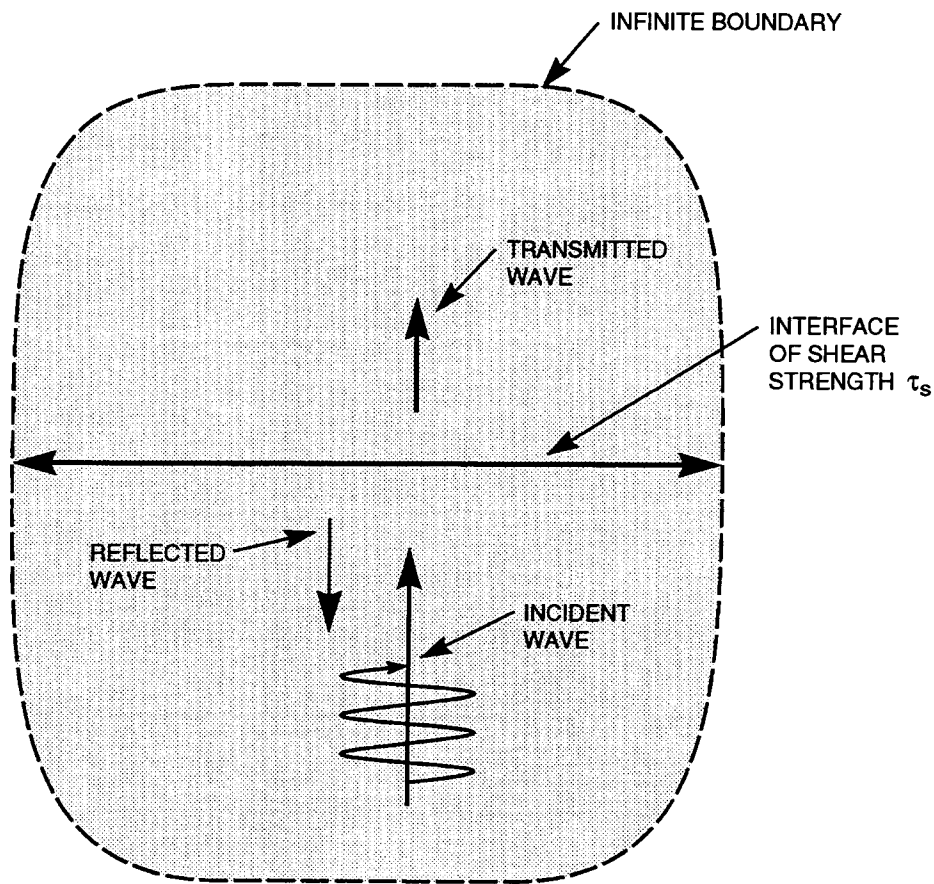
Figure A-10. Definition of the problem of wave propagation in an elastic medium with a single horizontal joint

where

$$C(D) = \frac{1}{\pi} \int_0^{2\pi} \tau_s \ (D \cos \theta - \omega D \sin \theta) \cos \theta \ d\theta$$

$$S(D) = \frac{1}{\pi} \int_0^{2\pi} \tau_s \ (D \cos \theta - \omega D \sin \theta) \sin \theta \ d\theta$$

$$\gamma_i = (p_i G_i)^{\frac{1}{2}}$$

If τ_s is independent of displacement, as is assumed for a cohesive interface, considerable simplification of these expressions is possible.

The phase angle is given by

$$\phi = \tan^{-1} \left\{ [S(D) - \omega \gamma_1 \gamma_2 \ D \ /(\gamma_1 + \gamma_2)] \ / \ C(D) \right\} \tag{A-22}$$

The transmitted and reflected waves are defined by

A-16

$$u_T(x,t) = TU \sin\left(\frac{\omega x}{C_2} - \omega t + \phi_T\right) \qquad \text{(A-23)}$$

$$u_R(x,t) = RU \sin\left(\frac{\omega x}{C_2} - \omega t + \phi_R\right) \qquad \text{(A-24)}$$

where

T and R = the transmission and reflection coefficients, respectively

ϕ_T and ϕ_R = phase shifts at the boundary (determined by ϕ)

By satisfying displacement conditions at the interface, it is found that

$$T = \left\{[(D/U)\sin\phi - 2]^2 + (D/U^2)\cos^2\phi\right\}^{\frac{1}{2}} \gamma_1 / (\gamma_1 + \gamma_2) \qquad \text{(A-24)}$$

$$R = \left\{(D/U)^2\cos^2\phi + [(D/U)\sin\phi + (\gamma_1 + \gamma_2) - 1]^2\right\}^{\frac{1}{2}} \gamma_2 / (\gamma_1 + \gamma_2) \qquad \text{(A-25)}$$

Equations (A-23) and (A-24) permit direct calculation of the transmission and reflection coefficients from the properties of the medium and the interface and the wave characteristics.

Material properties of continuous media and discontinuity are

Medium properties:

Mass density, ρ = 2.65 kg/m^3 = 0.165 pct (v. low)
Shear modulus, G = 16.667 GPa
Bulk modulus, K = 10.000 GPa   } Corrected

Discontinuity properties:

Normal stiffness, K_n = 10 GPa/m
Shear stiffness, K_s = 10 GPA/m
Friction angle, ϕ = 0°
Cohesion, C = 0.2 to 0.8333 MPa

A.3.2 UDEC Analysis

Figure A-11 shows the problem geometry modeled with UDEC. The plane of discontinuity EF was simulated with high normal stiffness and high shear stiffness but limited cohesion. The continuous media were modeled with elastic, fully deformable blocks which were further discretized into triangular finite-difference zones. In specifying the boundary conditions, viscous boundaries were applied at the
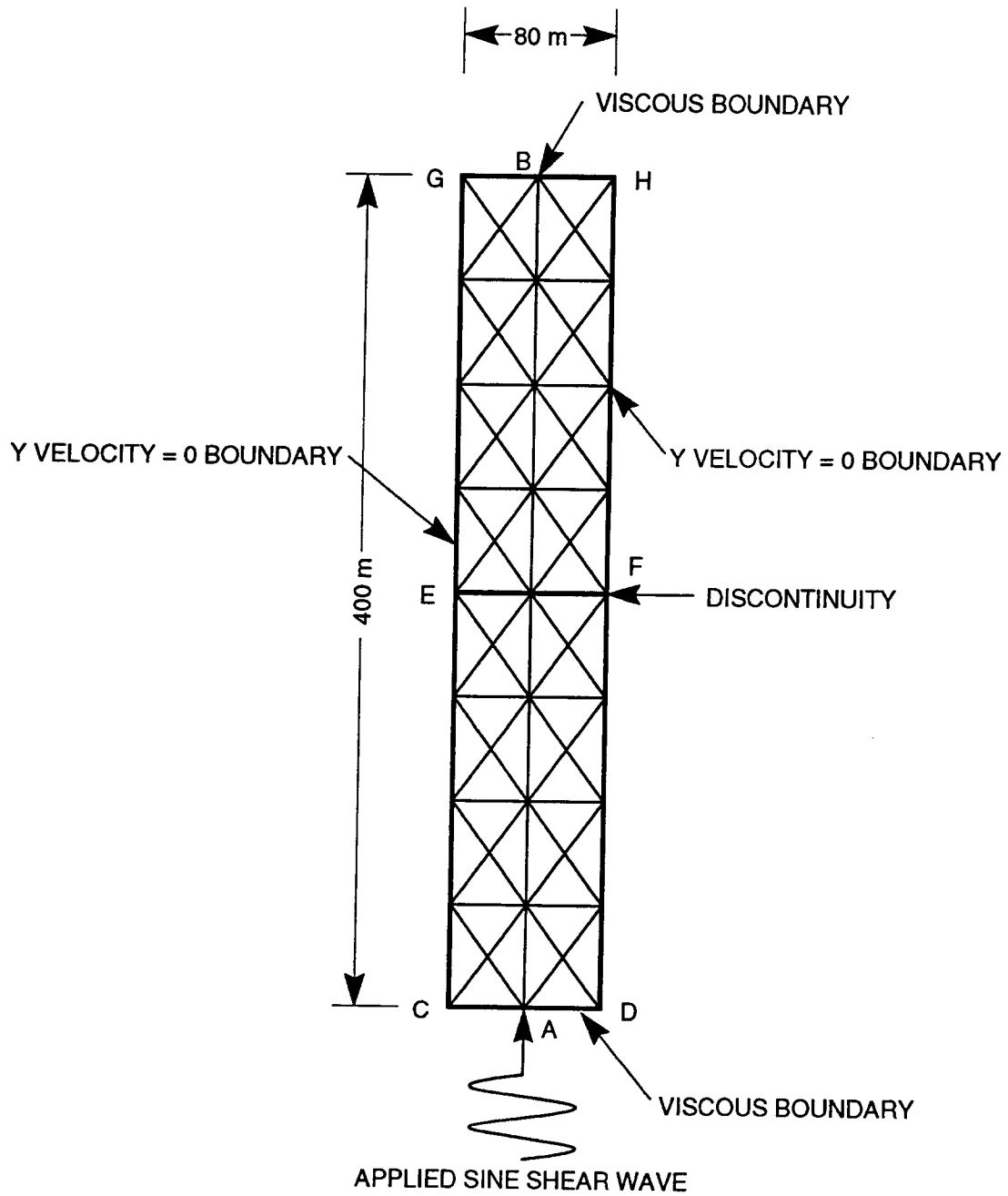
Figure A-11. UDEC model for the study of slip of the joint induced by a propagating harmonic shear wave

model boundaries, CD and GH, and the two vertical boundaries, CG and DH, were constrained to move in the horizontal direction. A sinusoidal wave was applied at the boundary, CD, the base of the model. The applied maximum stress and frequency of the incident wave were 1.0 MPa and 1 Hz, respectively.

In the current work, it is assumed that the coefficient of friction is zero and the shear resistance is cohesive. The implicit assumption is that the joint is elastic-perfectly plastic in shear. In UDEC, the only joint model that is absolutely compatible with this mode of joint shear is the Mohr-Coulomb joint. Therefore, the main basis for comparison of UDEC performance with the analytical solution is from the results using the Mohr-Coulomb joint model. In the current work for yielding joints, the joint cohesion has been taken in the range 0.02 to 0.8333 MPa.

A.3.3   ABAQUS Model   ⌐ 120. psi

The geometry of the model and the finite element mesh are shown in Figure A-12. It is 600 m in height and 80 m in width. Plane strain condition was assumed in the analysis. The discontinuity was represented by EF ($y=0$ m). Vertical boundaries of the model, AD ($x=0$ m) and BC ($x=80$ m), were restrained vertically. Infinite elements were placed at the horizontal boundaries, AB and CD, to create absorbing boundaries for simulating infinite material to wave propagation analysis. The harmonic shear wave was applied at a depth of 200 m below the interface at point G. The shear stress history was monitored at two points, J and K, located at 195 m above and below the discontinuity, respectively.

In the finite element model, the elastic medium was simulated using 8-noded quadrilateral elements and the discontinuity with 6-noded interface elements. There is no direct way to apply shear stress on the surface of solid elements in ABAQUS. Therefore, 3-noded beam elements were placed at $y=-200$ m, coincident with the base of a row of quadrilateral elements located at that elevation. Axial force was applied in the beam elements to transmit the desired magnitude of shear stress to the base of the quadrilateral elements. The stiffness of the beam elements was set to a small value relative to that of the solid elements. Material properties for the beam were

Young's modulus, E = 0.025 MPa
Poisson's ratio, ν = 0.25
Density, ρ = 2.65 kg/m^3

The applied axial force varied according to the following equation

$$F_x = A \sin (2\pi t) \tag{A-26}$$

where A is 2.0 MN/m and t is time in seconds. This produced a sinusoidal shear wave of amplitude 2.0 MPa at the base of the neighboring row of quadrilateral elements, thereby transmitting a horizontal shear stress wave of amplitude 1.0 MPa vertically through the medium.

The shear strength of an interface is defined in ABAQUS using classical Coulomb friction model (Amonton's law)

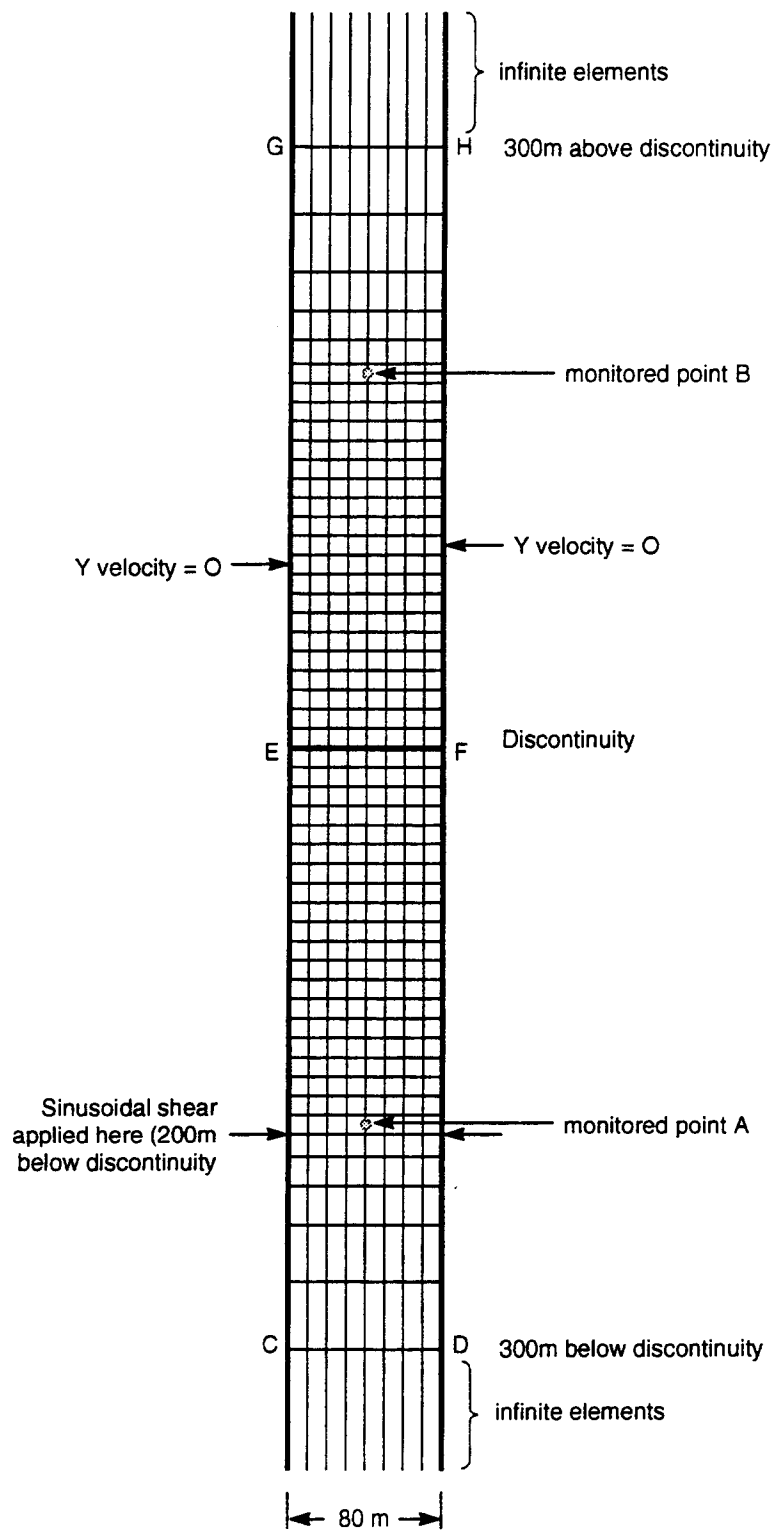$$\tau = \mu \ \sigma_n \tag{A-27}$$

A-19

Figure A-12. ABAQUS model for the study of slip of the joint induced by a propagating harmonic shear wave

where

μ = fricitional coefficient

σ_n = normal stress on the interface

On the other hand, the interface for this problem is required to be cohesive with zero friction. This required a modification of the ABAQUS friction subroutine to allow for the shear strength of an interface to be defined in terms of both cohesion and friction

$$\tau_s = C + \mu\sigma_n \qquad\qquad\qquad (A\text{-}28)$$

where C is the cohesion. This modification was accomplished through the user-supplied subroutine facility in ABAQUS. Four different values, 5.0, 0.75, 0.5, and 0.25 MPa, of cohesion were used in the analysis.

A.3.4   Results

The performance of ABAQUS and UDEC was assessed in terms of elastic transmission of a wave across the interface. Figure A-13 shows the time history of shear stress on opposite sides of the discontinuity using UDEC. Figure A-14 shows the results using ABAQUS with 5-MPa cohesion. UDEC and ABAQUS produced identical wave traces having peak amplitudes of 1 MPa and separated by a time increment equivalent to the wave transmission time between the monitored points. Identical waves confirm that the joint models in UDEC and ABAQUS transmit the elastic wave perfectly.

The figure is also interpreted to indicate that the infinite elements performed very well in this analysis. Waves reflected from the boundary (between infinite and finite elements) would have reached the monitoring points with a phase shift of about 0.1 sec, and the effect of the reflected wave would have been clearly noticeable in Figure A-14. The fact that there was no such effect means that waves hitting the boundary were perfectly transmitted. The infinite elements in ABAQUS are expected to be 100 percent effective when the infinite/finite boundary is normal to the direction of wave propagation; this expectation is confirmed in this analysis.

The capacity of UDEC and Mohr-Coulomb joint to model slip under dynamic conditions is indicated in Figure A-15. When the joint cohesion is 0.5 MPa, the shear wave transmitted across the interface has the peak amplitude of shear stress. This is confirmed in Figure A-15, where the transmitted wave is equivalent to the incident waveform clipped to a magnitude of 0.5 MPa. It is noted further that the time history for the point at the base of the model is the result of superposition of the incident wave and the reflected wave.

The results of the other three analyses (with C=0.75, 0.5, and 0.25 MPa) are presented in Figures A-16 through A-18, respectively. Each of the figures shows the following features:

(i)   The shear stress history at a point above the discontinuity is truncated at a value of shear stress equal to the shear strength of the interface, as the discontinuity cannot transmit shear stress larger than its shear strength. The incident energy gets partitioned into transmitted and reflected waves and absorption at the interface.

A-21
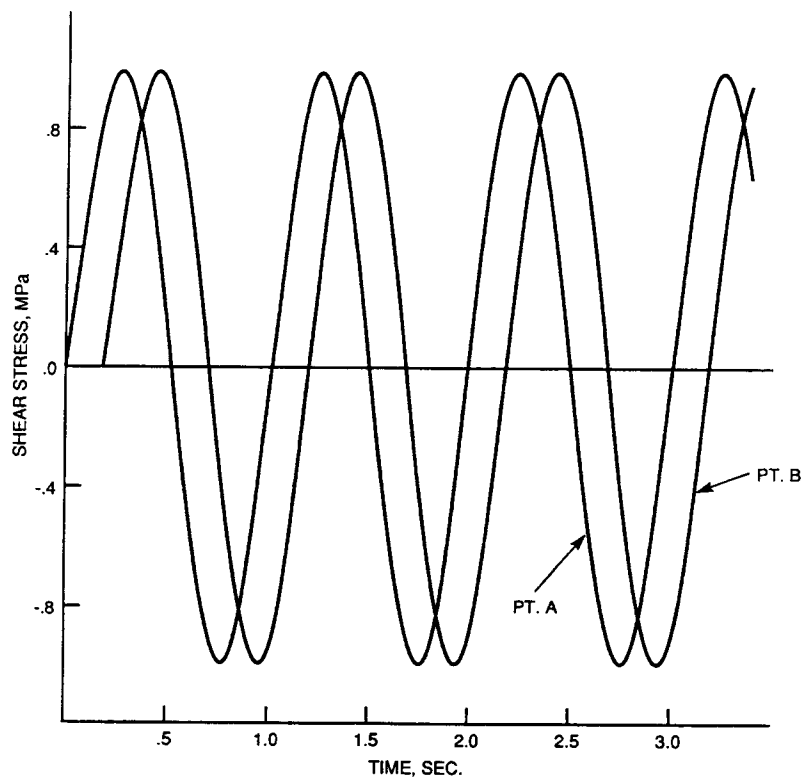
Time History of Shear Stress at Points A (-160,-200) and B (-160,200)
for the Case of Elastic Discontinuum

Figure A-13. History of shear stresses at points A and B of the UDEC model when the joint does not slip (cohesion 5 MPa)

(ii)   The shear stress history at a point below the discontinuity shows a peak of 1.0 MPa due to energy transmitted directly from the source and a secondary peak due to energy reflected from the interface. The secondary peak becomes more pronounced as the shear strength of the interface decreases (i.e., as the fraction of reflected energy increases).

These results are in agreement with those predicted in UDEC analyses (Brady et al., 1990).

A.4   PROBLEM 4: LINE SOURCE IN AN INFINITE MEDIUM WITH A DISCONTINUITY

This problem deals with the dynamic behavior of a single discontinuity under explosive loading. The basic geometry of the problem is illustrated in Figure A-19. It consists of a planar discontinuity of infinite lateral extent in an elastic medium and a dynamic load at a distance, h, from the discontinuity. The closed-form solution for crack slip as a function of time was derived by Day (1985) as a special symmetric condition for the general problem of slip on a discontinuity due to a dynamic point source
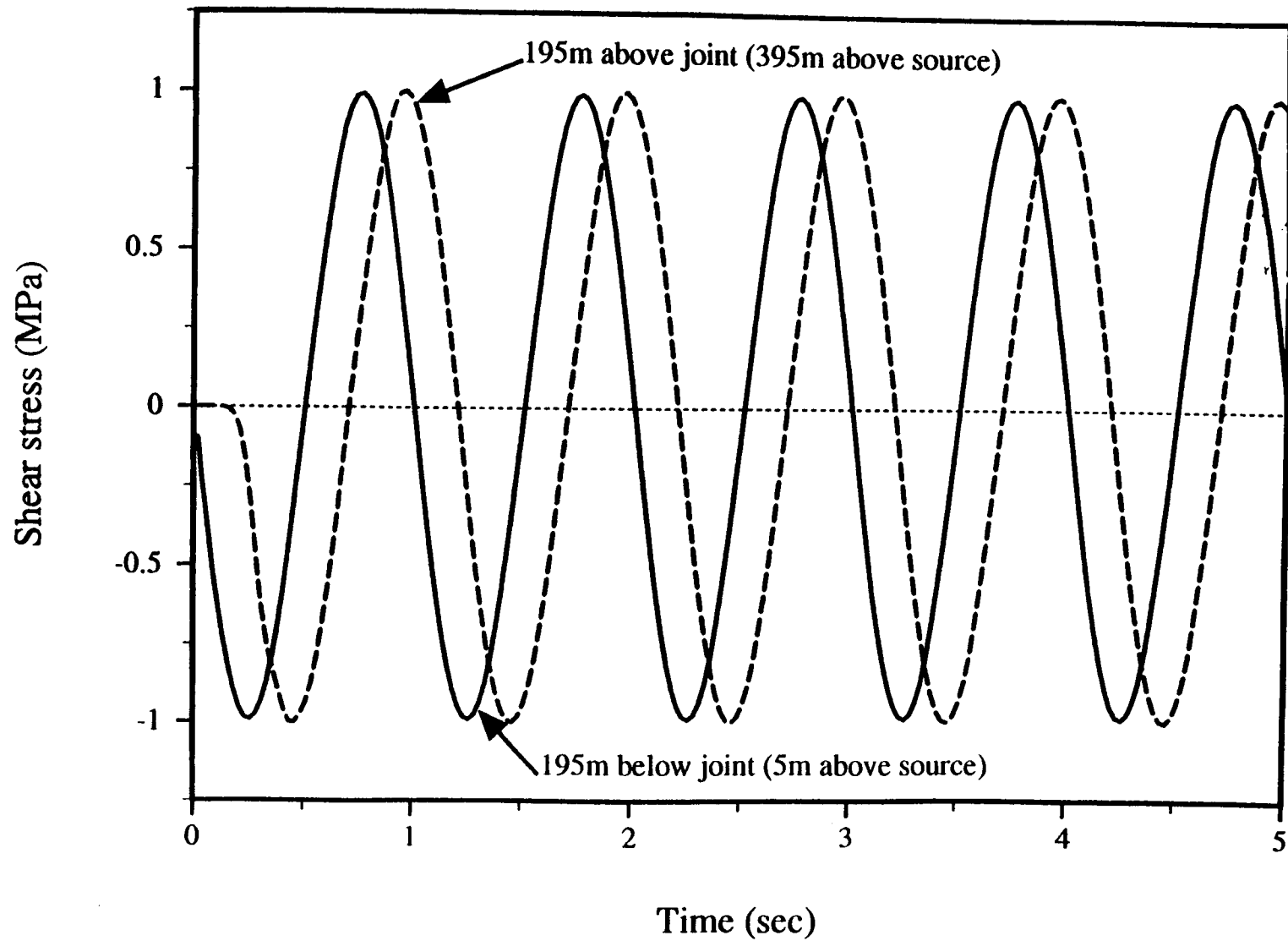
Figure A-14. History of shear stresses at points A and B of the ABAQUS model when the joint does not slip (cohesion 5 MPa)
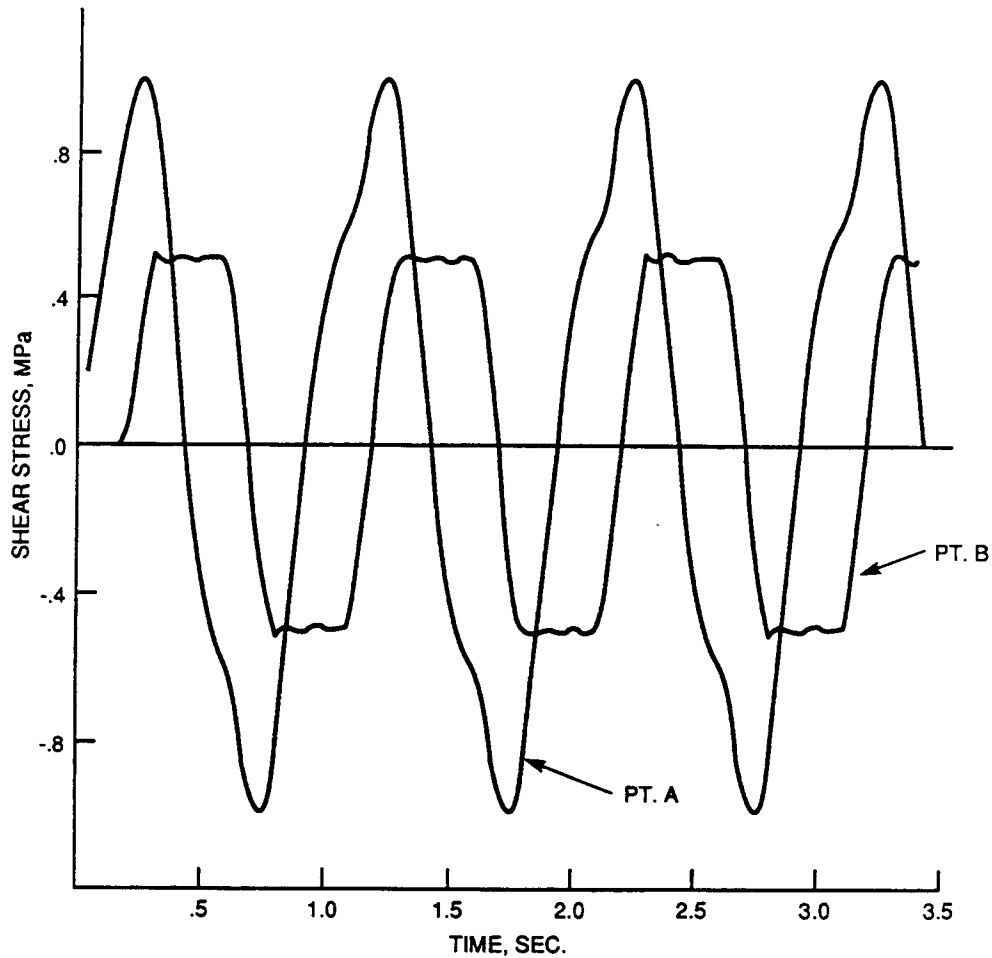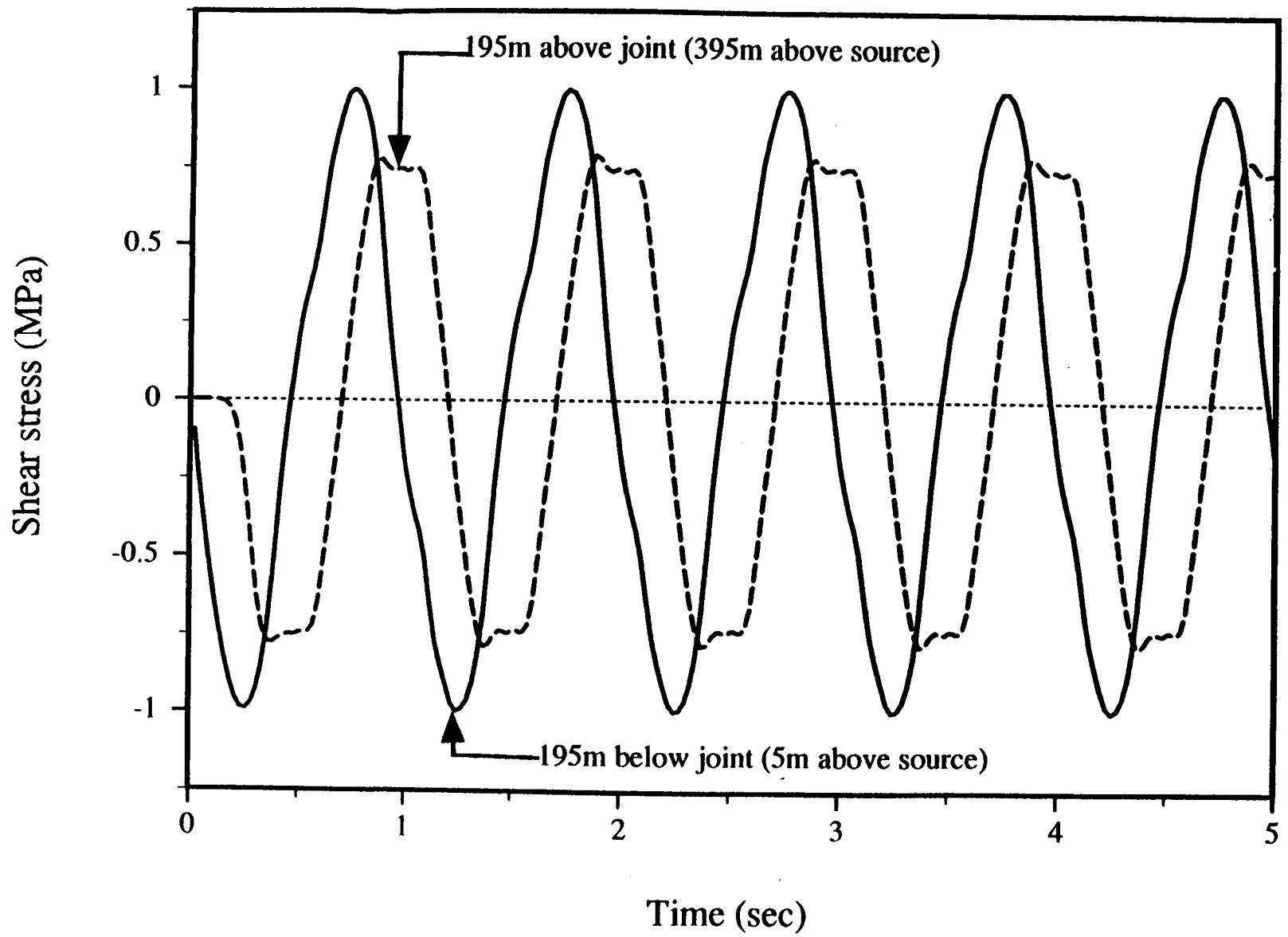
Figure A-15. History of shear stresses at points A and B of the UDEC model when the joint slips (cohesion 0.5 MPa)

(Salvador and Minster, 1980). The problem was also solved using UDEC (Brady et al., 1990). In this study, the analytical and UDEC solutions are compared with results obtained using ABAQUS. The purpose of this analysis is to examine the capabilities of UDEC and ABAQUS to: (i) simulate the dynamic response of a rock discontinuity under impulsive loading, (ii) simulate a high-frequency dynamic wave emanating from a buried explosive, and (iii) simulate nonreflecting boundary conditions.

A.4.1 Analytical Solution

The closed-form solution in terms of the slip on the discontinuity was derived by Day (1985)

$$\delta u(x,t) = \frac{2m_o\beta^2}{\pi\rho\alpha^2} \, \mathrm{Re}\left[\frac{p\eta_\alpha\eta_\beta}{R(p)}\right]\left[\tau + \frac{2r}{\alpha}\right]^{-1/2}\tau^{-1/2}H(\tau) \qquad (A\text{-}29)$$

A-24

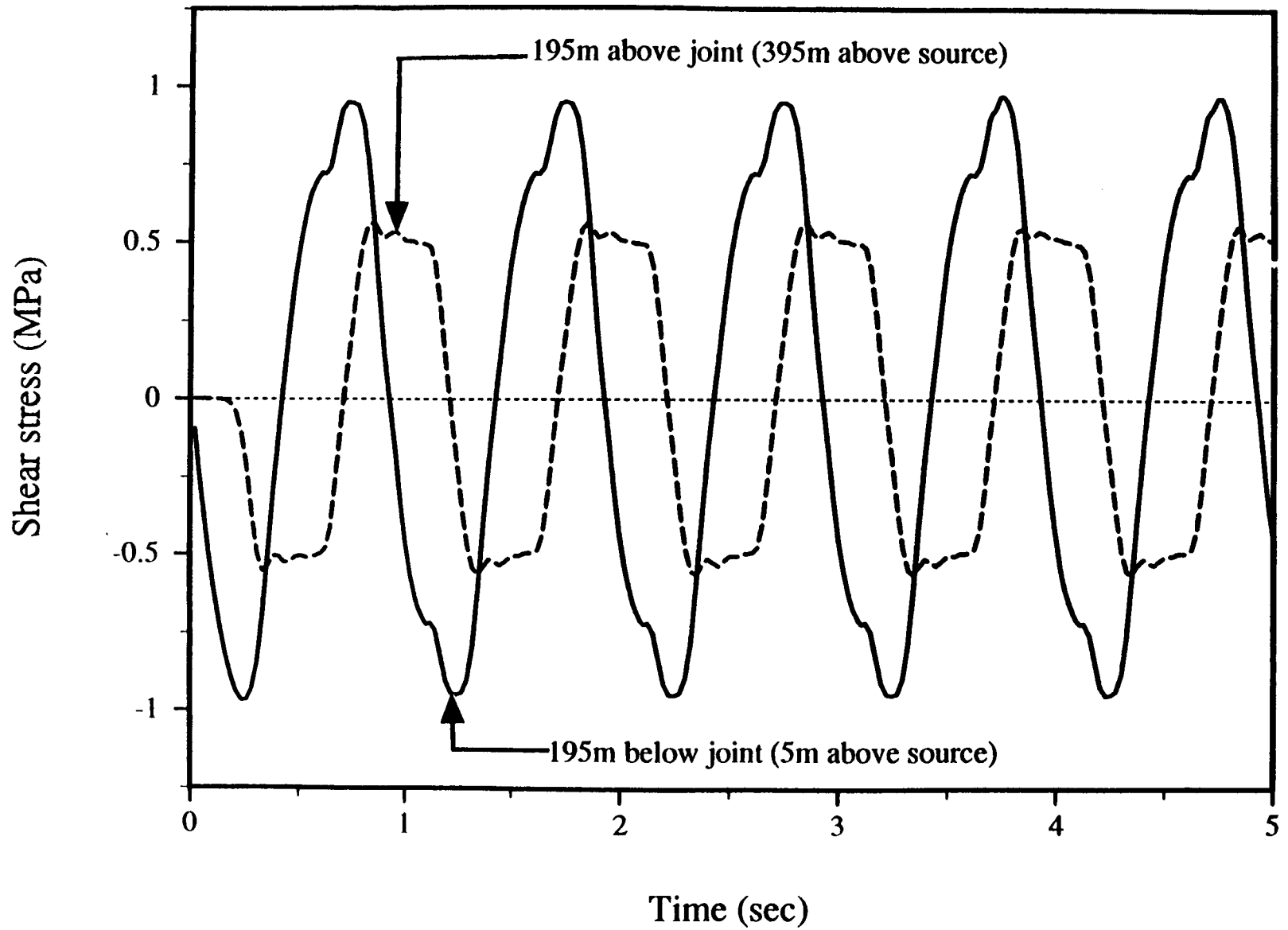195m above joint (395m above source)

195m below joint (5m above source)

Figure A-16. History of shear stresses at points A and B of the ABAQUS model when the joint slips (cohesion 0.75 MPa)

Figure A-17. History of shear stresses at points A and B of the ABAQUS model when the joint slips (cohesion 0.5 MPa)
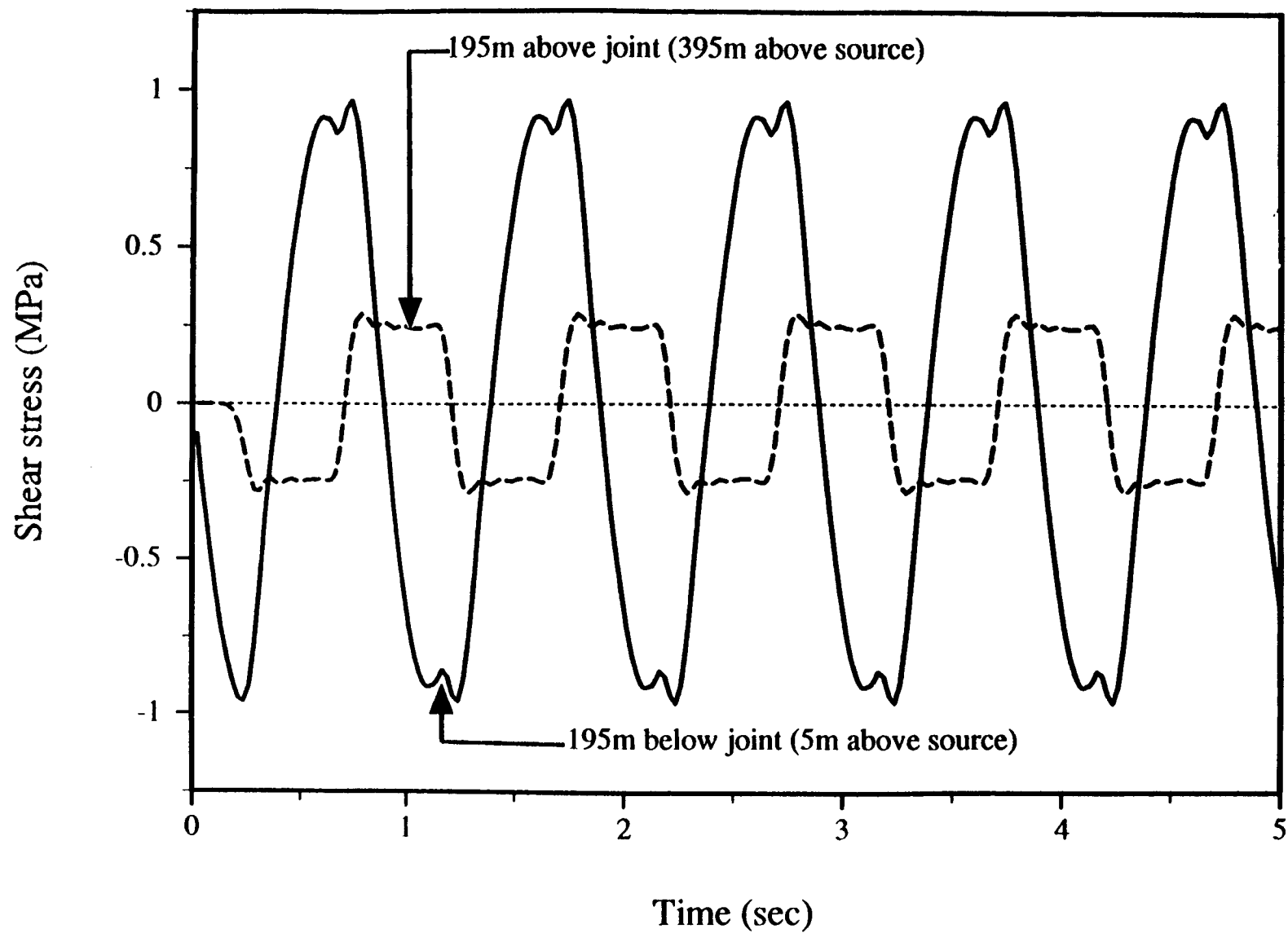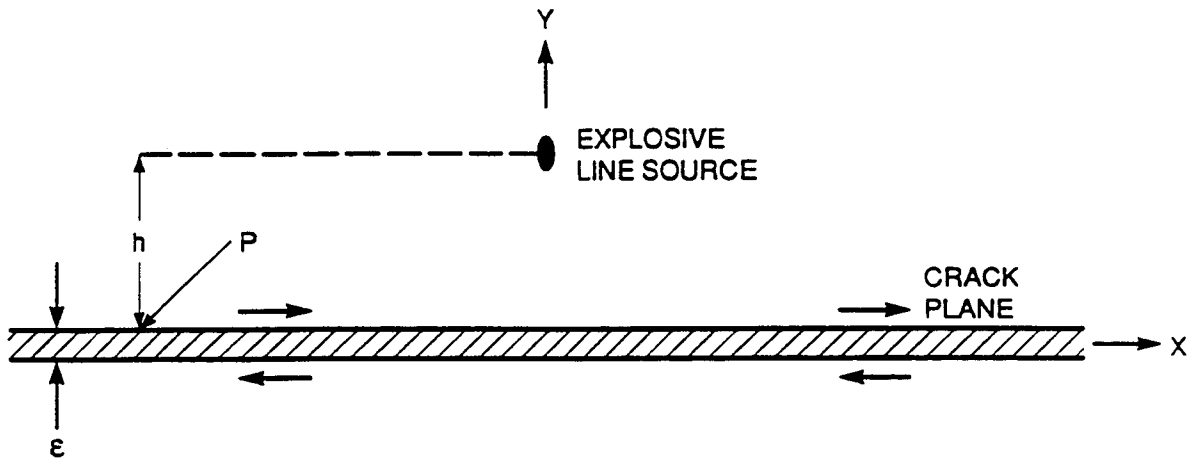
195m above joint (395m above source)

195m below joint (5m above source)

Shear stress (MPa)

Time (sec)

Figure A-18. History of shear stresses at points A and B of the ABAQUS model when the joint slips (cohesion 0.25 MPa)

Figure A-19. Problem geometry for an explosive source near a slip-prone discontinuity

where

r = $(x^2 + h^2)^{1/2}$, the distance from the point source to the point on the crack where the slip is monitored

$H(\tau)$ = step function

τ = $t - (r/\alpha)$

m_o = source strength

α = velocity of pressure wave

β = velocity of shear wave

ρ = density

η_α = $(\alpha^{-2} - p^2)^{1/2}$, Re $\eta_\alpha \geq 0$

η_β = $(\beta^{-2} - p^2)^{1/2}$, Re $\eta_\beta \geq 0$

$R(p)$ = $(1 - 2\beta^2 p^2)^2 + 4\beta^4 \eta_\alpha \eta_\beta p^2 + 2\beta \eta_\beta \gamma$

p = $\dfrac{1}{r^2}\left[\left[\tau + \dfrac{r}{\alpha}\right] x + i \left[\tau + 2\dfrac{r}{\alpha}\right]^{\frac{1}{2}} \tau^{\frac{1}{2}} h\right]$

i = $\sqrt{-1}$

The slip response of the discontinuity for any source history $S(t)$ can be obtained by convolution of Eq. A-29 and the source function $S(t)$.

The following material properties and dimensions were used in the analysis

Geometric Scale h: = 10 m

Block Properties:

    Mass density, ρ = 1 kg/m^3

    Shear modulus, G = 100 Pa

Velocity Input

Radial velocities corresponding to the dynamic solution for a line source in an infinite medium were enforced at the semicircular boundary. The velocities were calculated in the following manner.

The solution for the displacement due to a center of dilation in an infinite medium is (Achenbach, 1975)

$$U_i = \frac{1}{4\pi C p^2} \frac{\partial}{\partial x_i} \left[\frac{1}{4} f (t - r/C_P) \right] \tag{A-30}$$

where

$r^2 \quad = x^2 + y^2 + z^2$
$C_p \quad = \text{P-wave velocity}$
$f(t) \quad = \text{source time history}$

Integration of Eq. (A-30) along the z-axis leads to the solution for a line source of compression (Lemos, 1987) when $f(t)$ is taken as a step function

$$f (t) = 0, \ t<0 \atop 1, \ t\geq 0 \tag{A-31}$$

The 2D solution for radial displacement becomes

$$u = -\frac{1}{2\pi C_p} \frac{t}{r^2} \left[\frac{t^2 C_p^2}{r^2} - 1 \right]^{-\frac{1}{2}} , \ t > r/C_p \tag{A-32}$$

where

$r^2 = x^2 + y^2$

The corresponding velocity is

$$v = -\frac{1}{2\pi C_p} \frac{1}{r^2} \left[\frac{t^2 C_p^2}{r^2} - 1 \right]^{-\frac{3}{2}} , \ t > r/C_p \tag{A-33}$$

The actual input velocity record at $r=0.05h$ as shown in Figure A-20 was obtained by convoluting Eqs. (A-29), (A-33), and the source function $S(t)$.

A.4.2   UDEC Model

Figure A-21 shows the problem geometry modeled by UDEC. The source is located at the origin of the coordinate axes, and the discontinuity is located at $y=h$. The y-axis is a line of symmetry, and nonreflecting boundaries were used on the other three sides of the model. The dynamic input was applied at the semicircular boundary of radius 0.05 h. The slip movement is monitored at point P on the discontinuity.
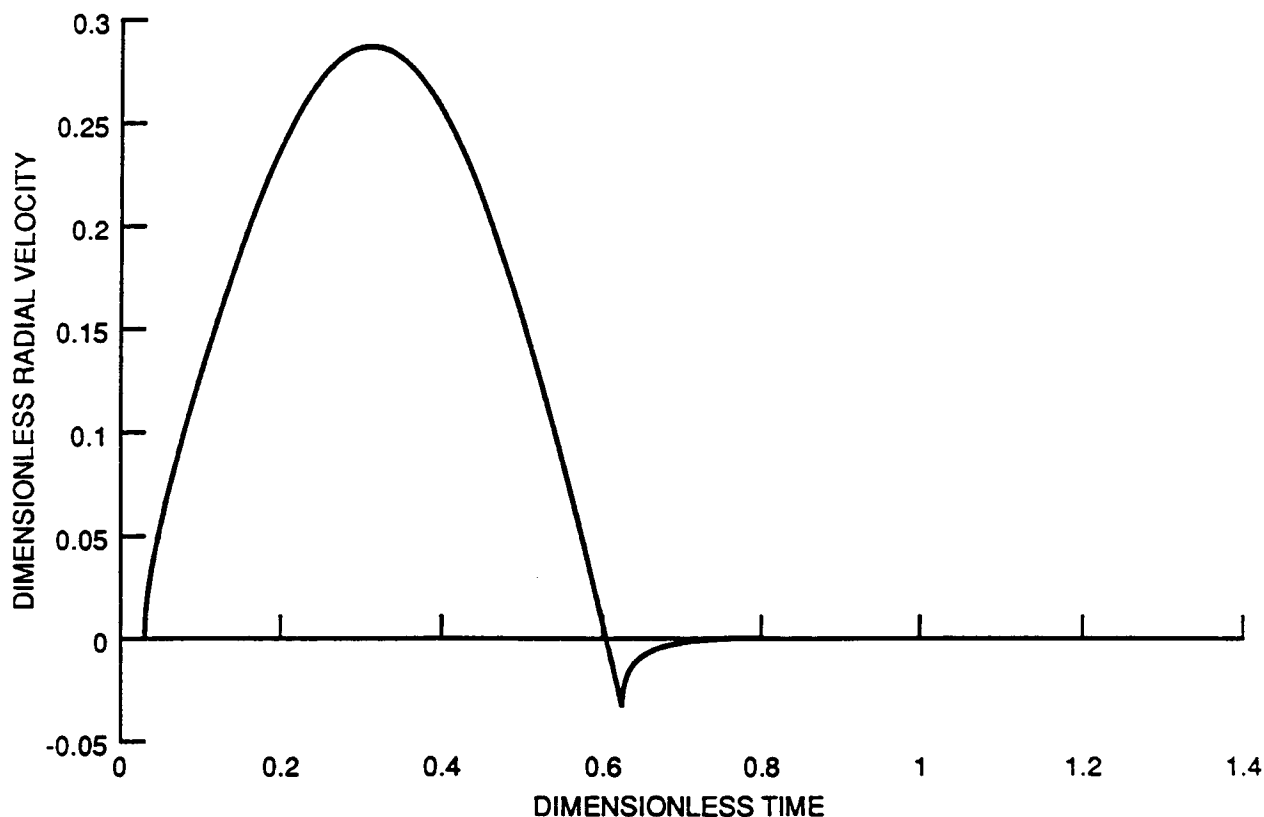
A-29

**Figure A-20. Input radial velocity time history prescribed at $r=0.05$ h.
Dimensionless velocity is $(h^2 \rho \beta / m_o)$ and dimensionless time $= t\beta/h$**

The continuous medium was modeled with elastic, fully deformable blocks, as shown in Figure A-22. Each block was further discretized into triangular finite-difference zones. All of the joints, except for the discontinuity were "glued," that is, assigned high cohesion, and had high normal and shear stiffness in order to model a continuous elastic medium. The discontinuity was assigned zero shear strength, a high normal stiffness, and high tensile strength in order to meet the assumption implied in the analytical solution.

A.4.3 ABAQUS Model

The model used in the analysis of the problem using ABAQUS is sketched in Figure A-23. The line source was assumed to be infinitely long. The continuous medium was assumed to be homogeneous, isotropic, and linear-elastic. Hence, any plane normal to the line source can be analyzed using a plane strain model to study the effects of the line source.
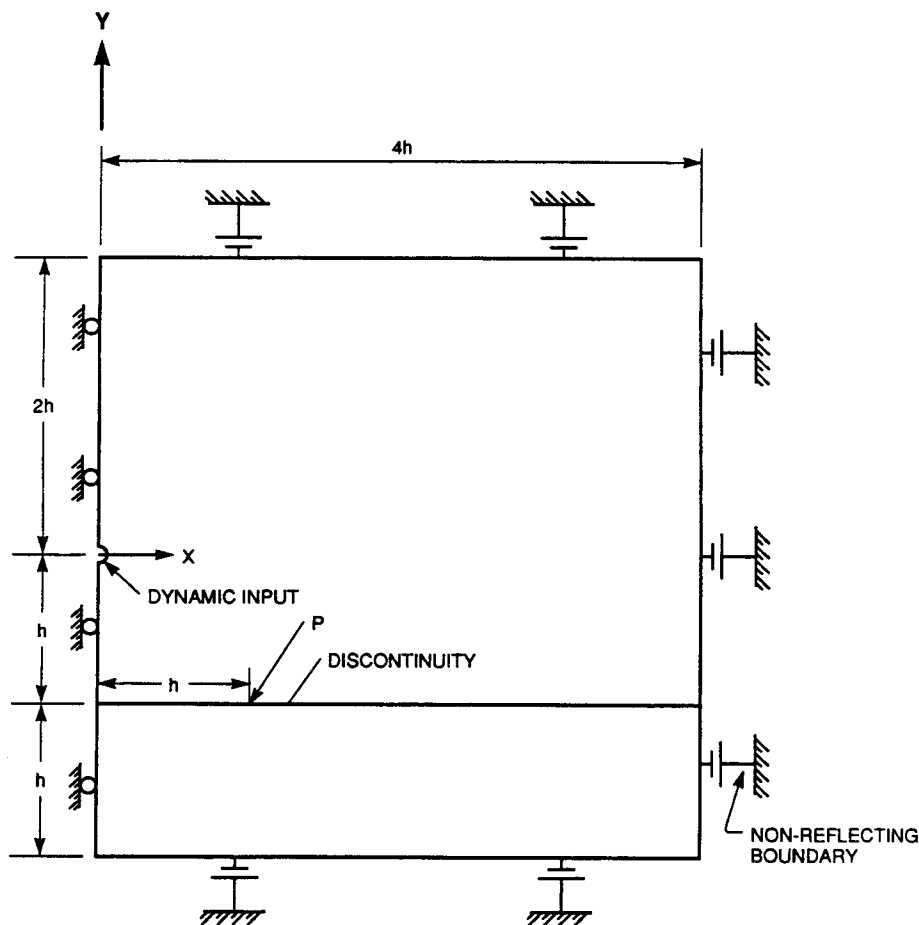
A-30

Figure A-21. Problem geometry and boundary conditions used in UDEC

The line source was modeled as a circular hole of radius 0.5 m, centered at $(x=0, y=0)$. The discontinuity lies at 10 m below the hole, along the line $y=-10$ m. The slip response of the discontinuity was monitored at the point $(x=10$ m, $y=-10$ m). The planar model is symmetrical about the vertical line $x=0$. Therefore, only one-half of the plane (to the right of this line) was analyzed; the model was restrained in the x-direction along the line $x=0$ to simulate symmetry. The other vertical boundary of the model, at $x=40$ m, and the horizontal boundaries, at $y=-20$ m and $y=20$ m, were surrounded with infinite elements to simulate absorbing boundaries.

The continuous medium was modeled using 4-noded quadrilateral elements and the discontinuity with 4-noded interface elements. The discontinuity was assigned zero shear strength (i.e., friction angle of 0.0) using the Coulomb friction model in ABAQUS. The slip tolerance, used by ABAQUS to set maximum elastic slip for the interface elements, was set to 1.0×10^{-4} m. As the friction angle used in this problem was zero, the value of slip tolerance had no effect. These material property values were the same as those used in the UDEC analysis (Brady et al., 1990).

Radial velocity history was applied at the nodes on the wall of the hole (radius 0.5 m; center at $(x=0$ m, $y=0$ m). ABAQUS checks for opening and closing of the contacts between two surfaces of an interface element by calculating the normal stress at the contacts. If there is no initial stress on the contacts,
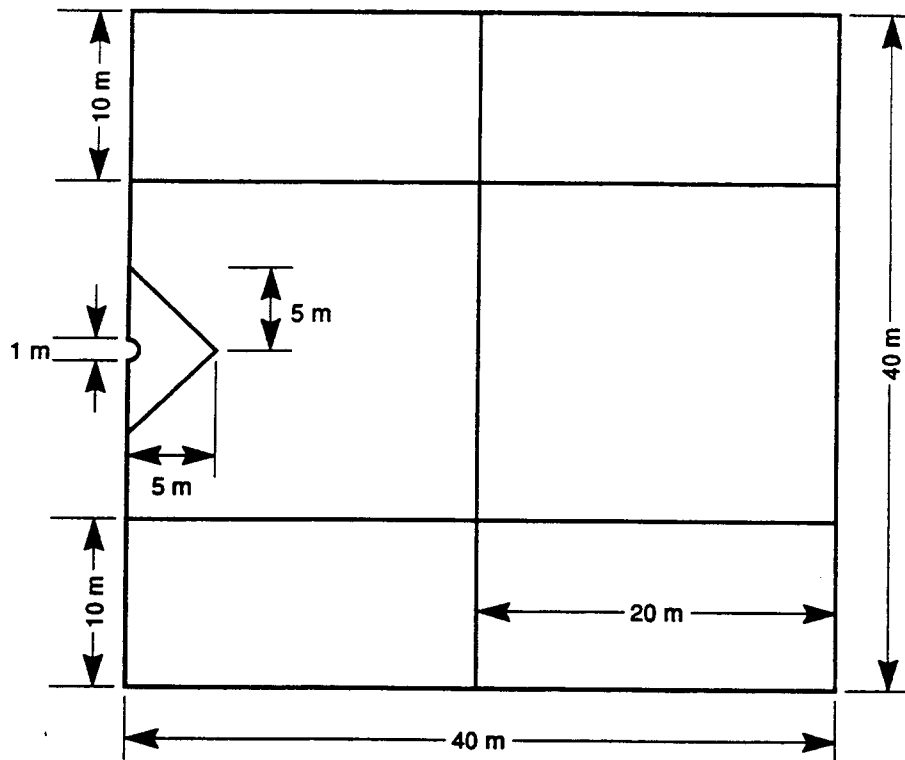
Figure A-22. UDEC model showing semicircular source and "artificial" or "glued" joints used to provide appropriate zoned discretization

numerical inaccuracies in representing real numbers in the computer cause difficulties in determining whether a contact is closed or open. Therefore, a small vertical stress was applied initially to overcome this problem. The slip response predicted at the point ($x=10$ m, $y=-10$ m) is plotted in Figure A-24 along with the analytical and UDEC solutions. The figure shows that both ABAQUS and UDEC predict responses close to the analytical solution.

A.5 PROBLEM 5: ANALYSIS OF INTERSECTING JOINTS

Two problems were solved to examine the capability of ABAQUS in analyzing rock deformation in the vicinity of intersecting discontinuities. Both problems dealt with two pairs of rock blocks arranged in such a way as to contain a pair of orthogonal discontinuities. The first problem considers simultaneous sliding on both discontinuities, and the second considers sliding on only one discontinuity.

A.6 PROBLEM 5.1: SIMULTANEOUS SLIP ON TWO ORTHOGONAL JOINTS

The geometry of the first problem along with the finite element mesh is illustrated in Figure A-25. Block B2 was restrained vertically on its top edge and horizontally on its right edge. Block B3 was restrained horizontally on its left edge and block B1 vertically on its bottom edge. Block B4 was displaced towards block B2 at a 45° angle the to x-axis.
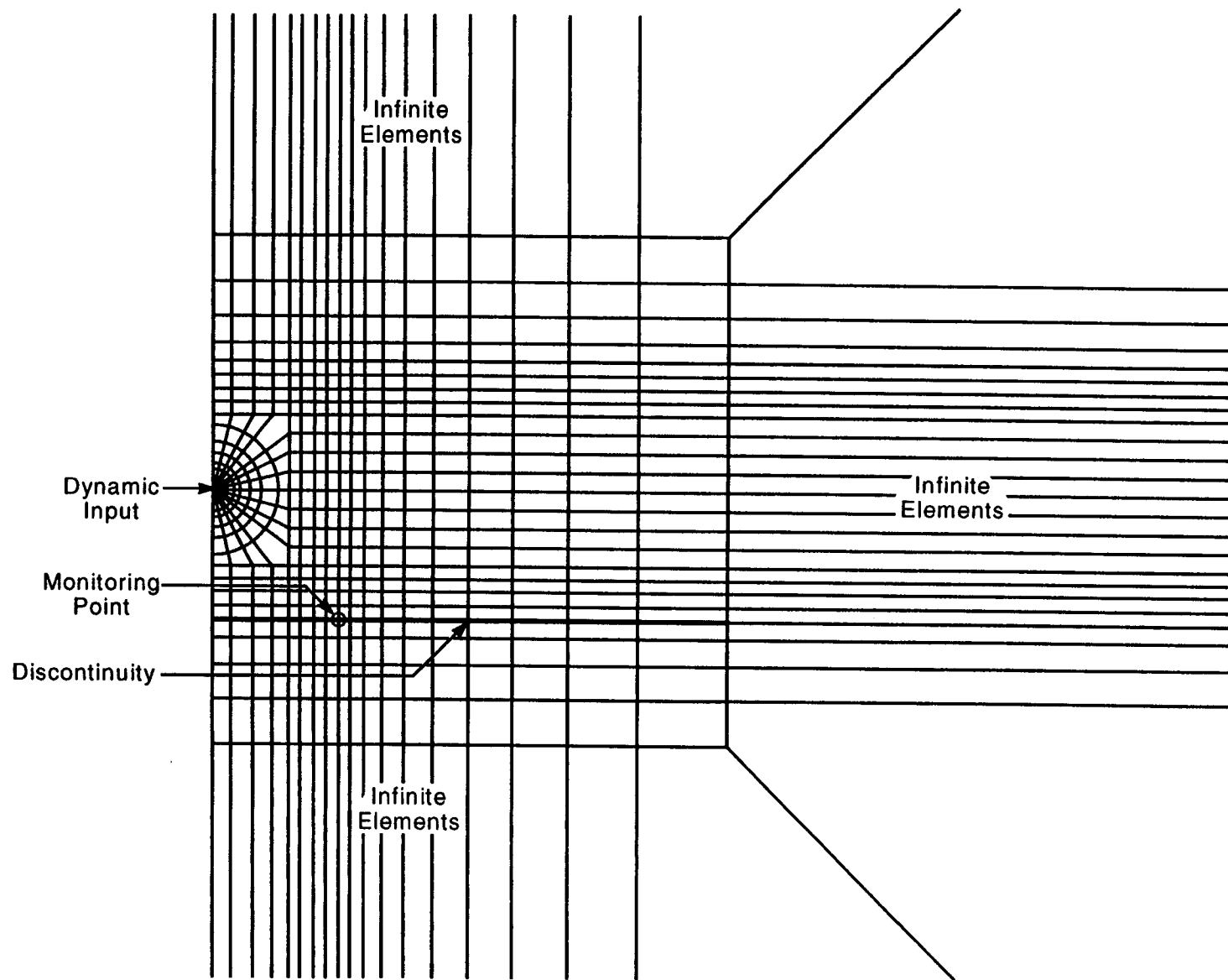
A-32

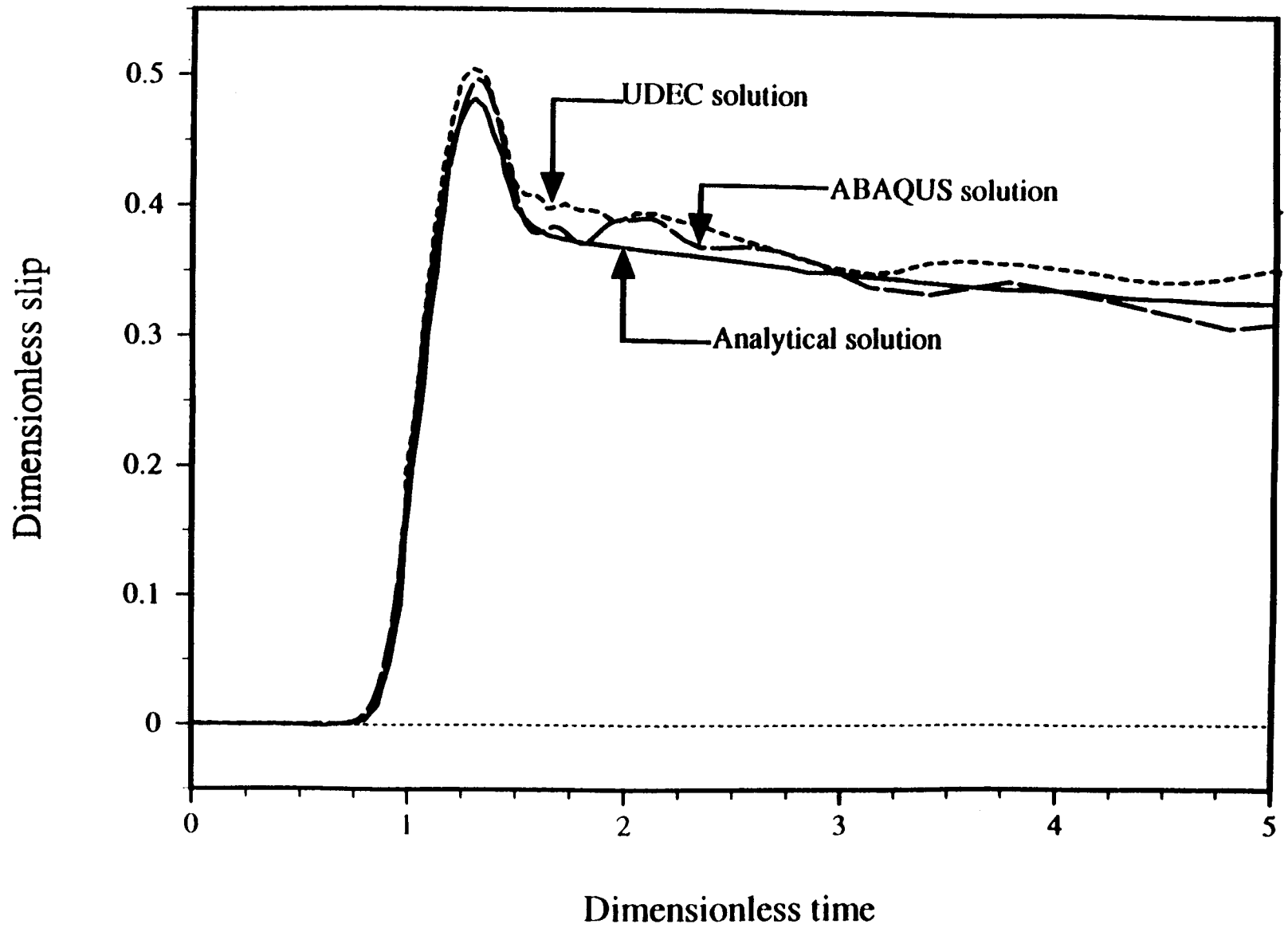Figure A-23. Finite element model used in ABAQUS analysis

Figure A-24. Comparison of ABAQUS and UDEC solutions with analytical solution for dimensionless slip versus dimensionless time
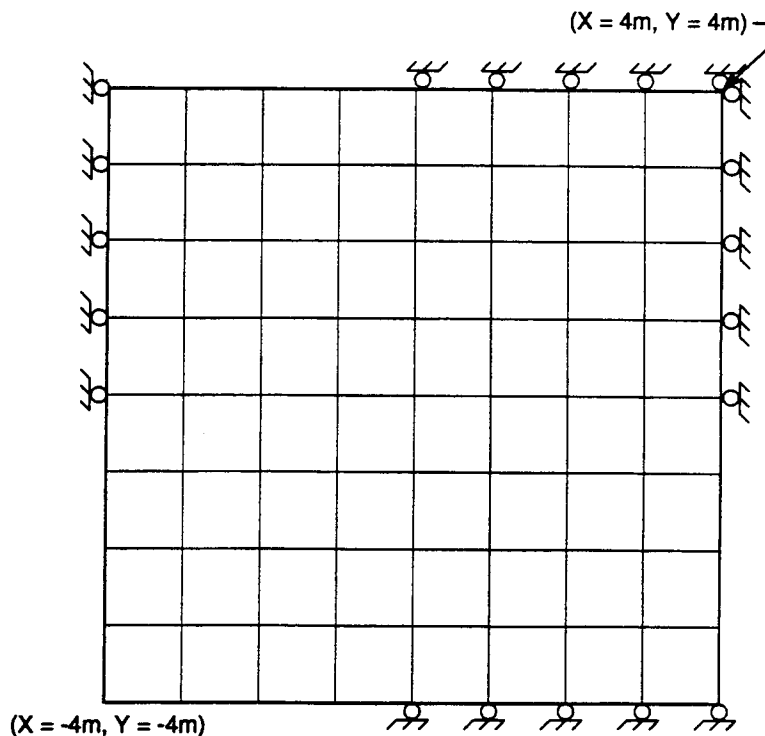
(X = 4m, Y = 4m)

(X = -4m, Y = -4m)

Figure A-25. Problem geometry and the mesh used to study the capability of ABAQUS to model intersecting joints

The model was analyzed in plane strain. Each block was modeled using 12, 4-noded quadrilateral elements. The discontinuities were modeled using 4-noded interface elements. The discontinuities were assigned zero shear resistance.

The deformed shape of the model is shown schematically in Figure A-26 after 27.4-cm displacement. There was no stress developed in the blocks — all movements occurred in rigid-body mode. Block B4 moved 27.4 cm diagonally. Block B3 moved 19.4 cm up, and B1 moved 19.4 cm to the right. Block B4 penetrated inside B2 without resistance.

The same model was analyzed using the distinct element program, UDEC. The program allowed block B4 to penetrate B2 only by the amount of a user-specified overlap tolerance. Thereafter, the program stopped with an error message indicating excessive overlap of the blocks. Moreover, the attempt to force block B4 into B2 caused a build-up of compressive stress around the contact point of the two blocks.

A.7 PROBLEM 5.2: SLIP ON ONE OF TWO ORTHOGONAL JOINTS

The geometry of the second problem is illustrated in Figure A-27. The problem was analyzed under plane strain conditions. Blocks B1 and B4 were restrained horizontally and vertically as shown in the figure. The analysis was run in two steps. First, block B3 was restrained horizontally on its left edge and a normal pressure of 5.0 MPa was applied on the top surface of B2 and B3; thereafter, block B3 was moved horizontally to the right. The blocks were modeled using 4-noded quadrilateral elements (eight
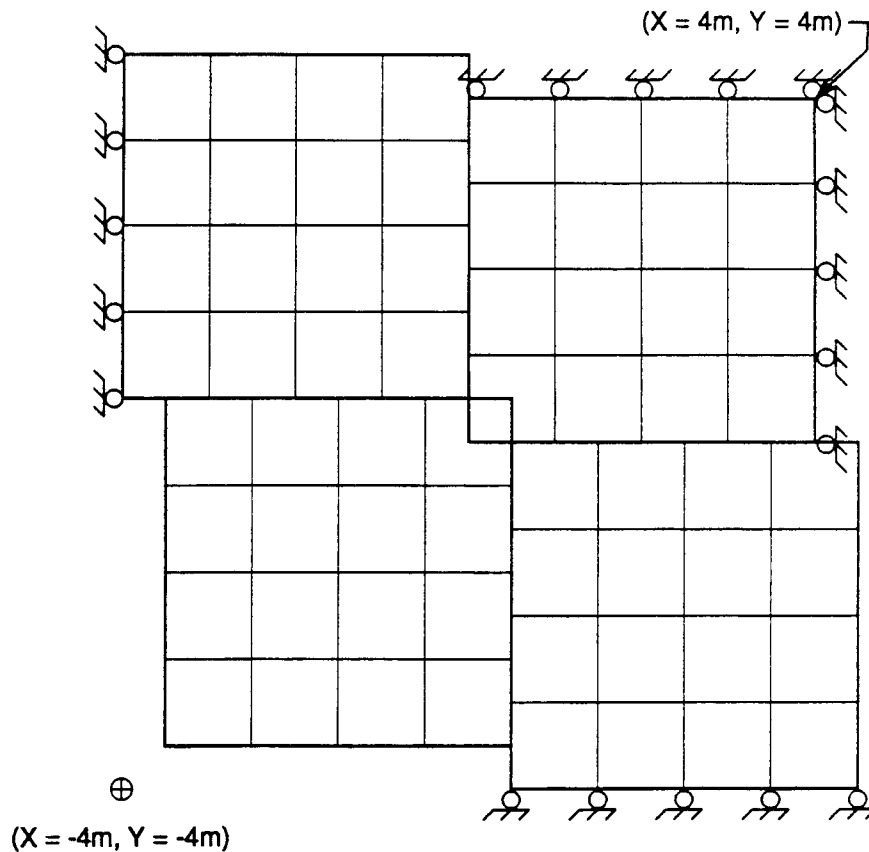
A-35

(X = 4m, Y = 4m)

(X = -4m, Y = -4m)

Figure A-26. Exaggerated displacement of the blocks used in the model with intersecting joints

elements for blocks B1 and B4, and four elements for blocks B2 and B3). The elements were 0.5 m wide and 0.5 m in length. The discontinuities were modeled using 4-noded interface elements of length 0.5 m.

Two different analyses of this problem were conducted. In the first analysis, the interface elements were free to open and slide. The result was that block B3 penetrated inside B2. In the second analysis, the interface elements were not allowed to open. In this case, both blocks B2 and B3 moved to the right by the same amount. The blocks were moved 0.5 m (one interface element length) horizontally to investigate the capability of the interface element to accommodate large-scale shear displacement.

The calculated response is shown in Figure A-28 in terms of normalized shear stress versus normalized shear displacement. Shear stress is normalized by dividing it by the applied normal stress. Shear displacement is expressed as the percentage of the interface element length. The calculated maximum normalized shear stress 0.287 is equal to the friction coefficient assigned to the interface between the blocks.
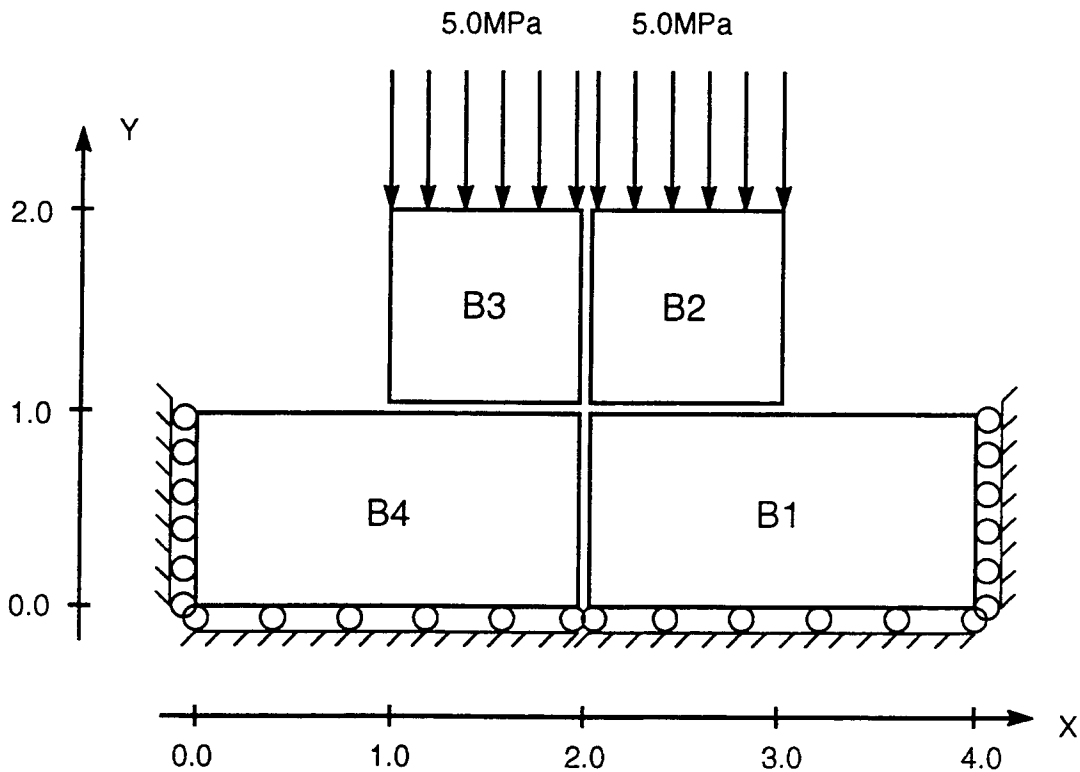
Figure A-27. Problem geometry for studying the capability of ABAQUS to model intersecting joints

A.7.1 Discussion of Results

Results from Problems 5.1 and 5.2 show that although ABAQUS can simulate the response of a single rock joint, its capability to simulate intersecting fractures is not adequate. The modeling scheme used in ABAQUS to define the fracture on the rough interface between two blocks using the interface element is not adequate to simulate the relative displacements between the blocks at opposite quadrants. As a result, one block can numerically penetrate the block at the opposite quadrant without generating any stress. Moreover, one interface element does not sense the existence of other interface elements. Consequently, ABAQUS can not model the redistribution of stresses and displacements when shear displacement takes place along the intersecting fractures.
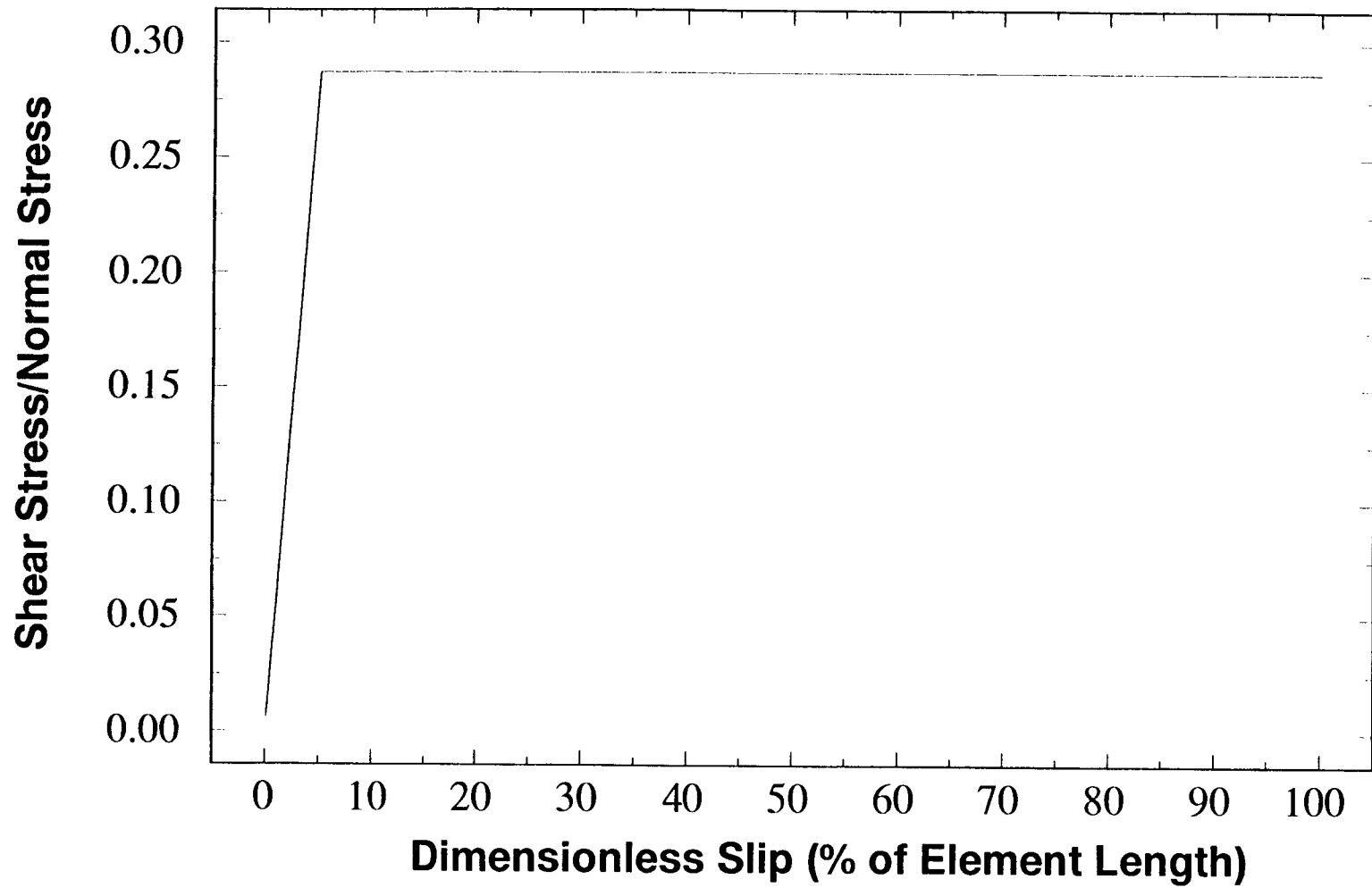
Figure A-28. Normalized shear stress (shear stress/normal stress) versus normalized slip (percentage of element length)

REFERENCES

Achenbach, J.D. 1975. *Ware Propagation in Elastic Solids*. New York, NY: North Holland Publishing Company.

Brady, B.H.G., and E.T. Brown. 1985. *Rock Mechanics for Underground Mining*. London, UK: George Allen & Unwin Ltd.

Brady, B.H.G., M.L. Cramer, and R.D. Hart. 1985. Preliminary analysis of a loading test on a large basalt block. *International Journal of Rock Mechanics and Mining Sciences & Geomechanics Abstracts* 22: 345-348.

Brady, B.H.G., S.M. Hsiung, and A.H. Chowdhury. 1990. *Qualification Studies on the Distinct Element Code UDEC Against Some Benchmark Analytical Problems*. CNWRA 90-004. San Antonio, TX: Center for Nuclear Waste Regulatory Analyses.

Day, S.M. 1985. *Test Problem for Plane Strain Block Motion Codes*. S-Cubed Inc. Memorandum to ITASCA Consulting Group, Inc.

Lemos, J. 1987. *A Distinct Element Model for Dynamic Analysis of Jointed Rock with Application to Dam Foundations and Fault Motion*. Ph.D. Thesis. University of Minnesota: 295.

Miller, R.K. 1978. The effects of boundary friction on the propagation of elastic waves. *Bulletin of the Seismological Society of America* 68: 987-998.

Olsson, W.A. 1982. Experiments on a slipping crack. *Geophysical Research Letters* 9(8): 797-800.

Salvado, C., and J.B. Minster. 1980. Slipping Interfaces: A possible source of S radiation from explosive sources. *Bulletin of the Seismological Society of America* 70: 659-670.

APPENDIX B

PRELIMINARY COMPARISON OF ABAQUS
AND UDEC CODES

B PRELIMINARY COMPARISON OF ABAQUS AND UDEC CODES

Fifteen codes were evaluated in Phase I study (Ghosh et al., 1993) based on the reported capabilities of modeling coupled processes, rock joint model, and responses from earthquakes and underground nuclear explosions. The comparison between the distinct element code UDEC, and the finite element code, ABAQUS, has been reproduced here. The symbol H_j was used to denote fluid flow through fractures on rock joints. H_m denoted flow through rock matrix.

Table B-1. Preliminary comparison of ABAQUS and UDEC codes based on published information (after Ghosh et al., 1993)

Criterion	UDEC (Version 1.8)	ABAQUS (Version 5.2-1)
Coupled Processes Modeled:		
$T{\rightarrow}M$	yes	yes
$T{\rightarrow}H_j$	no	no
$H_j{\rightarrow}T$	no	no
$M{\leftrightarrow}H_j$	yes	yes
$M{\leftrightarrow}H_m$	no	yes
$T{\rightarrow}H_m$	no	no
$H_m{\rightarrow}T$	no	no
Dynamic and Seismic Capabilities	yes	yes
Two-Phase Flow	no	yes[*]
Joint Simulation	Joint	Interface, Slideline
[*]No Phase Change		

REFERENCES

Ghosh, A., S.M. Hsiung, M.P. Ahola, and A.H. Chowhdury. 1993. *Evaluation of Coupled Computer Codes for Compliance Determination*. CNWRA 93-005. San Antonio, TX: Center for Nuclear Waste Regulatory Analyses.